



National Library
of Canada

Bibliothèque nationale
du Canada

Canadian Theses Service

Service des thèses canadiennes

Ottawa, Canada
K1A 0N4

NOTICE

The quality of this microform is heavily dependent upon the quality of the original thesis submitted for microfilming. Every effort has been made to ensure the highest quality of reproduction possible.

If pages are missing, contact the university which granted the degree.

Some pages may have indistinct print especially if the original pages were typed with a poor typewriter ribbon or if the university sent us an inferior photocopy.

Reproduction in full or in part of this microform is governed by the Canadian Copyright Act, R.S.C. 1970, c. C-30, and subsequent amendments.

AVIS

La qualité de cette microforme dépend grandement de la qualité de la thèse soumise au microfilmage. Nous avons tout fait pour assurer une qualité supérieure de reproduction.

S'il manque des pages, veuillez communiquer avec l'université qui a conféré le grade.

La qualité d'impression de certaines pages peut laisser à désirer, surtout si les pages originales ont été dactylographiées à l'aide d'un ruban usé ou si l'université nous a fait parvenir une photocopie de qualité inférieure.

La reproduction, même partielle, de cette microforme est soumise à la Loi canadienne sur le droit d'auteur, SRC 1970, c. C-30, et ses amendements subséquents.

λ



National Library
of Canada

Bibliothèque nationale
du Canada

Canadian Theses Service Service des thèses canadiennes

Ottawa, Canada
K1A 0N4

The author has granted an irrevocable non-exclusive licence allowing the National Library of Canada to reproduce, loan, distribute or sell copies of his/her thesis by any means and in any form or format, making this thesis available to interested persons.

The author retains ownership of the copyright in his/her thesis. Neither the thesis nor substantial extracts from it may be printed or otherwise reproduced without his/her permission.

L'auteur a accordé une licence irrévocable et non exclusive permettant à la Bibliothèque nationale du Canada de reproduire, prêter, distribuer ou vendre des copies de sa thèse de quelque manière et sous quelque forme que ce soit pour mettre des exemplaires de cette thèse à la disposition des personnes intéressées.

L'auteur conserve la propriété du droit d'auteur qui protège sa thèse. Ni la thèse ni des extraits substantiels de celle-ci ne doivent être imprimés ou autrement reproduits sans son autorisation.

ISBN 0-315-56072-X

**Reconstruction of Bandlimited Signal from
Unequally Distributed Samples**

Manimozhi Baskaran

A Thesis

in

The Department

of

Electrical and Computer Engineering

**Presented in Partial Fulfillment of the Requirements
for the Master of Engineering at
Concordia University
Montréal, Québec, Canada**

April, 1990

©Manimozhi Baskaran, 1990

ABSTRACT

Shannon's sampling theorem was introduced several decades ago to address the reconstruction of a band-limited signal from uniformly spaced samples. However, samples are not always equally spaced; in such a case exact reconstruction is not possible by using the uniform sampling theorem. Therefore, a different approach is essential to reconstruct a band-limited signal from unequally spaced samples. There exist numerous methods of signal reconstruction when a signal is given by a sequence of unequally spaced samples - various interpolation techniques as applied for band-limited signals, signal transformation methods, schemes for conversion of unequally spaced samples into their uniformly distributed counterparts, on-line iterative procedures and methods of multirate signal processing. From an extensive review of the literature, it is evident that conventional methods use special composing functions corresponding to a given set of unequally spaced samples; the functions are different for different sets of unequally spaced samples. Hence for each set, the corresponding composing functions have to be generated and they may not be well generalized. Moreover, the existing methods have not paid much attention for larger deviation of samples from their synchronous positions.

In the present study, an efficient simulation methodology for signal reconstruction from unequally spaced samples, using an iterative technique, is presented. This iterative technique is based on the approach of Plotkin and Swamy (1987). A user-friendly computer code is developed by implementing the partitioning scheme for the selection of samples. For the confirmation of newly developed code, preliminary simulations are performed for the same input conditions as that of Plotkin and Swamy (1987). Nevertheless, the present study is extended for larger deviation of samples from their

synchronous positions. It has been proved that the deviations can even exceed the Nyquist interval.

Deterministic signals, typically sinusoidal waveforms, are considered for restoring uniformly spaced samples from unequally sampled data at various subinterval lengths. Mean Square Errors (MSE) of the reconstructed signals are computed and they are found to decrease with increase in subinterval length. This algorithm is also applied for the reconstruction of random processes (Gaussian or uniformly distributed) from unequally spaced samples. The iterative procedure is implemented both for deterministic and random processes, and the calculated MSE levels decrease with increasing number of iterations. In addition, the present iterative procedure is extended for the summation of a deterministic signal and a random noise. Reconstructions are also performed for various Signal to Noise Ratio (SNR).

Recently Marvasti and Analoui, 1989 (MA) developed an iterative adaptive method for the reconstruction of bandlimited signals. To evaluate the efficiency of the present study (PS), considerable efforts have been made in simulating all the above cases by using the method of MA. Reconstructed results are analyzed and compared. From the comparisons it is clear that PS performs better than MA in all aspects. Moreover, PS can restore samples for larger deviation from the synchronous position. The performance of the PS is further analyzed by measuring the stability of the system. During the analysis, the sum of deterministic and random noise are considered by varying the two parameters namely the amplitude of the sinusoidal signal and variance of the random noise. It is found that the system is insensitive to the variation in the input parameters and hence stable.

ACKNOWLEDGEMENTS

Author would like to express her sincere thanks to Dr. E. I. PLOTKIN, for his constant guidance, stimulating suggestions and discussions. The author is also indebted to Dean M.N.S. SWAMY, for his advice and support. The author gratefully acknowledges the kindness and inspiration accorded during her study by her husband, A. BASKARAN. He provided the mental strength and stamina.

Dedicated to my father GANESAN

who instilled in me a desire for learning from my childhood days

TABLE OF CONTENTS

LIST OF FIGURES	ix
LIST OF ABBREVIATIONS AND SYMBOLS	xiii
CHAPTER I	
INTRODUCTION	1
1.1 General	1
1.2 Sampling Theorem for Band-limited Signals	4
1.3 Error Analysis	11
1.3.1 Truncation Error	11
1.3.2 Jitter Error	14
1.3.3 Round-off Error	19
1.4 Sampling Theorem for Unequally Spaced Samples	20
1.5 Thesis Organization	25
CHAPTER II	
SIGNAL RECOVERY FROM UNEQUALLY SPACED SAMPLES	27
2.1 A Review of the Existing Research	27
2.1.1 Reconstruction of Signal From a Finite Set of Arbitrarily Distributed Samples (Interpolation of band-limited Signals)	28
2.1.2 Reconstruction Procedure Based on Signal Transformation Method	30
2.1.3 Reconstruction Procedure Based on Conversion Method	40
2.1.4 Iterative Adaptive Method	42
2.1.5 Nonuniform Sampling for Sequences Using Multirate Signal Processing	44
2.2 Justifications of the Present Study	46
CHAPTER III	
SIMULATION METHODOLOGY	49

3.1	Governing Equations	49
3.2	Partitioning Scheme and Iterative Procedure	53
CHAPTER IV		
PRESENT COMPUTER CODE AND SIMULATED RESULTS FOR THE DETERMINISTIC PROCESSES		61
4.1	Description of the Present Computer Code	61
4.2	Simulated Results and Discussion for Deterministic Processes	66
4.2.1	Confirmation of the Present Study	66
4.2.2	Reconstruction Using Sine Wave	67
4.2.3	Reconstruction Using Sum of Sine Waves	89
4.3	Conclusion	99
CHAPTER V		
RECONSTRUCTION OF RANDOM PROCESSES FROM UNEQUALLY SPACED SAMPLES		100
5.1	Generation of a Random Process	100
5.2	Reconstruction from Unequally Spaced Samples for Random Processes	102
5.3	Reconstruction from Unequally Spaced Samples for the Sum of Deterministic and Random Processes	107
5.3.1	Gaussian Distribution	108
5.3.2	Uniform Distribution	119
5.4	Statistical Analysis of the Computed Errors	124
5.4.1	Sinusoidal Function with Uniformly Distributed Initial Phase	126
5.4.2	Uniformly Distributed Random Processes	133
5.4.3	Sinusoidal Function in the Presence of Uniformly Distributed Random Process	139
5.5	Conclusion	145

CHAPTER VI

STABILITY	147
6.1 Introduction	147
6.2 Effect of Amplitude on the Stability of the System	149
6.3 Influence of the Variation on the Stability of the System	152
6.4 Conclusion	157
CHAPTER VII CONCLUSIONS	158
REFERENCES	160

LIST OF FIGURES

Fig. 1.1	A physical interpretation of Shannon's sampling expansion (Jerri, 1977).	6
Fig. 1.2(a)	Fourier spectrum of $f(t)$ (Papoulis, 1966).	7
Fig. 1.2(b)	Periodic repetition of $f(\omega)$ (Papoulis, 1966).	7
Fig. 1.3	Kernel's spectrum in sampling expansion (Papoulis, 1966).	10
Fig. 1.4	Reconstruction of a band-limited signal using cardinal series (Mendelovitz and Sherman, 1975).	13
Fig. 1.5	Sampling and reconstruction of $f^*(t)$ (Thomas and Liu, 1974).	16
Fig. 2.1	Nonlinear transformation of axis (Papoulis, 1966).	32
Fig. 2.2	Geometric illustration of LCD operating to derive nonuniform sampling points (Plotkin et al., 1982).	35
Fig. 2.3	Modulation using nonuniform sampling (Plotkin et al., 1982).	38
Fig. 2.4	Block diagram for the reconstruction of $f(t)$ (Plotkin et al., 1984).	39
Fig. 2.5	A typical case for data-rate reduction (Valdhyathan and Liu, 1988).	45
Fig. 3.1	Data-block partitioning in restoring samples.	55
Fig. 3.2	Samples perturbed from their uniform location.	59
Fig. 4.1	Flow chart for the present computer code.	63
Fig. 4.2(a)	Confirmation of the present simulated results for sinusoidal waveform (without iterations).	68
Fig. 4.2(b)	Confirmation of the present simulated results for sinusoidal waveform (after two iterations).	69
Fig. 4.3	Nonuniform distribution of samples using sinusoidal waveform ($J=0.5$).	70

Fig. 4.4(a)	Reconstruction from nonuniformly distributed samples using sine waveform ($J=0.5$, PS).	72
Fig. 4.4(b)	Reconstruction from nonuniformly distributed samples using sine waveform ($J=0.5$, MA).	75
Fig. 4.5	Nonuniform distribution of samples using sinusoidal waveform ($J=1.0$).	76
Fig. 4.6(a)	Reconstruction from nonuniformly distributed samples using sine waveform ($J=1.0$, PS).	78
Fig. 4.6(b)	Reconstruction from nonuniformly distributed samples using sine waveform ($J=1.0$, MA).	79
Fig. 4.7	Reconstruction from nonuniformly distributed samples using sine waveform ($J=2.75$).	81
Fig. 4.8	A comparative study for the MSE between PS and MA.	82
Fig. 4.9	Effect of subinterval length on MSE.	85
Fig. 4.10	Influence of frequency ratio on RER.	88
Fig. 4.11	Nonuniformly distributed samples using sum of sine waves ($J=0.5$).	90
Fig. 4.12(a)	Reconstruction from nonuniformly distributed samples using sum of sine waves ($J=0.5$, PS).	91
Fig. 4.12(b)	Reconstruction from nonuniformly distributed samples using sum of sine waves ($J=0.5$, MA).	93
Fig. 4.13	Nonuniformly distributed samples using sum of sine waves ($J=1.0$).	94
Fig. 4.14(a)	Reconstruction from nonuniformly distributed samples using sum of sine waves ($J=1.0$, PS).	95
Fig. 4.14(b)	Reconstruction from nonuniformly distributed samples using sum of sine waves ($J=1.0$, MA).	97
Fig. 4.15	Reconstruction from nonuniformly distributed samples using complex waveform.	98
Fig. 5.1	Magnitude response of a Butterworth lowpass filter.	103

Fig. 5.2	Reconstruction from nonuniform samples using Gaussian distribution.	105
Fig. 5.3	Reconstruction from nonuniform samples using uniform distribution.	106
Fig. 5.4(a)	Reconstruction from nonuniformly spaced samples ($\text{SNR}_{\text{IN}} = -10\text{db}$, random Gaussian noise, PS).	110
Fig. 5.4(b)	Reconstruction from nonuniformly spaced samples ($\text{SNR}_{\text{IN}} = -10\text{db}$, random Gaussian noise, MA).	111
Fig. 5.5(a)	Reconstruction from nonuniformly spaced samples ($\text{SNR}_{\text{IN}} = 0\text{db}$, random Gaussian noise, PS).	113
Fig. 5.5(b)	Reconstruction from nonuniformly spaced samples ($\text{SNR}_{\text{IN}} = 0\text{db}$, random Gaussian noise, MA).	114
Fig. 5.6(a)	Reconstruction from nonuniformly spaced samples ($\text{SNR}_{\text{IN}} = +10\text{db}$, random Gaussian noise, PS).	115
Fig. 5.6(b)	Reconstruction from nonuniformly spaced samples ($\text{SNR}_{\text{IN}} = +10\text{db}$, random Gaussian noise, MA).	116
Fig. 5.7	Comparative study of MSE between PS and MA.	118
Fig. 5.8(a)	Reconstruction from nonuniformly spaced samples ($\text{SNR}_{\text{IN}} = 0\text{db}$, random uniform noise, PS).	120
Fig. 5.8(b)	Reconstruction from nonuniformly spaced samples ($\text{SNR}_{\text{IN}} = 0\text{db}$, random uniform noise, MA).	121
Fig. 5.9(a)	Reconstruction from nonuniformly spaced samples ($\text{SNR}_{\text{IN}} = +10\text{db}$, random uniform noise, PS).	122
Fig. 5.9(b)	Reconstruction from nonuniformly spaced samples ($\text{SNR}_{\text{IN}} = +10\text{db}$, random uniform noise, MA).	123
Fig. 5.10(a)	Mean of MSE for sinusoidal function with uniformly distributed initial phase ($M = 3$).	127
Fig. 5.10(b)	Standard deviation of MSE for sinusoidal function with uniformly distributed initial phase ($M = 3$).	129
Fig. 5.11(a)	Mean of MSE for sinusoidal function with uniformly distributed initial phase ($M = 5$).	131
Fig. 5.11(b)	Standard deviation of MSE for sinusoidal function with uniformly distributed initial phase ($M = 5$).	132

Fig. 5.12(a)	Mean of MSE for uniformly distributed random process ($M = 3$).	134
Fig. 5.12(b)	Standard deviation of MSE for uniformly distributed random process ($M = 3$).	136
Fig. 5.13(a)	Mean of MSE for uniformly distributed random process ($M = 5$).	137
Fig. 5.13(b)	Standard deviation of MSE for uniformly distributed random process ($M = 5$).	138
Fig. 5.14(a)	Mean of MSE for $SNR_{IN} = 20\text{db}$ ($M = 3$).	140
Fig. 5.14(b)	Standard deviation of MSE for $SNR_{IN} = 20\text{db}$ ($M = 3$).	142
Fig. 5.15(a)	Mean of MSE for $SNR_{IN} = 20\text{db}$ ($M = 5$).	143
Fig. 5.15(b)	Standard deviation of MSE for $SNR_{IN} = 20\text{db}$ ($M = 5$).	144
Fig. 6.1	Influence of amplitude variation on the stability of a random Gaussian process.	150
Fig. 6.2	Influence of amplitude variation on the stability of a random uniform process.	153
Fig. 6.3	Influence of variance on the stability of a random Gaussian process.	155
Fig. 6.4	Influence of variance on the stability of a random uniform process.	156

LIST OF ABBREVIATIONS AND SYMBOLS

A_s	<i>amplitude of the sinusoidal signal</i>
C_n	<i>Fourier coefficient</i>
E_e	<i>total energy</i>
$e_j(t)$	<i>jitter error</i>
$e_N(t)$	<i>truncation error</i>
$e_r(t)$	<i>round-off error</i>
$F(\omega), X(\omega)$	<i>Fourier transform of $f(t), x(t)$ respectively</i>
f_0	<i>operating frequency</i>
f_s	<i>sampling frequency</i>
$f(n/2W)$	<i>sample value of $f(t)$</i>
$f(t), x(t)$	<i>signal in consideration</i>
$f^*(t), \hat{x}(t)$	<i>estimated signal</i>
$f_s(t)$	<i>source signal</i>
J	<i>jitter parameter</i>
k_1, k_2	<i>real positive constants</i>
$k(t)$	<i>impulse response of the filter</i>
L	<i>number of samples retained</i>
M	<i>subinterval length</i>
MSE	<i>Mean Squared Error</i>
N	<i>number of samples</i>
NT	<i>number of trials</i>
$\{\frac{N}{2W}\}$	<i>sampling interval</i>
n	<i>number of iterations</i>
P_1, S_1	<i>band-limiting operators</i>
R	<i>normalized sampling rate</i>
RER	<i>Reconstruction ERror</i>
SNR	<i>Signal to Noise Ratio</i>
SNR_{IN}	<i>SNR at input</i>
$s(t)$	<i>filter output</i>
T	<i>upperlimit of the observation interval</i>
t_E	<i>elapsed time</i>
t_k, t_n	<i>sampling time instants</i>

$x(n)$	<i>discrete sequence</i>
$\hat{x}(k\Delta t), \tilde{x}(k\Delta t)$	<i>reconstructed samples</i>
$y(t)$	<i>modulating signal</i>
\bar{y}	<i>time average of y</i>
λ	<i>constant</i>
γ_k	<i>equally distributed levels</i>
γ_n	<i>deviation synchronous position</i>
$\Delta\gamma$	<i>distance between equally distributed levels</i>
γ_{\max}	<i>maximum value of the distributed levels</i>
Δt	<i>average sampling time</i>
Δ_k, μ_n	<i>sample time deviations</i>
$\delta(t - t_i)$	<i>unit impulse at t_i</i>
ω_m	<i>band-limited range</i>
σ_n^2	<i>variance of random noise</i>

CHAPTER 1

INTRODUCTION

1.1 GENERAL

Research efforts in signal processing continue to grow, as most of the engineering processes can be represented by means of signals. In general, the signals vary with time and it can be mathematically expressed as $f(t)$, where "t" represents an independent variable. Thus $f(t)$ represents the instantaneous value of the waveform as a function of this variable. A signal whose Fourier spectrum vanishes outside an interval can be easily realized using a physical system, namely, a band-limited filter. Then the realized signal is called as a band-limited signal. It can be classified as either analog or discrete signal. Analog signals can be represented by a series of discrete samples, each of which represents a value of $f(t)$ at a particular sampling point. One of the simplest ways of discretizing an analog signal is by equally spaced sampling. Such a type of sampling procedure is usually called as uniform sampling.

Shannon is one of the pioneers to reconstruct a band-limited signal from its uniform samples and it is called as Shannon's sampling theorem. It has been later extended by many authors into various generalized versions. One of the simplest version is: "A continuous time signal $f(t)$, band-limited to $|\omega| < W$ can be reconstructed from its equally spaced samples, if the sampling frequency (f_s) is at least equal to the Nyquist frequency". Thus to recover the signal $f(t)$ which is band-limited to W Hertz, it is necessary that f_s is greater than or equal to $2W$. A typical

practical example is the voice signal in telephone systems where the highest frequency is approximately equal to 3.3kHz. For the above system, f_s is chosen as 8kHz even though the theoretical minimum is only 6.6 kHz. If the minimum sampling rate is not met, the spectral components will overlap. In this case, the components of the original spectrum will appear with that of the other components and can not be uniquely determined. This process is called aliasing.

Whittaker E.T (1915) and Whittaker J.M (1929) are the first to give a mathematical expression for the sampling theorem. Whittaker (1915) derived an analytical expression for the function $f(t)$ by knowing its values at equidistant points $a, a+W, \dots, a+nW$, and is given by

$$f(t) = \sum_{n=-\infty}^{\infty} f(a+nW) \frac{\sin \frac{\pi}{W}(t-a-nW)}{\frac{\pi}{W}(t-a-nW)} \quad (1.1)$$

where $f(a+nW)$ are the values of $f(t)$ and a is a constant at its equidistant points. The sampling theorem which uses the cardinal series is sometimes called as Whittaker sampling theorem.

Kotelnikov (1933) presented the sampling theorem of the form (Equation 1.1) with applications to Communication Theory in Russian literature. Later, Shannon (1949) formally introduced sampling theorem to Information Theory based on Whittaker's mathematical derivation (Equation 1.1) and statement of Kotelnikov, which in brief is known as WKS sampling theorem to represent the works of Whittakers, Kotelnikov and Shannon respectively. Shannon sampling theorem allows the replacement of a continuous band-limited signal by a discrete sequence of

its samples without loss of any information. It also specifies the lowest rate necessary for the reproduction of the original continuous signal. The WKS sampling theorem is primarily used for band-limited deterministic processes and can be extended for band-limited random processes.

WKS sampling theorem was further extended in 1957 by Kramer and since then it is called as WKSK sampling theorem. Kramer considered the samples at nonequidistant values instead of equidistant values. The WKSK sampling theorem has many extensions, such as sampling for the case of N dimensions, for using derivatives, for random processes, for nonequally spaced samples, and for known and unknown distributions of sampling points. An excellent tutorial review of the extensions can be found from Jerri (1977). These extensions are also reviewed in the various contexts by Papoulis (1977a. and 1977b.) and Brown (1981). Papoulis (1977a. and 1977b.) studied the derivative sampling theorem, by formulating an unified framework in terms of linear filtering operation. Brown (1981) interpreted Papoulis work and showed that the reconstruction of signal can be obtained from its "generalized samples".

The following section discusses the proof of Shannon's sampling theorem for band-limited signals. Errors that occur in physical realization of band-limited signals are classified and discussed in the third section. Even though Shannon's sampling theorem allows the reconstruction of a band-limited signal by its discrete samples, during the process of reconstruction, the samples may deviate from their uniform positions. To accomplish the reconstruction of a signal from nonequally spaced samples, "nonuniform sampling theorem" is presented in the fourth section. The lay out of the thesis is discussed.

1.2 SAMPLING THEOREM FOR BAND-LIMITED SIGNALS

The statement of Shannon for WKS theorem is given below (Jerrl 1977):

"If a function $f(t)$ contains no frequencies higher than W cycles per second it is completely determined by giving its ordinates at a series of points spaced $(1/2W)$ seconds apart"

A signal $f(t)$ can be represented by its inverse Fourier transform as follows:

$$f(t) = \frac{1}{2\pi} \int_{-\infty}^{\infty} F(\omega) e^{j\omega t} d\omega \quad (1.2)$$

For a band-limit of $(-2\pi W, 2\pi W)$ the above equation can be rewritten as:

$$f(t) = \frac{1}{2\pi} \int_{-2\pi W}^{2\pi W} F(\omega) e^{j\omega t} d\omega \quad (1.3)$$

where $F(\omega)$ is the Fourier spectrum of $f(t)$ and assumed to have zero value outside the band $(-2\pi W, 2\pi W)$. The Fourier series expansion of $F(\omega)$ is:

$$F(\omega) = \sum_{n=-\infty}^{\infty} C_n e^{-j\omega \frac{n}{2W}} \quad (1.4)$$

where

$$\begin{aligned} C_n &= \frac{1}{4\pi W} \int_{-2\pi W}^{2\pi W} F(\omega) e^{j\omega \frac{n}{2W}} d\omega \\ &= \frac{1}{2\pi} \frac{1}{2W} \int_{-2\pi W}^{2\pi W} F(\omega) e^{j\omega \frac{n}{2W}} d\omega \end{aligned} \quad (1.5)$$

When $t = n/2W$, C_n can be rewritten as:

$$C_n = \frac{1}{2W} f\left(\frac{n}{2W}\right) \quad (1.6)$$

C_n and $f(n/2W)$ represent respectively the Fourier coefficient and the sample value of $f(t)$. From Equation (1.6), it can be observed that C_n is proportional to $f(n/2W)$ which in turn depends on $F(\omega)$. Shannon constructed $f(t)$ by substituting Equations

(1.4) and (1.6) in Equation (1.3). The following sampling series is obtained by further representing the integration as summation.

$$f(t) = \sum_{n=-\infty}^{\infty} f\left(\frac{n}{2W}\right) \frac{\sin \pi(2Wt - n)}{\pi(2Wt - n)} \quad (1.7)$$

Jerrl (1977) gave a physical interpretation for the above theorem as shown in Fig.

1.1. A band-limited signal $f(t)$ and its Fourier transform $F(\omega)$ are shown in Fig. 1.1(a), $F(\omega)$ has a zero value outside the region $(-2\pi W, 2\pi W)$. Fig. 1.1(b) shows $k(t)$, the impulse response of an Ideal Low Pass Filter (LPF) which is expressed as:

$$k(t) = \frac{\sin 2\pi Wt}{\pi t} \quad (1.8)$$

$K(\omega)$ is the system function of $k(t)$ with its cut off frequency equal to $2\pi W$. The continuous signal is sampled at various times $n/2W$, $n = 0, \pm 1, \pm 2, \dots$ as shown in Fig. 1.1(c), then these samples are successively applied to the LPF. The output of the filter is nothing but the original function, $f(t)$.

A more generalized representation for WKS sampling theorem has been introduced by Papoulls (1966). A signal $f(t)$ and its Fourier transform $F(\omega)$ are shown in Fig. 1.2 (a).

$$F(\omega) = \int_{-\infty}^{\infty} f(t) e^{-j\omega t} dt \quad (1.9)$$

If the signal is band-limited by W_1 then

$$F(\omega) = 0 \quad \text{for } |\omega| \geq W_1 \quad (1.10)$$

The generalized representation of Equation (1.7) given by Papoulls is as follows:

$$f(t) = \sum_{n=-\infty}^{\infty} f(nT) \frac{\sin W_0(t-nT)}{W_2(t-nT)} \quad (1.11)$$

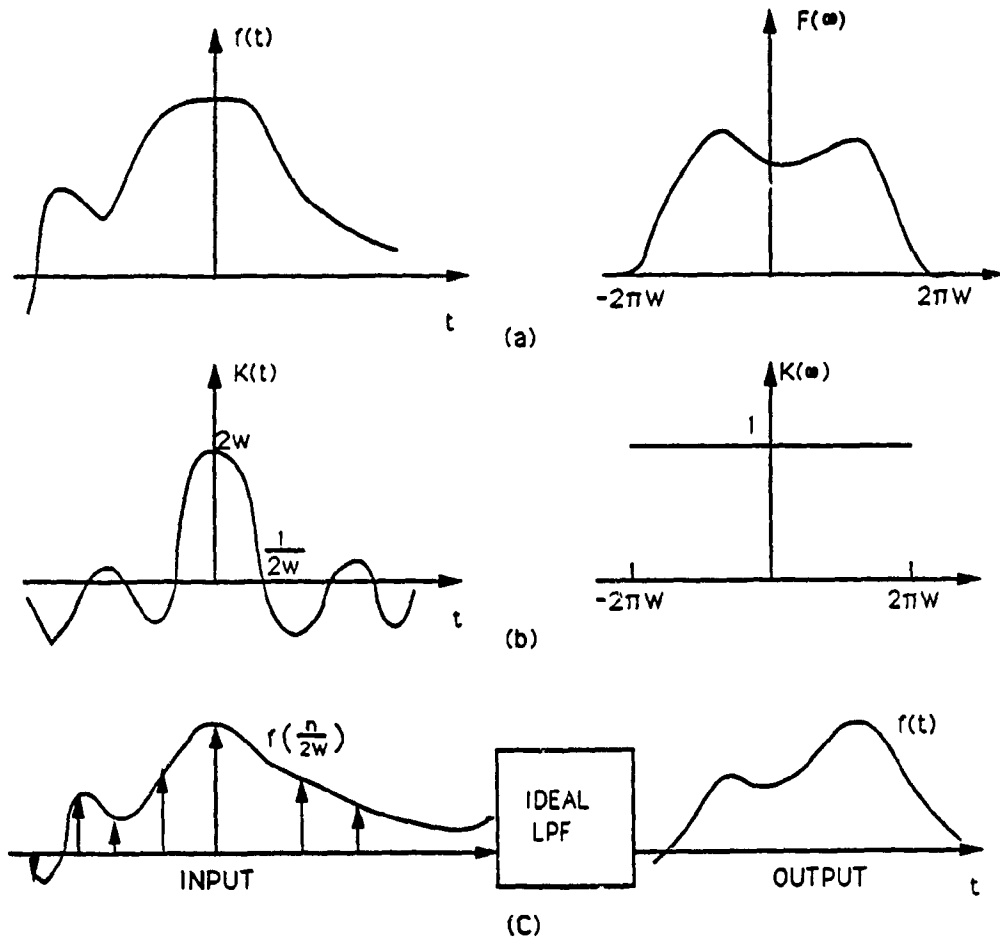


Fig. 1.1: A physical interpretation of Shannon's sampling expansion, (Jerri,1977)

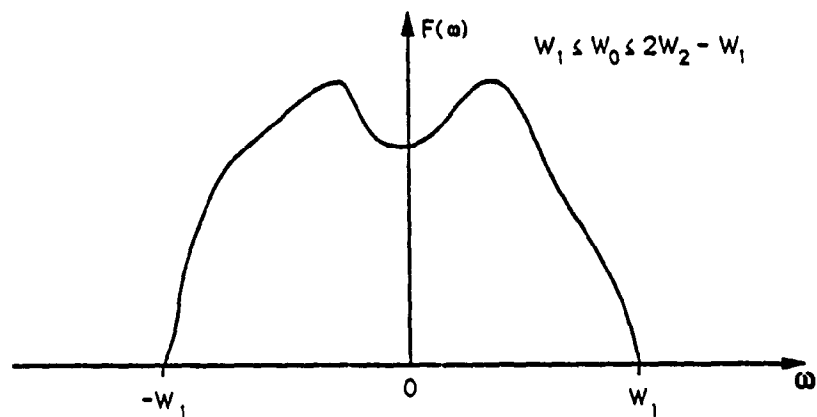


Fig. 1.2 (a): Fourier spectrum of $f(t)$, (Papoulis, 1966)

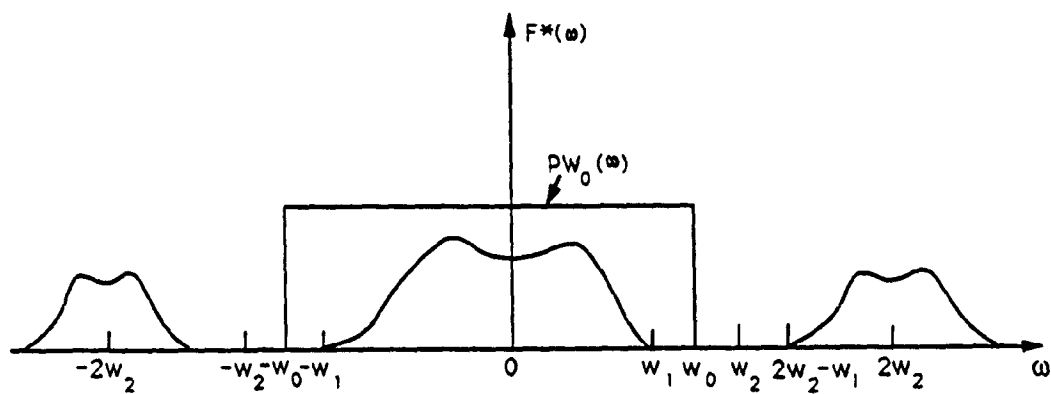


Fig. 1.2 (b): Periodic repetition of $F(\omega)$, (Papoulis, 1966)

where

$$W_2 \equiv \left\lceil \frac{\pi}{T} \right\rceil \geq W_1 \quad (1.12)$$

W_0 is an arbitrary constant between W_1 and $(2W_2 - W_1)$ such that

$$W_1 \leq W_0 \leq 2W_2 - W_1 \quad (1.13)$$

and $f(nT)$ are the sampled values with a sample spacing T .

To prove Equation (1.11) we consider the Fourier inversion formula for $f(nT)$:

$$f(nT) = \frac{1}{2\pi} \int_{-W_1}^{W_1} F(\omega) e^{jnT\omega} d\omega \quad (1.14)$$

By expanding $F(\omega)$ in the interval $(-W_2, W_2)$ and using Equation (1.12), $f(nT)$ can be expressed as:

$$f(nT) = \frac{1}{2W_2T} \int_{-W_2}^{W_2} F(\omega) e^{jnT\omega} d\omega \quad (1.15)$$

The above equation can also be expressed in terms of the Fourier coefficient, $f(nT)$ as:

$$F(\omega) = \sum_{n=-\infty}^{\infty} T f(nT) e^{-jnT\omega} \quad \text{for } |\omega| \leq \frac{\pi}{T} \quad (1.16)$$

In Fig. 1.2(b), $F^*(\omega)$ is nothing but a periodic repetition of $F(\omega)$ and therefore Equation (1.16) can be written as:

$$\begin{aligned} F^*(\omega) &= \sum_{n=-\infty}^{\infty} T f(nT) e^{-jnT\omega} \\ &= \sum_{n=-\infty}^{\infty} F\left(\omega + \frac{2\pi n}{T}\right) \end{aligned} \quad (1.17)$$

If $P_{W_0}(\omega)$ represents the impulse response of the filter, then $F(\omega)$ can also be expressed as:

$$F(\omega) = \sum_{n=-\infty}^{\infty} T f(nT) e^{-jnT\omega} P_{W_0}(\omega) \quad (1.18)$$

The terms on the right hand side of Equations (1.18) and (1.11) can be related as follows:

$$\begin{aligned} T e^{-jnT\omega} P_{W_0}(\omega) &\longleftrightarrow \frac{\sin W_0(t-nT)}{W_2(t-nT)} \\ \text{i.e., } e^{-jnT\omega} P_{W_0}(\omega) &\longleftrightarrow \frac{\sin W_0(t-nT)}{TW_2(t-nT)} \end{aligned} \quad (1.19)$$

Using Equation (1.12):

$$e^{-jnT\omega} P_{W_0}(\omega) \longleftrightarrow \frac{\sin W_0(t-nT)}{\pi(t-nT)} \quad (1.20)$$

From the above $f(t)$ can be expressed as:

$$f(t) = \sum_{n=-\infty}^{\infty} T f(nT) \frac{\sin W_0(t-nT)}{\pi(t-nT)} \quad (1.21)$$

What follows is Equation (1.11), which is obtained again by using Equation (1.12).

$$f(t) = \sum_{n=-\infty}^{\infty} f(nT) \frac{\sin W_0(t-nT)}{W_2(t-nT)} \quad (1.11)$$

Equation (1.11) can be further generalized for a relaxed filter condition $K(\omega)$ such that:

$$K(\omega) = \begin{cases} 1 & -W_1 \leq \omega \leq W_1 \\ 0 & 2nW_2 - W_1 \leq \omega \leq 2nW_2 + W_1, \quad n \neq 0 \end{cases} \quad (1.22)$$

Fig. 1.3 shows the magnitude response for the relaxed filter condition. It is clear from the figure that the value of $K(\omega)$ is unity for $-W_1 \leq \omega \leq W_1$ and it is zero when n is substituted as unity in the above equation.

With the above relaxed filter condition Equation (1.18) can be written as:

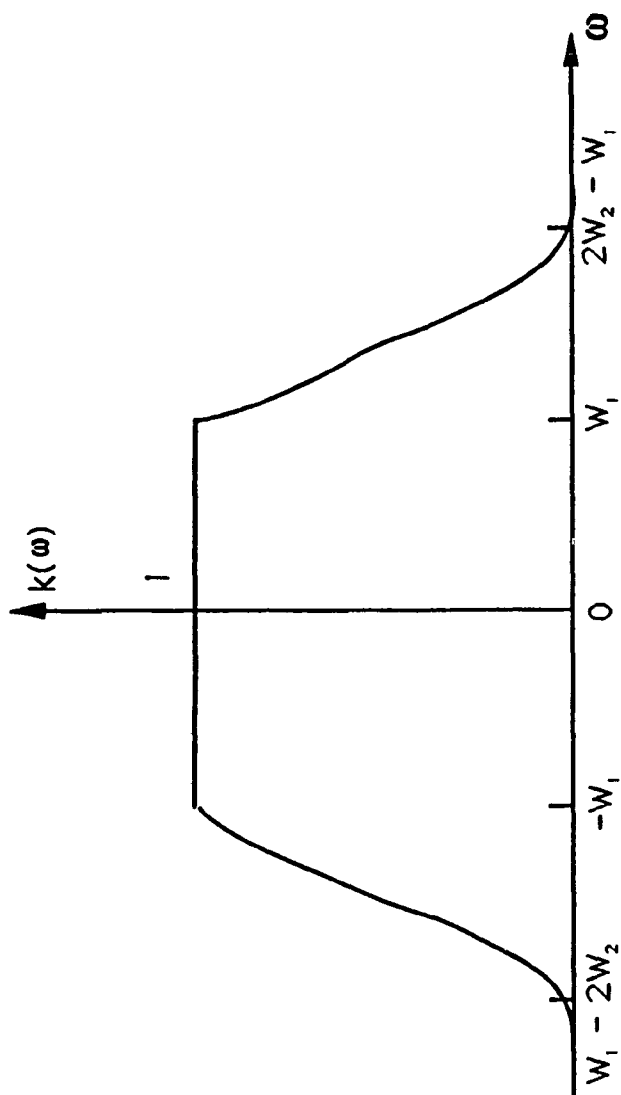


Fig. 1.3: Kernel's spectrum in sampling expansion, (Papoulis, 1986)

$$\begin{aligned} F(\omega) &= F^*(\omega)K(\omega) \\ &= \sum_{n=-\infty}^{\infty} T f(nT) e^{-jnT\omega} K(\omega) \end{aligned} \quad (1.23)$$

Hence $f(t)$ can be reconstructed from the sample values $f(nT)$ as:

$$f(t) = \sum_{n=-\infty}^{\infty} T f(nT) K(t - nT) \quad (1.24)$$

Thus the above equation also represents an extension of the WKS sampling theorem.

1.3 ERROR ANALYSIS

This section will present a review of the various errors that arise in the implementation of the sampling theorems. It includes truncation error which results when only a finite number of samples are used instead of infinite number of samples in the sampling representation, the jitter error, caused by the sampling at instants different from the uniformly distributed sample points, and finally, the round-off error due to the result of uncertainty in measuring the amplitude of the samples.

1.3.1 Truncation Error

As discussed in section 1.2, uniform sampling theorem can be used to reconstruct the original signal from its samples. Equation (1.7) represents an infinite series; however, conventionally the summation is obtained by truncating and assuming zero value after a finite interval. The truncation error can be further explained by recalling equation (1.7).

$$f(t) = \sum_{n=-\infty}^{\infty} f\left(\frac{n}{2W}\right) \frac{\sin 2\pi W(t - \frac{n}{2W})}{2\pi W(t - \frac{n}{2W})} \quad (1.25)$$

With $1/2W = T$ the above equation can be rewritten as:

$$f(t) = \sum_{n=-\infty}^{\infty} f(nT) \frac{\sin \frac{\pi}{T}(t-nT)}{\frac{\pi}{T}(t-nT)} \quad (1.26)$$

Substituting $\pi/T = \omega_1$

$$f(t) = \sum_{n=-\infty}^{\infty} f(nT) \frac{\sin \omega_1(t-nT)}{\omega_1(t-nT)} \quad (1.27)$$

where $f(nT)$ is the sample value with infinite number of samples. If a finite sum is used to reconstruct the signal, then Equation (1.27) can be rewritten as:

$$f_N(t) = \sum_{n=-N}^N f(nT) \frac{\sin \omega_1(t-nT)}{\omega_1(t-nT)} \quad (1.28)$$

The truncation error can then be calculated by finding the difference,

$$e_N(t) = f(t) - f_N(t) \quad (1.29)$$

Fig. 1.4 compares the truncation error in the reconstruction of a signal using cardinal series. The results from Brown (1969), Yao and Thomas (1966) and Mendelovlcz and Sherman (1975) are presented respectively as three curves. The method of Mendelovlcz and Sherman uses the generalized approach of Papoulls (1967) for energy bounded band-limited functions. However, Papoulls (1967) considered the truncation error performance of the cardinal series not only for the band-limited energy bounded signals but also for the band-limited random signals. For the former class of signals, the absolute value of the error is calculated at every time instant whereas for the latter class of signals, mean squared error is computed.

The horizontal axis of Fig. 1.4 represents the normalized sampling rate (R) defined as the ratio of the sampling frequency (f_s) to the operating frequencies (f_0),

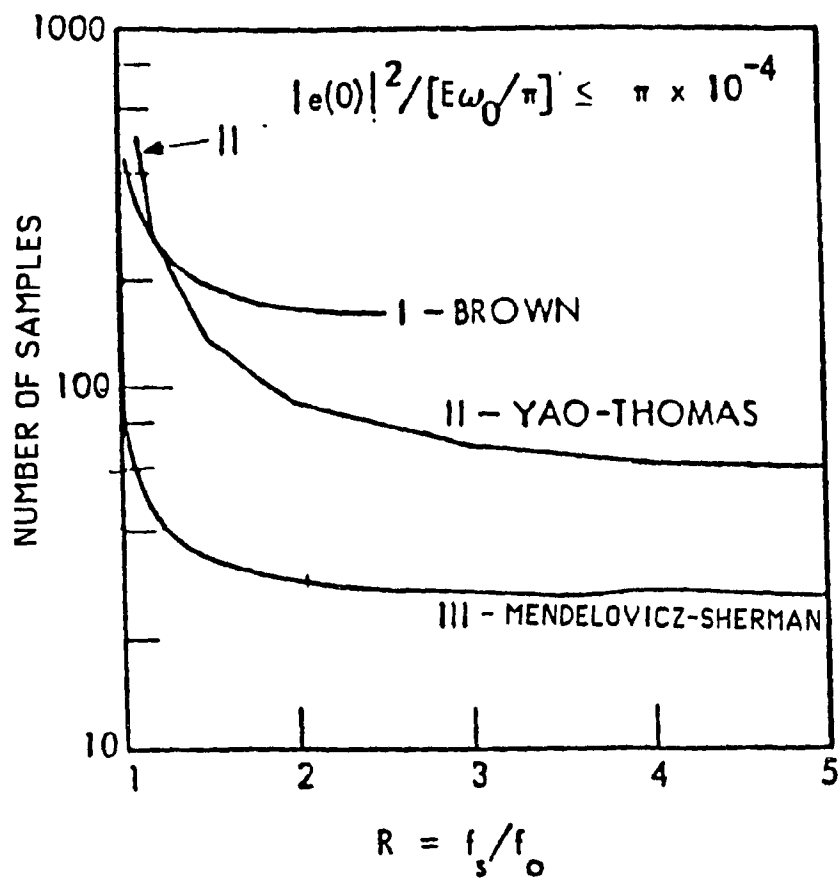


Fig. 1.4: Reconstruction of a band-limited signal
using cardinal series, (Mendelovicz and Sherman, 1975)

whereas the vertical axis represents the number of samples (N) in an observation interval. For all the three curves, the number of samples decrease for a certain range of R before stabilizing. For example, the third curve which is the most favourable one amongst the other curves, where for a value of $R = 1$, at least 100 samples are necessary to perform the reconstruction of the signal. By applying the cardinal series this is the minimum value of N necessary to reconstruct the signal, whereas it is even higher for the other two methods.

1.3.2 Jitter Error

Second kind of sampling error, namely jitter error, is discussed here. According to WKS sampling theorem, the sample instants are taken at synchronous positions nT . In some cases the samples may be shifted from their synchronous positions by a deviation γ_n , such that:

$$t_n = nT + \gamma_n \quad (1.30)$$

where γ_n are random numbers. Substituting t_n instead of nT in Equation (1.27), $f(t)$ can be written as:

$$\begin{aligned} f(t) &\approx \sum_{n=-\infty}^{\infty} f(t_n) \frac{\sin \omega_1(t-nT)}{\omega_1(t-nT)} \\ &= \sum_{n=-\infty}^{\infty} f(nT + \gamma_n) \frac{\sin \omega_1(t-nT)}{\omega_1(t-nT)} \end{aligned} \quad (1.31)$$

Balakrishnan (1963) treated the jitter error assuming a random model for both deterministic and stochastic signals. The spectrum of jittered process $[f(nT + \gamma_n)]$ is calculated and various measures of error due to jitter are evaluated. An optimal result

for the reconstruction of $f(t)$ using Equation (1.31) has also been presented. Brown (1964) treated two basic types of jitter, namely, the read-in jitter and read-out jitter. When these two types of jitters are equal it is known as locked jitter. Jitter spectrums are also obtained for read-in, read-out and locked jitters. If the actual sampling time occurs at $\{nT + x(nT)\}$ instead of the original sampling time, $\{nT\}$, then the data available after sampling are represented by a new function $g(nT)$ as follows:

$$g(nT) = f[(nT + x(nT))] \quad (1.32)$$

In the above equation $g(nT)$ equals $f(nT)$ if there is no jitter error in the sampling time. $x(nT)$ in this equation depicts the jitter and such jitter is termed as read-in jitter. Thus the motivation of the above process is that the sampling is done in order to store data. The stored data may be later used to reconstruct the signal $f(t)$ as denoted by $\hat{f}(t)$.

$$\hat{f}(t) = \sum_{n=-\infty}^{\infty} k(t - nT)g(nT) \quad (1.33)$$

where $k(t)$ is the impulse response of the filter. To obtain $\hat{f}(t)$, the stored samples $g(nT)$, are read-out of storage sequentially in the form of narrow pulses by passing through the filter. If the pulses are not read-out of storage exactly, there may be a second type of jitter coming into picture. This is called read out jitter.

Thomas and Liu (1964) have also elaborately illustrated the following example for the jitter error. Fig. 1.5 shows the steps involved in signal reconstruction for a real wide-sense stationary random process $f(t)$. $f(t)$ is first sampled at times $t = t_n$ and the resulting $f(t_n)$ used to construct an estimate $\hat{f}^*(t)$ of the original $f(t)$. In the figure, $f(t_n)$ and $\hat{f}^*(t)$ are respectively the input and the output of the filter whose impulse response is $h(t)$. Usually the sampled instants t_n are taken to be

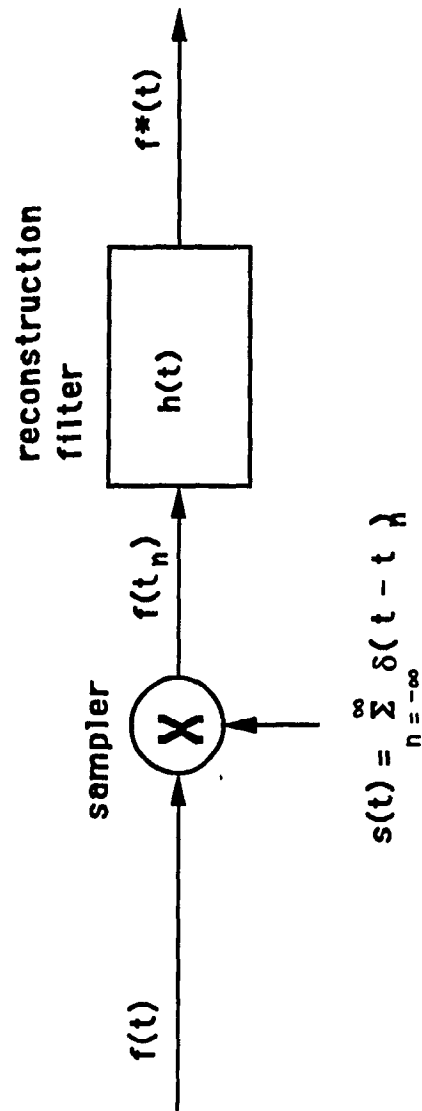


Fig. 1.5: Sampling and reconstruction of $f^*(t)$, (Thomas and Liu, 1974)

equally spaced ($t_n = nT$). Then the spectrum of the discrete process $[f(nT)]$ is uniquely related to that of the original continuous process $[f(t)]$, if the latter is properly band-limited. This is nothing but recovery from uniform samples. When the jitter is present at the sampler, the samples are taken at $t_n = nT + \gamma_n$ instead of nT . Thus a different discrete process $[f(nT + \gamma_n)]$ is obtained as a result of jittered sampling.

Instead of equation (1.30) Thomas and Liu also treated the jittered sampling instants as follows:

$$t_n = nT + \gamma_n - \alpha \quad (1.34)$$

where α is a parameter denoting the phase of the sampling function $s(t)$ relative to the signal $f(t)$ (-refer Fig. 1.5). They assumed γ_n as a discrete wide-sense stationary random process and α as a random variable, uniformly distributed in the observation interval. Due to the inclusion of α in the above equation, the estimate $f^*(t)$ is constructed from the jittered samples $[f(nT + \gamma_n - \alpha)]$ by using $h(t)$ instead of $[f(nT + \gamma_n)]$. Therefore $f^*(t)$ can be written as:

$$f^*(t) = \sum_{n=-\infty}^{\infty} f(nT + \gamma_n - \alpha)h(t - nT - \gamma_n + \alpha) \quad (1.35)$$

The expected error of such a reconstruction is estimated as:

$$E[(f - f^*)^2] = E[f^2] + E[f^{*2}] - 2E[ff^*] \quad (1.36)$$

where E is the expectation of the respective process. The error will be zero when $f^*(t)$ and $f(t)$ are equal. On the otherhand, the error will occur depending upon two characteristics. One of the characteristics is due to the jitter in time and the other

due to the selection of $h(t)$.

Papoulis (1966) considered the delays γ_n , as random numbers and estimated $f(t)$ from $f(nT + \gamma_n)$. The estimated $f(t)$ is denoted by $f_j(t)$ and is expressed as follows:

$$f_j(t) = \sum_{n=-\infty}^{\infty} f(nT + \gamma_n) \frac{\sin \omega_1(t - nT)}{\omega_1(t - nT)} \quad (1.37)$$

The estimated $f_j(t)$ differs from $f(t)$ by "jitter error", $e_j(t)$ as:

$$e_j(t) = f(t) - f_j(t) \quad (1.38)$$

On the otherhand, the difference between the original sample values, $f(nT)$ and recorded sample values, $f(nT + \gamma_n)$ can be calculated as:

$$\delta_n = f(nT) - f(nT + \gamma_n) \quad (1.39)$$

Then $e_j(t)$ can be expressed in terms of δ_n as:

$$e_j(t) = \sum_{n=-\infty}^{\infty} \delta_n \frac{\sin \omega_1(t - nT)}{\omega_1(t - nT)} \quad (1.40)$$

Following a similar procedure, Plotkin et al. (1984) classified the jitter error into two kinds of partial jitters. The first kind of partial jitter error is due to the difference in the amplitudes of samples (equally and unequally spaced) and it is expressed as:

$$e_{j1}(t) = \sum_{n=-\infty}^{\infty} \delta_n \frac{\sin \omega_1(t - nT)}{\omega_1(t - nT)} \quad (1.41)$$

The second kind of partial jitter is due to the shifting in the composing functions, while the values of amplitudes $f(nT)$ are supposed to be equal. The synchronous samples (nT) are shifted by γ_n in the "sinc" composing functions and the difference

between the original function and the shifted function is $e_{j_2}(t)$ and defined as:

$$\begin{aligned} e_{j_2}(t) &= \sum_{n=-\infty}^{\infty} \left[\text{sinc} \omega_1(t-nT) - \text{sinc} \omega_1(t-nT-\gamma_n) \right] \\ &= 1 - \sum_{n=-\infty}^{\infty} \text{sinc} \omega_1(t-nT-\gamma_n) \end{aligned} \quad (1.42)$$

The compositions of these two jitter errors may be considered as a total jitter error. In spite of the fact that the rule of the compositions can not be explicitly determined, it can be observed that if $f(nT + \gamma_n)$ is the same as that of $f(nT)$ then δ_n is zero in Equation (1.41) and total jitter is only due to second kind of partial jitter.

$$e_j(t) = e_{j_2}(t) \quad (1.43)$$

On the contrary, if the composing functions $\text{sinc} \omega_1(t - nT)$ are placed uniformly at nT , the second kind of jitter does not occur and therefore the total jitter error is due to the first kind of error only.

$$e_j(t) = e_{j_1}(t) \quad (1.44)$$

The error $e_j(t)$ in the above equation is equivalent to the round-off error which will be presented and discussed in the following subsection.

1.3.3 Round-off Error

The round-off error is nothing but an amplitude error and is caused due to the uncertainty in measuring the amplitude of the sample values. These uncertainties will occur either in quantization or fluctuation. If the restored values represent $\bar{f}(nT)$ instead of $f(nT)$ in Equation (1.27), then the signal recovered will have a round-off error and is given by:

$$f_r(t) = \sum_{n=-\infty}^{\infty} \bar{f}(nT) \frac{\text{sinc} \omega_1(t - nT)}{\omega_1(t - nT)} \quad (1.45)$$

The difference in $f(nT)$ and $\bar{f}(nT)$ is:

$$\epsilon_n = f(nT) - \bar{f}(nT) \quad (1.46)$$

The round-off error is:

$$e_r(t) = \sum_{n=-\infty}^{\infty} \epsilon_n \frac{\sin \omega_1(t - nT)}{\omega_1(t - nT)} \quad (1.47)$$

In Equation (1.45), $f_r(t)$ is band-limited and hence $e_r(t)$ is also band-limited by ω_1 ; the bounds for $e_r(t)$ based on the total energy (E_e) is as follows:

$$|e_r(t)| \leq \sqrt{\frac{\omega_1 E_e}{\pi}} \quad (1.48)$$

Further inherent details of the above equation can be found in Papoulis (1966).

1.4 SAMPLING THEOREM FOR UNEQUALLY SPACED SAMPLES

A band-limited function $f(t)$ need not be always equally spaced as defined by uniform sampling theorem. In such a case the exact reconstruction is obviously not possible through the sampling series and therefore a different approach is necessary for the reconstruction. The theorem that brings the principle of unequally spaced samples distribution is categorized as nonuniform sampling theorem.

Nonuniform sampling theorem may find applications in various practical situations. Some examples are:

(1) In mobile communication systems, there are several moving transmitters. They may generate a sequence $x(n)$. It is then up to the receiver (central fixed receiving station with sufficient signal processing facilities) to reconstruct the original $x(n)$. For this ideal situation, the data-rate reduction technique of nonuniform sampling may be applicable (Valdhyathan and Liu, 1988).

- (2) Sampling strategy may be random for some physical measurements. For example, wind varies with time and its velocity records contain unequally spaced samples. Then sampling theorem for unequally spaced samples may be applicable for the reconstruction of the velocity signal.
- (3) Some of the equally spaced samples may be missing in an observation interval. This leads to a nonuniform sample distribution.
- (4) In biomedical engineering, ECG (Electrocardiogram) and EMG (Electromyogram) signals are measured in human body. Sampling rate of these signals may vary depending upon the stress of the human body.
- (5) The sensors of a given array may be allocated in irregular fixed points, then the collected data falls under the category of nonuniform samples distribution.

In this section only a general review of some of the existing works on signal reconstruction procedures using unequally spaced samples is discussed. However, based on this general review five classifications are made. This will include, reconstruction of a signal from a finite set of arbitrarily distributed samples, reconstruction using signal transformation method, reconstruction based on conversion method, reconstruction using adaptive method and finally reconstruction from unequally spaced samples for sequences using multirate signal processing. All these methods will be discussed in detail with illustrative examples in the next chapter. In what follows now is the preview of signal reconstruction procedure from its unequally spaced data.

A thorough understanding of nonuniform sampling using explicit reconstruction formulas are given by Yen (1956). This study examined some special nonuniform sampling processes and the results presented in four generalized theorems. Three

theorems deal with nonuniform sample distributions which possess simple reconstruction formulas. Theorem 4 discusses "minimum energy signals". This class of signal is more suitable for nonuniform sampling involving a finite number of sample points. The complexity and accuracy of the reconstruction procedures as well as some important properties of bandwidth-limited signals are deduced from these four theorems. Further details of these theorems are presented in the next chapter.

Gardner (1972) extended Yen's (1956) nonuniform sampling procedure to higher dimensions. Sankur and Gerhardt (1973) also considered various methods for reconstructing a continuous signal from its nonuniform samples. They employed and compared a number of techniques namely, low pass filtering, Spline interpolation and Yen's interpolation. They observed that even though Yen's method was difficult to realize, it is still superior in comparison to other methods.

Beutler (1961) presented an approach to nonuniform sampling for wide-sense stationary random processes and concluded that the sampling times need not be periodic but may vary from its true periodicity by over 20 percent if the sinc composing function is used. Later, in 1966 he proved what is called "folk theorem" in the sense that a signal $f(t)$ may be represented by any linear combination of irregularly spaced samples $f(t_n)$, provided that the average sampling rate exceeds the Nyquist rate. This means that the number of samples per unit time exceed (on the average) twice the highest frequency of the signal.

By following the technique of Beutler (1961), Yao and Thomas (1968) derived sampling representation for band-limited functions when the sampling instants are not

necessarily uniformly spaced but deviate less than 0.22 from its Nyquist instant as required by WKS sampling theorem. They termed this as "semi-uniform" distribution and used the nonharmonic Fourier series for its derivations. Finally they remarked that sample representation is not possible when all the sampling instants are allowed to space nonuniformly by 25 percent from their corresponding Nyquist instant. It is found also that the true reconstruction is not possible if sample instants are placed arbitrarily or if additional sample instants are added.

Many procedures are developed based on the signal transformation method, such as time-wrapping and amplitude modulation techniques. Papoulis (1966) considered the time-wrapping technique as applied for unequally spaced samples. The positions of the samples are supposed to deviate by μ_n from their synchronous positions nT . Then a new set of sample positions will be formed at $nT - \mu_n$. This creates the problem of determining $f(t)$ in terms of $f(nT - \mu_n)$, instead of the original sample values $f(nT)$. In such a case the samples $nT - \mu_n$ are transformed into the points of nT . This transformation is called as the time-wrapping technique.

The second transformation method is the amplitude modulation technique. Plotkin and coworkers (1982 and 1984) used this technique for producing a sample whenever the integral of the modulating function crosses a threshold level by using a Level Crossing Detector (LCD) and thus LCD was used as a nonuniform sampler for this technique. They illustrated the concept of signal reconstruction by a numerical example. Two possible applications for employing this technique are identified namely as asynchronous Pulse Position Modulation (PPM) and signal approximation.

One of the problems in Yen's reconstruction procedure is the use of a special composing function. For each set of samples, the composing function may possess different forms. Hence for each set of sampling points, a set of composing function has to be generated and it may not be well generalized. To overcome this problem Dunlop and Phillips (1974) described a conversion method using nonuniform samples. The uniform samples are obtained from nonuniform samples by solving a set of simultaneous equations and this technique is discussed in detail in the next chapter. The method of obtaining uniform samples from nonuniform samples is called direct reconstruction procedure and by this procedure perfect reconstruction is not always possible. To reduce the error an iterative procedure has been suggested by Plotkin and Swamy (1987). This work forms primary interest of this thesis and it will be investigated in depth later.

In 1976, Marvasti and Gerhardt gave a practical treatment for signal transmission using nonuniform sampling. Their recent work (Marvasti and Analoul, 1989) showed that the iterative procedure can also be implemented based on Sandberg's theorem (1963) which is basically an extension of the work of Wiley (1977 and 1978) and Marvasti (1986). The above procedure is also called adaptive method. The iterative procedures of Plotkin and Swamy (1987) and Marvasti and Analoul (1989) are observed to be the simplest for signal reconstruction using the "sinc" composing function.

A special class of nonuniform sampling procedure is related to the so called multichannel signal processing. The derivative sampling theorem and nonuniform sampling theorem are given a new lucid interpretation by Papoulis (1977 a). Later Brown

(1981) reinterpreted the framework of Papoulis and showed the reconstruction of a signal is possible from its generalized samples. Recently Valdhyanadhan and Liu (1988) applied the idea of multichannel sampling to multirate signal processing. They exploited the analogy between sampling theorem framework and multirate filter bands. The multirate processing involved the downsampling of sequences at various stages and subsequently reconstruction of the signal.

1.5 THESIS ORGANIZATION

The thesis is divided into seven chapters. Chapter 2 will discuss, in detail, the various procedures for the reconstruction of a band-limited signal from unequally spaced data. It will also discuss the objectives of the present study. In chapter 3, a simulation methodology using an iterative procedure is presented. A computer code is developed for the reconstruction of a band-limited signal and chapter 4 will discuss the details of the computer algorithm. Various interesting simulations have been performed for the deterministic processes and the results are presented under two subdivisions, one dealing with the reconstruction of sine waves, and the other with the reconstruction of a deterministic signal given by sum of sine waves. The present computer code is extended in chapter 5 to verify the reconstruction technique for a random process. The results are discussed under four sections namely, generation of a random process; reconstruction from unequally spaced samples of a random process; reconstruction of a deterministic signal in the presence of a random noise; and statistical analysis of the computed errors. To evaluate the performance of the present iterative procedure, simulations are also carried out for all the above cases by applying the

algorithm of Marvasti and Analoul (1989) and the results compared.

Chapter 6 is dedicated to an examination of the stability of the system for changes in the input parameters. The amplitude of the sinusoid waveform and the variance of a random noise are varied and their effects on the system output studied. The concluding chapter summarizes the various findings of the present research work.

CHAPTER 2

SIGNAL RECOVERY FROM UNEQUALLY SPACED SAMPLES

A review of the existing research in signal recovery from unequally spaced samples is presented in this chapter. Particular emphasis is given for band-limited signals as this forms the basis of the present study. The need for further study is analyzed and justified based on the review of the existing works. Thus this chapter comprises two sections. First section has five subdivisions. The first subdivision discusses the classical theory of Yen (1956) using a finite set of arbitrarily distributed sample points. Second subdivision discusses the reconstruction of a signal based on signal transformation method and contains two techniques namely, time modulation technique of Papoulis (1966) and amplitude modulation technique of Plotkin and coworkers (1982 and 1984). The third subdivision deals with the conversion method of Dunlop and Phillips (1974). Fourth subdivision discusses the adaptive method of Marvasti and Analoul (1989) and the final subdivision discusses the multirate technique of Brown (1981), and Valdhyanadhan and Liu (1988).

2.1 A REVIEW OF THE EXISTING RESEARCH

As discussed in the previous chapter, the WKS sampling theorem for signal reconstruction assumes uniform sample distribution as follows:

$$f(t) = \sum_{k=-\infty}^{\infty} f(k\Delta t) \text{sinc} \omega_m(t-k\Delta t) \quad (2.1)$$

However a basic problem in many signal processing applications is the reconstruction of a band-limited signal $f(t)$, from its unequally spaced samples $\{t_k\}$. If $f(t_k)$ is employed in Equation (2.1) instead of $f(k\Delta t)$ the sampling series is:

$$\hat{f}(t) = \sum_{k=-\infty}^{\infty} f(t_k) \text{sinc} \omega_m(t - t_k) \neq f(t) \quad (2.2)$$

where $\text{sinc} \omega_m(t - t_k)$ is called the composing function for the sample points t_k . Note, that in this expression, the composing function becomes nonorthogonal and thus reconstructed signal, $\hat{f}(t)$ will differ from its original signal, $f(t)$. In other words, the distortions in $\hat{f}(t)$ will depend upon the distribution of the sampling points, $\{t_k\}$ for their deviation from the corresponding synchronous positions, $\{k\Delta t\}$. Thus the nonequally spaced samples can be conveniently presented as a shifted version of the synchronous positions as follows:

$$t_k = k\Delta t + \Delta_k \quad (2.3)$$

where Δ_k 's are random variables.

Various methods have been proposed to avoid the distortions in $\hat{f}(t)$. One of the methods is to compute a special composing function instead of $\text{sinc} \omega_m(t - t_k)$ and then perform the reconstruction without distortions. The computed special composing function is an infinite product based on the distribution of the sampling points. Yen (1956) performed a typical reconstruction procedure from a finite set of arbitrarily distributed samples, using the Lagrange's interpolation function. This is discussed in the following subdivision.

2.1.1 Reconstruction of Signal from a Finite Set of Arbitrarily Distributed Samples (Interpolation of Band-limited Signals)

One of the early studies in nonuniform sampling for band-limited signal is due to Yen (1956). He summarized the main results under four generalized sampling theorems containing simple reconstruction formulas. One of the simplest methods to illustrate the sequence of unequally spaced samples is to form the migration of finite number of uniformly distributed samples. This is stated in Theorem 1 as follows:

Theorem 1: "If a finite number of uniform sample points in a uniform distribution are migrated to new distinct positions thus forming a new distribution then, the band-width limited signal is uniquely defined."

When the number of shifted uniform sample points increases without bound, Theorem 1 is no longer valid. The resulting sample point distribution may or may not allow the unique determination of the signal. For such a distribution the following theorem holds.

Theorem 2: "It involves the shifting of half the uniform sample points, say all those with $t > 0$, by an equal amount with respect to the rest."

Another simple spacing of nonuniform samples is the recurrent nonuniform distribution as described in Theorem 3. For the recurrent nonuniform distribution, sample points are divided into different groups of N points. The groups have recurrent period of $N/2W$ seconds, where W cps is the band-limit of the signal. Yen determined the signal $f(t)$ uniquely and reconstructed it in terms of its values at $t = t_p + (mN / 2W)$, $p = 1, 2, \dots, N$ and $m = \dots, -1, 0, 1, \dots$ as follows:

Theorem 3: "A band-limited signal is uniquely determined by its values at a set of recurrent sample points $t = \tau_{pm} = t_p + (mN/2W)$, $p = 1, 2, \dots, N$; $m = \dots, -1, 0, 1, \dots$.

Theorem 4 addresses the reconstruction of a signal from a finite set of arbitrarily distributed samples. A band-limited signal $f(t)$ can be reconstructed from a finite set of arbitrarily distributed sample points $t = \tau_p$ and p can vary from $1, 2, \dots, N$ under the condition of minimum energy signal. Then the reconstruction can be defined as follows:

$$f(t) = \sum_{p=1}^N f(\tau_p) \Psi_p(t) \quad (2.4)$$

where

$$\Psi_p(t) = \sum_{q=1}^N a_{qp} \frac{\sin 2\pi W(t - \tau_q)}{2\pi W(t - \tau_q)} \quad (2.5)$$

a_{qp} are the coefficients of the inverse matrix whose elements are given by:

$$a_{qp} = \frac{\sin 2\pi W(\tau_p - \tau_q)}{2\pi W(\tau_p - \tau_q)} \quad (2.6)$$

The right hand side of Equation (2.5) is a product of two sinc functions and hence become more and more complicated as the sample points deviate more and more from their uniform positions. This is due to the fact that for a nonuniform distribution, the composing functions no longer possess the same form. In other words, these functions differ for each set of sample points and hence have to be regenerated for every data-block. Thus the functions are complicated to realize.

2.1.2 Reconstruction Procedure Based on Signal Transformation Method

(a) Time-warping Technique

Usually in sampling theory, a signal $f(t)$ is sensed from its sampled values $f(nT)$. But in real applications the sampled numbers are obtained with some deviations, μ_n . Problem arises in reconstructing $f(t)$ from the deviated sample values $f(nT - \mu_n)$. Papoulls (1966) considered this deviation as timing errors in the recovery mechanism and presented some excellent observations using the time warping technique which is discussed below.

Assuming the delays μ_n are known numbers, he developed a method for determining $f(t)$ from $f(nT - \mu_n)$. To reconstruct the signal $f(t)$, consider a band-limited signal $\theta(\tau)$:

$$\theta(\tau) = \sum_{n=-\infty}^{\infty} \mu_n \operatorname{sinc} \omega_m(\tau - nT) \quad (2.7)$$

where

$$\mu_n = \theta(nT) \quad (2.8)$$

Fig. 2.1 shows the transformation of X and Y-axes. $\gamma(t)$ is a nonlinear function that determines the relationship between these two axes and can be expressed as:

$$\tau = \gamma(t) \quad (2.9)$$

Suppose $\gamma(t) = 1$, then τ on the Y-axis is transformed into τ on the X-axis. When $\gamma(t) \neq 1$, τ in Y-axis is transformed into t in X-axis which can be mathematically expressed as:

$$t = \tau - \theta(\tau) \quad (2.10)$$

$$\text{If } \tau = nT \text{ then } t = nT - \theta(nT) = nT - \mu_n \quad (2.11)$$

Implementing the above principle of nonlinear transformation of the axis, $f(t)$ is reconstructed from $f(nT - \mu_n)$. Using Equation (2.10), $f(t)$ can be expressed as:

$$f(t) = f[\tau - \theta(\tau)] \quad (2.12)$$

Calling $f(t)$ by a new function $g(\tau)$:

$$g(\tau) = f[\tau - \theta(\tau)] \quad (2.13)$$

When it is band-limited by ω_m , then by sampling series:

$$g(\tau) = \sum_{n=-\infty}^{\infty} g(nT) \text{sinc } \omega_m(\tau - nT) \quad (2.14)$$

Using Equation (2.9), the above equation can be rewritten as:

$$g[\gamma(t)] = \sum_{n=-\infty}^{\infty} g(nT) \text{sinc } \omega_m[\gamma(t) - nT] \quad (2.15)$$

Substituting $\tau = nT$ and using Equation (2.8), Equation (2.13) can be rewritten as:

$$g(nT) = f(nT - \mu_n) \quad (2.16)$$

Substituting this value of $g(nT)$ into Equation (2.15):

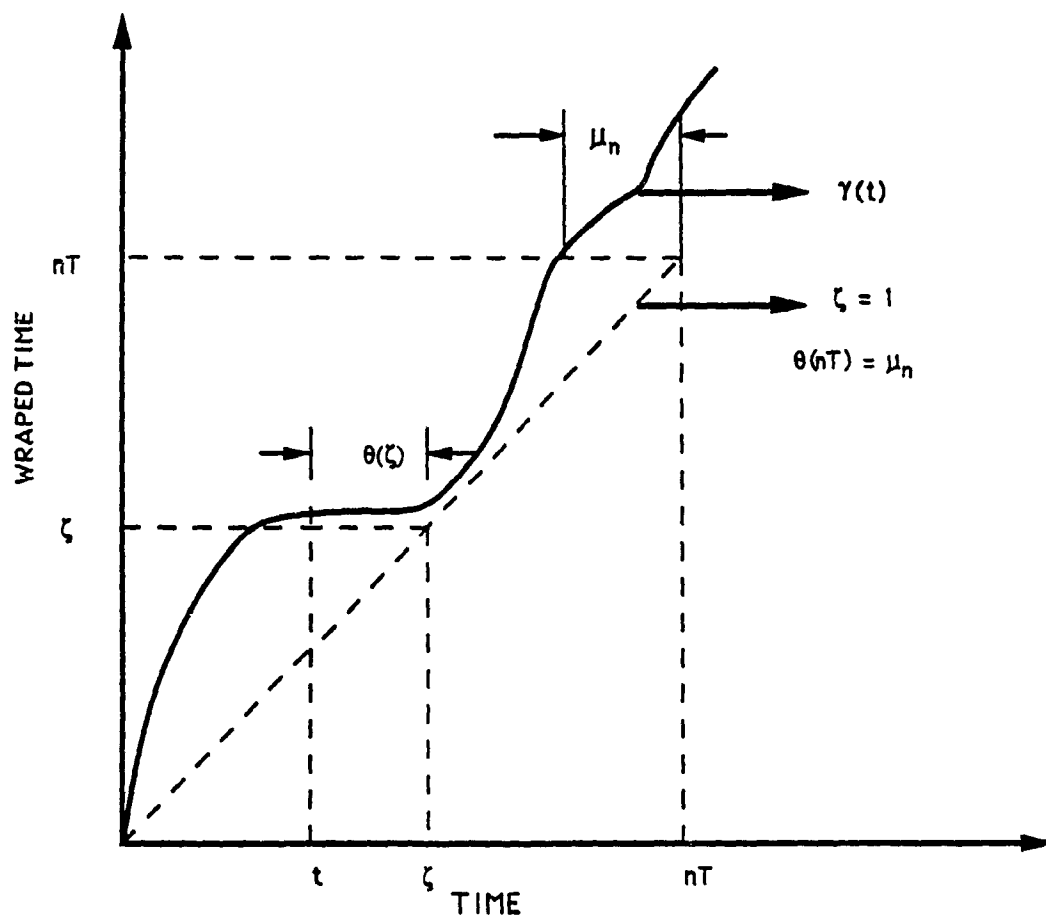


Fig. 2.1: Non-linear transformation of axis, (Papoulis, 1986)

$$g[\gamma(t)] = \sum_{n=-\infty}^{\infty} f(nT - \mu_n) \text{sinc } \omega_m [\gamma(t) - nT] \quad (2.17)$$

Since $g(\tau)$ is nothing but $f(t)$; the reconstructed function is:

$$f(t) = \sum_{n=-\infty}^{\infty} f(nT - \mu_n) \text{sinc } \omega_m [\gamma(t) - nT] \quad (2.18)$$

To derive the boundaries for the jitter error, consider $F(\omega)$ as the Fourier transform of the signal $f(t)$. Let the first order moment of $F(\omega)$ be defined as:

$$M_1 = \frac{1}{\pi} \int_0^{\omega_m} \omega |F(\omega)| d\omega \quad (2.19)$$

According to Papoulis (1962 a), for any t_1 and t_2 in $f(t)$,

$$|f(t_1) - f(t_2)| = M_1 |t_1 - t_2| \quad (2.20)$$

Applying the above expression in Equation (1.39), it can be concluded that:

$$|\delta_n| = |f(nT) - f(nT - \mu_n)| \leq M_1 |\mu_n| \quad (2.21)$$

Let μ_n be a random variable having zero mean such that:

$$E\{\mu_n\} = 0 \quad (2.22)$$

where E corresponds to the mathematical expectation. The variance is expressed as:

$$E\{\mu_n^2\} = \sigma^2 \quad (2.23)$$

In Equation (2.21), for a given n , δ_n depends only upon μ_n . Hence, δ_n is also independent and its mean and variance can be expressed respectively as:

$$E\{\delta_n^2\} \leq M_1^2 \sigma^2 \quad (2.24)$$

Having known the $E\{\delta_n^2\}$, Papoulis (1966) derived an expression for the expectation of $e_j^2(t)$ as follows:

$$E\{e_j^2(t)\} = \sum_{n=-\infty}^{\infty} E\{\delta_n^2\} \frac{\sin^2 \omega_m (t - nT)}{\omega_m^2 (t - nT)} \leq M_1^2 \sigma^2 \quad (2.25)$$

This is the boundary condition for $e_j(t)$.

(b) Amplitude Modulation Technique

Plotkin and coworkers (1982 and 1984) presented a modulation technique to reconstruct a signal from nonequally spaced samples such that the distortions in the reconstructed signal are minimized (Equation 1.37). Consider a modulated signal $z(t)$ band-limited to the frequency range $|\omega| < \omega_m$ given by:

$$\begin{aligned} z(t) &= y(t) \cdot x(t) \\ &= \sum_{k=0}^N x(t_k) \text{sinc} \omega_m(t - t_k) \end{aligned} \quad (2.26)$$

$x(t)$ is a signal whose values $x(t_k)$ are given at a set of nonequally spaced sample points, $\{t_k\}$ which are known apriori. The function $y(t)$ in the above equation is called a "correction function" and the problem of reconstruction of $x(t)$ is now reduced to the problem of finding this correction function. Hence the reconstructed signal becomes:

$$x(t) = y^{-1}(t) \cdot z(t) \quad (2.27)$$

It is clear from the above equation that $y(t)$ has to be a positive, single valued function. Plotkin and coworkers (1982) have presented the steps involved in finding $y(t)$ based on a knowledge of the spacing of sample points $\{t_k\}$.

The parameters used for the modulation technique is shown in Fig. 2.2 which is taken from Plotkin et al. (1982). X-axis represents a set of nonequally spaced sampling times, $\{t_k\}$. This set of $\{t_k\}$ may be transformed into uniformly distributed levels γ_k on the Y-axis depending upon the characteristic of modulating function $y(t)$. \bar{y} is the time-average value of the modulating function in the interval $(0, T)$ and is defined as:

$$\bar{y} = \frac{1}{T} \int_0^T y(t) dt \quad (2.28)$$

Δt and $\Delta \gamma$ are respectively the distance between two adjacent levels on the X and

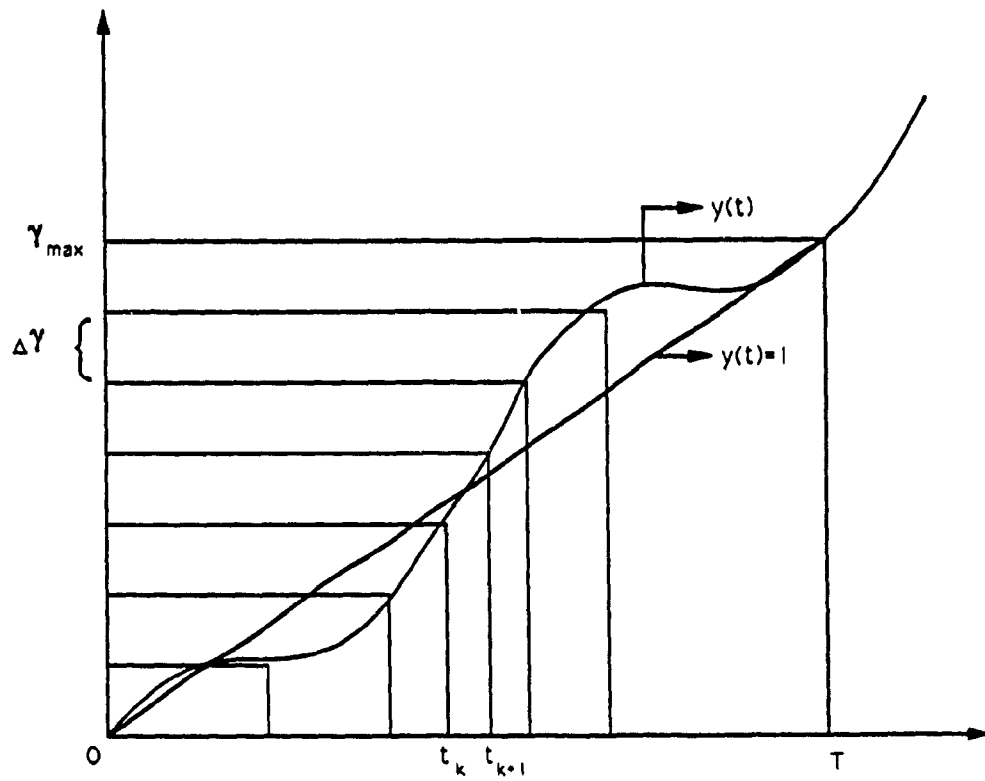


Fig. 2.2: Geometric illustration of LCD, operating to derive nonuniform sampling points, (Plotkin et al., 1982)

Y-axes. They are expressed as:

$$\Delta t = \frac{T}{N} \quad (2.29)$$

$$\Delta \gamma = \frac{\gamma_{\max}}{N} \quad (2.30)$$

An estimate for $z(t)$ is represented as $\hat{z}(t)$ and can be expressed as follows:

$$\hat{z}(t) = \bar{y} \sum_{k=0}^N x(t_k) \text{sinc} \omega_m(t - t_k) \quad (2.31)$$

This estimated function, $\hat{z}(t)$, is represented in terms of unequally spaced sample instants $\{t_k\}$ and the modulating function $y(t)$.

Recall that Equation (2.3) for unequally spaced sample instants t_k

$$t_k = k\Delta t + \Delta_k \quad (2.3)$$

where $k\Delta t$ and Δ_k are respectively the uniform sample position and random value at k th instant. Once γ_k levels and t_k instants are known, the function $y(t)$ can be found and used for determining $\hat{x}(t)$ as follows:

$$\hat{x}(t) = y^{-1}(t) \hat{z}(t) \quad (2.32)$$

By using Equation (2.31):

$$\hat{x}(t) = \bar{y} \cdot \frac{\sum_{k=0}^{\infty} x(t_k) \text{sinc} \omega_m(t - t_k)}{y(t)} \quad (2.33)$$

In the above equation, " \hat{x} " emphasizes that this procedure is obtained with a certain error in the reconstruction due to the approximation in finding the function $y(t)$.

If $y(t) = 1$ in Fig 2.2, then the nonuniform sampling is reduced to uniform sampling and therefore Equation (2.3) reduces to:

$$t_k = k\Delta t \quad (2.34)$$

Then the Equation (2.31) can be modified as:

$$\hat{z}(t) = \sum_{k=0}^N x(k\Delta t) \text{sinc} \omega_m(t - k\Delta t) = z(t) \quad (2.35)$$

Note that $\bar{y} = 1$ when $y(t) = 1$. For this case $\hat{z}(t)$ is exactly equal to the original signal $z(t)$.

A practical implementation of Equation (2.31) is shown in Fig. 2.3, which is also taken from Plotkin and coworkers (1982). $\delta(t - t_k)$ is due to the realization of the source modulating function $y(t)$. $x(t_k)$ represents the value of unequally spaced sampling instants for the set $\{t_k\}$, and ω_m is the cut-off frequency of Low Pass Filter (LPF). The nonuniform sampler is basically a Level Crossing Detector (LCD), a device consisting of a number of uniformly spaced levels. A single sample is taken whenever the input to the LCD crosses a threshold level. The above mentioned procedure may be defined as an asynchronous Pulse Position Modulation (PPM), because the sequence $\delta(t - t_k)$ is due to the realization of the source modulating function using the nonuniform sampling procedure, LCD. An extension of the above work has been published in Plotkin et al. (1984). In Equation (2.31), when \bar{y} takes a value other than unity, it can not be reduced as Equation (2.35) and therefore expressed as:

$$\begin{aligned} z(t) &\approx \bar{y} \cdot \hat{x}(t) \\ y(t) \cdot x(t) &\approx \bar{y} \cdot \hat{x}(t) \end{aligned} \quad (2.36)$$

Note that in the Equation (2.36), the left hand side is approximately equal to the right hand side and therefore the above relation can be equated by introducing a new factor $\hat{x}(t)$ as:

$$y(t) \cdot \hat{x}(t) = \bar{y} \cdot \hat{x}(t) \quad (2.37)$$

Thus

$$\hat{x}(t) = \bar{y} \cdot \frac{\hat{x}(t)}{y(t)} \quad (2.38)$$

$\hat{x}(t)$ in Equation (2.38) can be found by using Fig. 2.4 which illustrates the various involved steps. An ideal LPF with input of unequally spaced samples $x(t_k)$ is used to get $\hat{x}(t)$. The bottom branch is used to find a distribution function, $y(t)$.

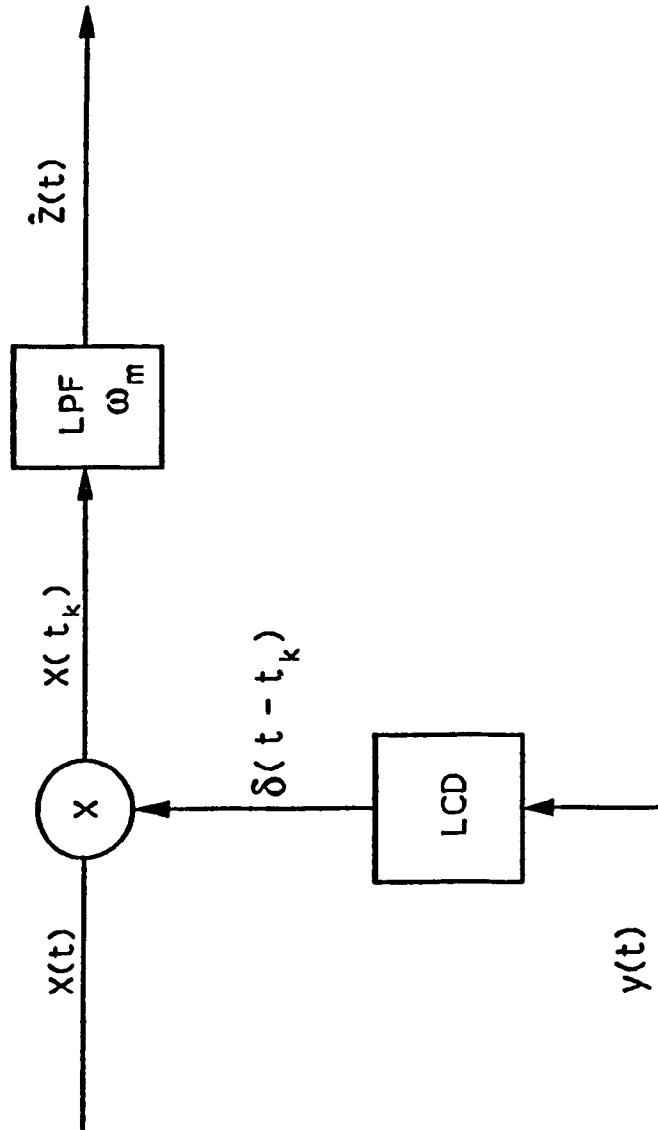


Fig. 2.3: Modulation using nonuniform sampling, (Plotkin et al., 1982)

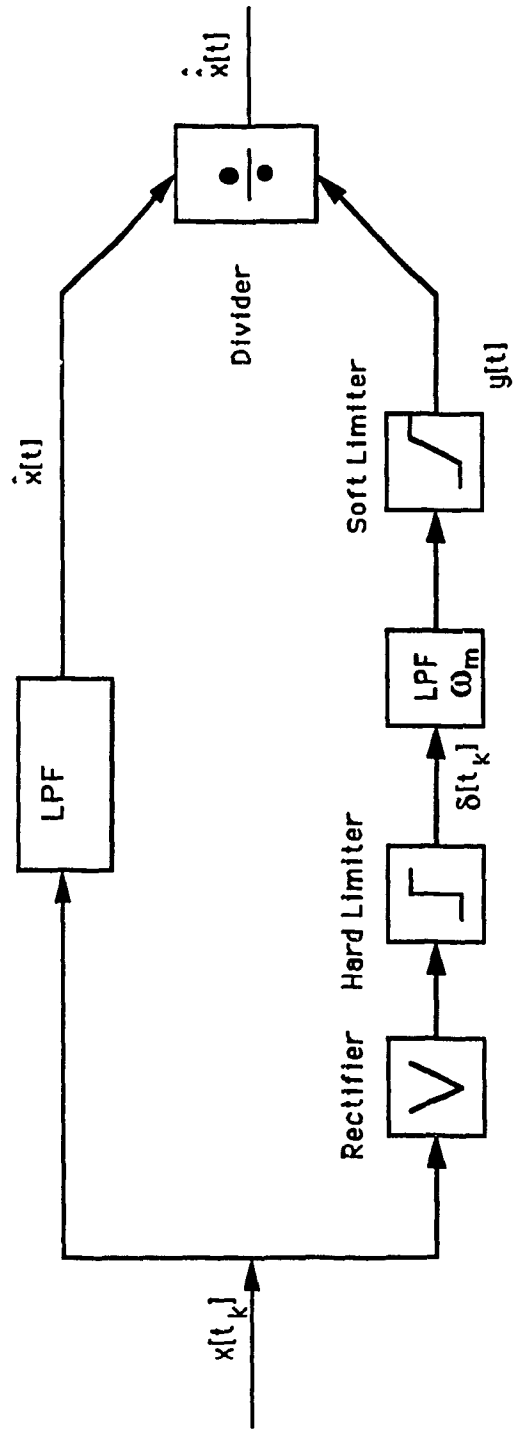


Fig. 2.4: Block diagram for the reconstruction of $\hat{x}(t)$, (Plotkin et al.,

1984)

It consists of a rectifier, a hard limiter and a soft limiter. By inputting $y(t)$ and $\hat{x}(t)$ into a divider, $\hat{x}(t)$ can be obtained. Further details considering the design of the various components can be found in Plotkin and coworkers (1984).

The efficiency of this amplitude modulation technique depends on the deviation of the sample points $\{t_k\}$ from their synchronous positions $\{k\Delta t\}$. They have shown that an increase in sampling time deviations from their synchronous positions decreases the efficiency of the method. However these deviations should not exceed $\pm\Delta t/2$.

2.1.3 Reconstruction Procedure Based on Conversion Method

Yen's (1956) reconstruction procedure uses special composing functions in the Fourier series expansion (refer to Equation 2.4); these are difficult to realize. To overcome this problem different methods have been suggested and one of the methods utilizes the sinc function. This method is developed by Dunlop and Phillips (1974). During the reconstruction procedure, nonuniform samples are converted into uniform samples based on the impulse response of a filter and this approach is named as the conversion method. The conversion method is otherwise called as direct method, because nonuniform samples are first used to reconstruct a set of uniform samples and these samples are then used for reconstruction of the signal itself.

Consider a signal $f(t)$, band-limited to W Hz. It can be recovered from its amplitude samples which are spaced at intervals $1/2W$ sec. or less. Then the relation can be expressed as:

$$f(t) = \sum_{n=-\infty}^{\infty} A(n) \frac{\sin\left\{2\pi W\left(t - \frac{n}{2W}\right)\right\}}{2\pi W\left(t - \frac{n}{2W}\right)} \quad (2.39)$$

where $A(1), A(2), \dots A(n)$ are the values of the samples. Equation (2.39) shows that the signal $f(t)$ can be recovered from its samples by multiplying each sample by a general sinc function and summing these products over all time.

It is evident from Equation (2.39) that the original function $f(t)$ can be obtained completely from the uniform samples $A(n)$ taken at time $t = n/2W$. However if the samples are not taken at equal intervals of time, then the nonuniform samples occur. The knowledge of these nonuniform samples should be sufficient to calculate the uniform samples $A(n)$. Let $b(m)$ represent a sample at time τ_m . These samples would then enable the samples $A(n)$ to be obtained from the following expression:

$$b(m) = \sum_{n=-\infty}^{\infty} A(n) \frac{\sin\left\{2\pi W\left(\tau_m - \frac{n}{2W}\right)\right\}}{2\pi W\left(\tau_m - \frac{n}{2W}\right)} \quad (2.40)$$

All the $A(n)$ values then would determine $f(t)$ using Equation (2.39).

The right hand side of Equations (2.39 and 2.40) are infinite series. $A(n)$ values thus persists for all time and this must be included in the expression to find $f(t)$ in Equation (2.39). In order to render a feasible calculation it is necessary to limit the number of simultaneous equations. Consider a region of time τ_m and suppose $f(t)$ has to be determined at this region of time then $A(n)$ values had to be determined first using the nonuniform samples $b(m)$. A finite number of samples $A(n)$ in τ_m region determines $f(t)$. This can be easily implemented by truncating " $\sin \omega t / \omega t$ " and assuming zero after a finite time. The error is well pronounced if the number of equations is small.

If the infinite series on the right hand side of the Equation (2.40) is truncated

with a finite number say for example five, then it can be reconstructed as:

$$b(m) = \sum_{n=1}^5 A(n) \frac{\sin\left\{2\pi W\left(\tau_m - \frac{n}{2W}\right)\right\}}{2\pi W\left(\tau_m - \frac{n}{2W}\right)} \quad (2.41)$$

There are two kinds of errors arising due to the practical implementation of this scheme. The first kind of error is the truncation error and the second kind of error arises due to the ill-conditioning of the matrix that may arise during the conversion. When the nonuniform samples are converted into uniform samples, the inverse matrix may take a value zero and create ill-conditioning. Hence a high degree of precision is necessary to avoid the occurrence of ill-conditioning. These errors limit the practical implementation of the above method.

2.1.4 Iterative Adaptive Method

Marvasti and Analoui (1989) derived an algorithm extending the work of Wiley(1977). This method uses an iterative algorithm to reconstruct a band-limited signal from unequally spaced samples. The recovered uniform samples of the current iteration are used for simulating uniform samples in next iteration and therefore called iterative adaptive method. The procedure is also applied for other nonuniform sampling like, natural samples and sampled and held version.

Consider a source function $f_s(t)$ as:

$$f_s(t) = \sum_i f(t_i) \delta(t - t_i) \quad (2.42)$$

where $f(t_i)$ is the value of the unequally spaced samples at $\{t_i\}$. Then the following iterative algorithm is implemented such that the original band-limited finite energy signal $f(t)$ is recovered from its n th iteration value.

$$f(t) = \lim_{n \rightarrow \infty} f_n(t) \quad (2.43)$$

where Lt is the limit of number of iterations and when it tends to ∞ , the recovered signal lies very close to the original signal, $f(t)$. The n th iterative value $f_n(t)$ can be related with that of $(n + 1)$ iteration as follows:

$$f_{n+1}(t) = \lambda P_1 S_1 f(t) + (P_1 - \lambda P_1 S_1) f_n(t) \quad (2.44)$$

The value of λ is properly determined depending upon the constant values k_1 and k_2 and defined as:

$$\lambda = \frac{k_1}{k_2} \quad (2.45)$$

The value of λ is chosen based on the range of convergence satisfying some criteria. These criteria are obtained from experimental results and can be inferred from Marvasti and Analoui (1989). P_1 and S_1 are operators for band-limiting and ideal nonuniform sampling respectively. $P_1 S_1 f(t)$ in Equation (2.44) is the nonuniform sample output from a low pass filter. For example, the 1st and 2nd iteration functions are obtained as follows:

$$\begin{aligned} f_1(t) &= \frac{k_1}{k_2} P_1 S_1 f(t) \\ f_2(t) &= \frac{k_1}{k_2} \left(P_1 S_1 f(t) - \frac{k_1}{k_2} P_1^2 S_1^2 f(t) \right) + \frac{k_1}{k_2} (P_1 S_1 f(t)) \end{aligned} \quad (2.46)$$

The Mean Squared Error (MSE) is calculated during each iteration and been used as the index of convergence. A significant reduction in error can be obtained only when an appropriate value for λ in Equation (2.45) is chosen. The selected value of λ influences the convergence criterion of the iterative process.

Equation (2.44) holds good only for a small range of deviation of nonuniform sample points from their synchronous positions. Also from Equation (2.45) it is clear that the constant factor, λ , has to be properly chosen in order to reduce the MSE level. In otherwords, proper attention is needed in selecting the value of real positive

constants namely k_1 and k_2 . However, it is obvious that the method does not involve too much computational complexity and also practically easy to implement. Moreover, the present study as well, as this method, implements the iterative scheme using sinc functions. Hence, various interesting simulations are also performed by using MA method and the results compared with that of the present study.

2.1.5 Nonuniform Sampling for Sequences Using Multirate Signal Processing

Multirate digital signal processing is basically concerned with problems in which more than one sampling rate is required, and it is especially an important criterion in digital transmission systems where data are transmitted at various sampling rates. The multirate sampling can occur in the form of decimation or interpolation of a discrete sequence; the process of lowering the sampling rate is called decimation and the process of raising the sampling rate is called an interpolation. Thus multirate sampling can be analogous to the occurrence of "nonuniform sampling".

The derivative sampling theorem and nonuniform sampling theorem are given a new lucid interpretation in the work of Papoulis (1977 a) where a unified framework is formulated in terms of linear filtering operation prior to sampling. Brown (1981) reinterpreted the work of Papoulis and showed that reconstruction is possible from its "generalized samples".

Recently, the principle of multirate signal processing has been applied by Valdhyanadhan and Llu (1988 a). Further underlying steps of this technique is also discussed in Valdhyanadhan (1988 b). A discrete version of a band-limited signal $|\omega| < 2\pi/3$ is considered for illustrative purpose. The Fourier transform of this

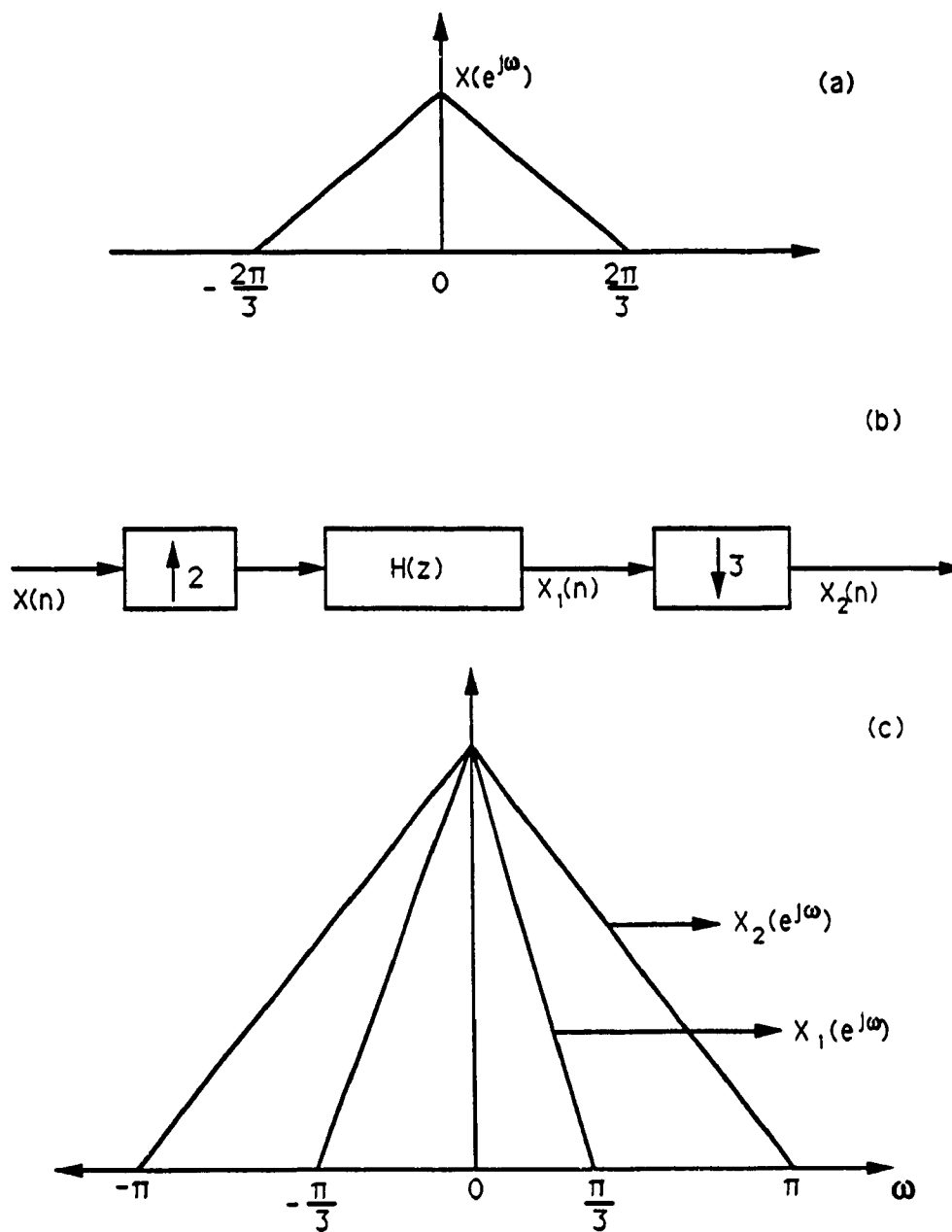


Fig. 2.5: A typical case for data-rate reduction, (Vaidhyadnan and Liu, 1988)

sequence is shown in Fig. 2.5 (a) and the steps involved in reconstructing $x(n)$ are shown in Fig. 2.5 (b). First, the signal rate is increased by a factor of 2 and this can be easily implemented by inserting a zero valued sample between every two adjacent samples of $x(n)$. It is then filtered to ensure that the image created by this zero insertion is eliminated. The resultant of this operation is $x_1(n)$ and it is further decimated by a factor of 3 without causing aliasing. The Fourier transforms as a result of the first and second operations are shown in Fig. 2.5 (c) respectively as $X_1(e^{j\omega})$ and $X_2(e^{j\omega})$. The Fourier spectrum of $x_2(n)$ is same as that of $X(e^{j\omega})$ except that it is stretched by a factor of 3/2 due to data-reduction.

The above process is called "data-rate" reduction technique and it can not only be performed this way but also achieved by dropping one out of every three samples of $x(n)$ which is stated by Valdhyanadhan and Liu (1988 a) as:

"Let $x(n)$ be a sequence band-limited to $|\omega| < (L/M)\pi$ where L and M are integers and $L \leq M$ and considering that time axis is divided into intervals of M , it ought to be able to retain L out of M samples in each of these intervals and discard the rest".

The following procedure is implemented to accomplish the result using a polyphase filter bank framework for the same example (Fig. 2.5). The selected design values are $M=3$ and $L=2$. They considered a real sequence $x(n)$ of finite length. Due to this finite length, $X(e^{j\omega})$ the Fourier transform of $x(n)$ is band-limited to $|\omega| < 2\pi/3$. A linear phase Low Pass Filter (LPF) and a linear phase Finite Impulse Response (FIR) filter are used during the reconstruction. By the suggested technique they proved that the Fourier transform of the reconstructed sequence, that is $\hat{X}(e^{j\omega})$, lies very close to the original Fourier spectrum $X(e^{j\omega})$. However it is necessary to pay attention in designing filters to reconstruct $\hat{X}(e^{j\omega})$ accurately.

2.2 JUSTIFICATIONS OF THE PRESENT STUDY

It is evident from the existing literature that the main disadvantage of the classical method is that a set of special composing functions is necessary for signal reconstruction. In other words, a new special composing function has to be constructed for every possible pattern of unequally spaced samples. For example, the reconstruction procedure considered by Yen (1956) uses interpolation technique and it is evident that this method incorporates multiplication of two sinc functions. Secondly, most of the existing methods do not pay much attention for larger deviation of samples from their synchronous positions.

The present study is mainly focussed to overcome the above two disadvantages. As a part of the current research a simulation methodology is presented and discussed for the signal reconstruction from unequally spaced samples using iterative technique. The study of Plotkin and Swamy (1987) is used as the basis for this thesis. Thus preliminary simulations have been carried out with the same input parameters as those of Plotkin and Swamy (1987).

The present algorithm is also extended for larger deviations of the sampling instants $\{t_k\}$ from their synchronous positions. It is proved that this deviation could exceed the Nyquist space given by π / ω_m up to 150 percent. Signals are reconstructed for various subinterval lengths and the calculated errors are found to decrease with increasing subinterval length.

Secondly, the present iterative procedure is applied to random processes. Random uniform and Gaussian distributions are taken as the test signals under analysis. By proceeding one step further, the proposed procedure is also treated for various Signal to Noise Ratio's (SNR) by considering the deterministic sinusoidal signal in the

presence of a random noise. In all cases, SNR's typically representing -10 db., 0 db., and +10 db., are considered and errors are calculated and compared. Since the generated random numbers vary from trial to trial, their statistical functions namely mean and standard deviation, are also studied.

In the literature, many innovative techniques have been proposed for signal reconstruction and each technique has its own limitations. It is common to use stability as an index of the performance of the system developed. Sankur and Gerhardt (1973) defined stability as: "the insensitiveness for the sample migration". Present study also analyzes the stability criterion based on Sankur and Gerhardt's (1973) approach.

The proposed methodology uses iterative techniques to recover signals from unequally spaced data. As mentioned in the previous section, Marvasti and Analoul (1989) also use an iterative method for reconstructing a band-limited signal. To evaluate the efficiency and establish the superiority of the proposed method, considerable amount of effort has been made in simulating the various cases discussed above. From this study it is clear that the present procedure is not only better in mean squared error performance, but also it is proved that the current algorithm works for larger deviations of samples in comparison to the method of Marvasti and Analoul (1989).

CHAPTER 3

SIMULATION METHODOLOGY

In the previous chapter various procedures were reviewed for reconstructing a band-limited signal from unequally spaced samples. Although the existing techniques can be applied for various interesting problems, there is still an urgent need for a method of reconstructing a band-limited signal, when the samples deviate by a larger range from their uniform samples. The purpose of this chapter is to present a simulation algorithm which is developed as a part of this current research. First section of this chapter groups the necessary equations for the proposed procedure, and a partitioning scheme for the iterative procedure is presented in the second section.

3.1 GOVERNING EQUATIONS

This section brings out the system of equations necessary for the reconstruction procedure. As discussed in the previous chapter, the present reconstruction methodology for a band-limited signal is basically an extension of the work of Plotkin and Swamy (1987). A signal with unequally spaced instants $\{t_k\}$ can be represented as follows:

$$x(t) = \sum_{k=-\infty}^{\infty} x(t_k) \text{sinc} \omega_m(t - t_k) \quad (3.1)$$

where $x(t)$ is a signal band-limited to $|\omega| \leq \omega_m$ and it has been reconstructed from its sample values $x(t_k)$. When $t_k = k\Delta t$, Equation (3.1) represents uniform sampling theorem. To reconstruct the equally spaced samples, $x(k\Delta t)$, a system of $N + 1$ algebraic equations are necessary and it can be written as:

$$x(t_n) = \sum_{k=0}^N x(k\Delta t) \text{sinc} \omega_m(t_n - k\Delta t) \quad (3.2)$$

where $\{t_n\}$ is the deviation of sampling point from the synchronous position represented with its value $x(t_n)$ in the observation interval $(0, T)$ where

$$T = (N+1)\Delta t \quad (3.3)$$

$$\Delta t = \frac{\pi}{\omega_m} \quad (3.4)$$

The uniformly spaced samples can be evaluated from their unequally spaced counterparts, $x(t_n)$ in Equation (3.2) based on the principal of conversion (Dunlop and Phillips, 1974). Having known the amplitude of unequally spaced samples, the uniform samples can be computed, and then further used to reconstruct the signal using Shannon's theorem:

$$\hat{x}(t) = \sum_{k=0}^N \hat{x}(k\Delta t) \text{sinc} \omega_m(t - k\Delta t) \quad (3.5)$$

Assume that $x(t_n)$ in Equation (3.2) are known. This would enable us to estimate the uniform samples; let them be denoted by $\hat{x}(k\Delta t)$. The newly calculated samples are called as "estimated samples" and they can be used in Equation (3.5) to reconstruct $\hat{x}(t)$. To obtain $\hat{x}(k\Delta t)$, it is necessary to process an entire data-block of unequally spaced samples. Therefore Equation (3.2) becomes:

$$\begin{aligned} x(t_0) &= \sum_{k=0}^N \hat{x}(k\Delta t) \text{sinc} \omega_m(t_0 - k\Delta t) \\ x(t_1) &= \sum_{k=0}^N \hat{x}(k\Delta t) \text{sinc} \omega_m(t_1 - k\Delta t) \end{aligned}$$

and so on

$$x(t_N) = \sum_{k=0}^N \hat{x}(k\Delta t) \text{sinc} \omega_m(t_N - k\Delta t) \quad (3.6)$$

To obtain the uniform samples, the above set of equations are transformed into the matrix form:

$$\mathbf{C} = \mathbf{A} \mathbf{B} \quad (3.7)$$

where:

$$\mathbf{C} = \begin{bmatrix} x(t_0) \\ x(t_1) \\ \vdots \\ x(t_N) \end{bmatrix}$$

$$\mathbf{A} = \begin{bmatrix} a_{00} & a_{01} & \dots & a_{0N} \\ a_{10} & a_{11} & \dots & a_{1N} \\ \vdots & \vdots & \ddots & \vdots \\ \vdots & \vdots & \vdots & \vdots \\ a_{N0} & a_{N1} & \dots & a_{NN} \end{bmatrix}; \quad a_{nk} = \text{sinc } \omega_m(t_n - k \Delta t) \quad (3.8)$$

n and k represents row and column respectively,

and

$$\mathbf{B} = \begin{bmatrix} x(0\Delta t) \\ x(1\Delta t) \\ \vdots \\ x(N\Delta t) \end{bmatrix} \quad (3.9)$$

From Equation (3.7), \mathbf{B} can be computed as:

$$\mathbf{B} = \mathbf{A}^{-1} \mathbf{C} \quad (3.10)$$

where \mathbf{A}^{-1} is the inverse matrix. If the coefficients of matrix \mathbf{A} having $(N+1)*(N+1)$ elements turn out to be zero, then the determinant value of the inverted matrix will be influenced and hence most of the information about the restored matrix will be lost. It is clear that the inverted matrix needs high accuracy during its computation even when the coefficients have a very small value. If this is

not so, the determinant value of the matrix A may become zero and then ill-conditioning may occur. To avoid or minimize the problem of ill-conditioning, a large size of the data-block (N) is reduced by short subinterval lengths. For example, by considering a subinterval length of 3, the coefficients of the matrices in Equation (3.8) has their values as follows:

$$\begin{aligned} C &= \begin{bmatrix} x(t_0) \\ x(t_1) \\ x(t_2) \end{bmatrix} \\ A &= \begin{bmatrix} a_{00} & a_{01} & a_{02} \\ a_{10} & a_{11} & a_{12} \\ a_{20} & a_{21} & a_{22} \end{bmatrix} \\ B &= \begin{bmatrix} x'(0\Delta t) \\ x'(1\Delta t) \\ x'(2\Delta t) \end{bmatrix} \end{aligned} \tag{3.11}$$

In the above equation A is reduced to a matrix of dimension 3×3 instead of $(N+1) \times (N+1)$ (Equation 3.8). Even if one of the coefficients in the matrix A is zero, not much information is lost in the process of computing the uniform samples. Considering the matrix dimension as 5×5 , it is observed that the system may be more sensitive to the problem of ill-conditioning, still not much of the information is lost as compared to the matrix dimension of $(N+1) \times (N+1)$. Thus, the sensitivity towards ill-conditioning is minimized.

An important characteristic of the proposed methodology is the complexity index. The complexity index is defined by the number of arithmetic operations, R , needed for reconstructing one sample and can be defined as:

$$R = \frac{2}{3} (M + 1)(M + 2) + (M + 1) \quad (3.12)$$

M is the subinterval length used in the partitioning scheme. For $M \gg 1$

$$R = \frac{2}{3} M^2 \quad (3.13)$$

Thus the arithmetical operation is a characteristic of the proposed simulation methodology. This in turn influences the Central Processor Unit (CPU) time. When $M = N$, the computational complexity is very high. For example, when M is chosen as 3, the simulation takes approximately 27 sec. of CPU time on VAX/8550 under batch mode operation.

In solving Equation (3.10), the resultant matrix is of 3*1 dimension. In this matrix, only the centre sample is considered and the two boundary samples are excluded. For each subinterval of length M, only one uniform sample is evaluated and stored. By repeating the procedure, all uniformly spaced samples are revealed.

3.2 PARTITIONING SCHEME AND ITERATIVE PROCEDURE

Plotkin and Swamy (1987) proposed two data-block partitioning schemes for the recovery of uniform samples, namely, first and second partitioning scheme in which they used the second partitioning scheme. The scheme implements M samples in a subinterval. It has fixed-length overlapping subintervals shifted by the constant factor $q = M - p$, where p is the number of mutual samples belonging to any two adjacent subintervals. They considered a typical case of $M=6$, $p=2$ and $q=M - p=4$. Only 4 samples are stored within every subinterval and two boundary samples are excluded. The boundary samples of each subinterval become regular samples of the preceding and following subintervals. Thus the complexity of the N-

order system is reduced in computation of a 6th order system.

A typical partitioning scheme with $M=3$ and $p=2$ is displayed in Fig. 3.1. The scheme uses fixed-length overlapping subintervals shifted by a constant factor 2. By this partitioning scheme only the centre sample is restored for every subinterval and the boundary samples are excluded. For $M=3$, let the centre sample in a subinterval i be denoted as $\hat{x}_{ic}(k\Delta t)$, for which the boundary samples are $\hat{x}_{ic-1}(k\Delta t)$ and $\hat{x}_{ic+1}(k\Delta t)$. However, the two excluded boundary samples will be restored as centre samples respectively in the preceding and following subintervals, namely, $(i-1)$ and $(i+1)$ interval. Typically, considering the first boundary sample $\hat{x}_{ic-1}(k\Delta t)$, it will be restored as the centre sample in the subinterval $(i-1)$ where the boundary samples are respectively $\hat{x}_{ic-2}(k\Delta t)$ and $\hat{x}_{ic}(k\Delta t)$. Considering the second boundary sample, $\hat{x}_{ic+1}(k\Delta t)$, it will be treated as the centre sample in the subinterval $(i+1)$, and hence the boundary samples of this subinterval will be $\hat{x}_{ic}(k\Delta t)$ and $\hat{x}_{ic+2}(k\Delta t)$. Thus the two boundary samples are restored in the preceding and the following subintervals. However, in the above process, first and the last sample in the sequence can not be restored and hence discarded.

Recalling Equation (3.11), \mathbf{C} corresponds to the values of unequally spaced samples $x(t_0)$, $x(t_1)$ and $x(t_2)$. $\hat{x}(0\Delta t)$, $\hat{x}(1\Delta t)$ and $\hat{x}(2\Delta t)$ are the restored values in the matrix \mathbf{B} . When the partitioning scheme is implemented, only $\hat{x}(1\Delta t)$ is recovered while $\hat{x}(0\Delta t)$ and $\hat{x}(2\Delta t)$ are discarded. For such a scheme a minimum subinterval length is 3 with a overlapping factor of 2. The partitioning scheme is more effective if the subinterval length increases. For example, if 5 samples are considered in a subinterval, then centre sample is only restored and rest of the 4 samples

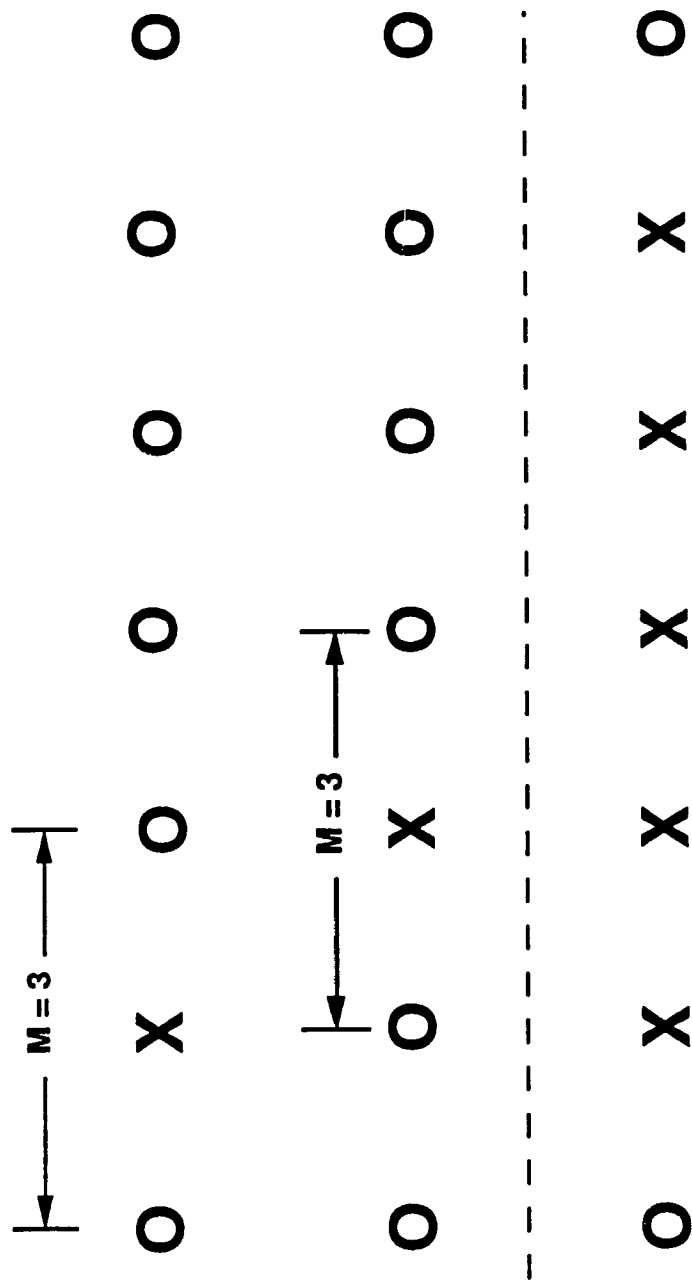


Fig.3.1 Data-Block Partitioning in Restoring Samples

are discarded.

The solved vector $\hat{x}(k\Delta t)$ differs from its original samples, $x(k\Delta t)$. The main source of the reconstruction error is truncation error and it is due to the short length of every subinterval. Therefore an index is defined as follows:

$$\bar{e}_0^2 = \frac{\sum_{k=0}^N \left[x(k\Delta t) - \hat{x}(k\Delta t) \right]^2}{\sum_{k=0}^N x^2(k\Delta t)} \quad (3.14)$$

The above index is named as Mean Squared Error (MSE) and it can be minimized in an effective way during the reconstruction by a repeated processing, called "iterative procedure". This can be further explained in the following paragraph.

With respect to the i -th subinterval:

$$x_i(t) = A_i x_i(k\Delta t) \quad (3.15)$$

Let all such samples, except the first and the last, be combined to form a string of uniformly spaced samples, $\{\hat{x}_c(k\Delta t)\}$ and used for the signal reconstruction as:

$$\hat{x}(t) = \sum_{ic=2}^{N-1} \hat{x}_{ic}(k\Delta t) \text{sinc} \omega_m(t - k\Delta t) \quad (3.16)$$

The above equation can also be written with respect to the i -th subinterval as follows:

$$\hat{x}_i(t) = A_i \hat{x}_i(k\Delta t) \quad (3.17)$$

The newly calculated $\hat{x}_i(t)$ differs from its previous value $x_i(t)$ by a correction term which can be written as follows:

$$\begin{aligned} \Delta_i x(t) &= x_i(t) - \hat{x}_i(t) \\ &= x_i(t) - A_i \hat{x}_i(k\Delta t) \end{aligned} \quad (3.18)$$

By using Equation (3.15) in Equation (3.18)

$$\begin{aligned}\Delta_i x(t) &= A_i x_i(k\Delta t) - A_i \hat{x}_i(k\Delta t) \\ &= A_i [x_i(k\Delta t) - \hat{x}_i(k\Delta t)] \\ &= A_i \Delta_i x(k\Delta t)\end{aligned}\tag{3.19}$$

In the above equation, $\Delta_i x(t)$ depends upon $\Delta_i x(k\Delta t)$. The difference between $x_i(k\Delta t)$ and $\hat{x}_i(k\Delta t)$ diminishes when the restored samples lie closer to the original samples. In other words, MSE (Equation 3.14) will be minimum. Note that the coefficients in the matrix A is factorized only once and used for further iteration which in turn reduces the CPU time.

The estimated $\Delta_i x(k\Delta t)$ is added to the $\hat{x}_i(k\Delta t)$ to obtain $\hat{\hat{x}}_i(k\Delta t)$. This is obtained as a result of implementing the iterative procedure once and hence $\hat{x}_i(k\Delta t)$ are the recovered samples of the "first iteration" whereas $\hat{\hat{x}}_i(k\Delta t)$ are obtained "without implementing iteration". Further, the MSE can be computed by substituting $\hat{\hat{x}}(k\Delta t)$ in Equation (3.14) instead of $\hat{x}(k\Delta t)$. When the iterative procedure is repeated twice, the restored samples, $\hat{\hat{x}}(k\Delta t)$ lie closer to $x(k\Delta t)$ and hence the MSE of the "second iteration" is reduced and the iterative procedure tends to converge. Thus the above mentioned steps emphasise the effect of the iterative procedure by studying the convergence of the MSE levels.

The subinterval length chosen for the partitioning scheme influences the MSE levels. If the subinterval is 3, only the centre sample is restored and the boundary samples are excluded. However if the subinterval is 5, then 4 boundary samples are excluded and the centre sample is restored. Further convergence in MSE can be observed, if the subinterval is chosen 7, 9, 11, etc. Therefore the restored samples,

$\hat{x}(k\Delta t)$ lie more and more close to $x(k\Delta t)$ in Equation (3.14) and the MSE level is reduced; or in other words the truncation error is reduced. Let $x(t)$ be the original signal and $x_N(t)$ be the reconstructed signal due to finite sum of samples, N . Then, the difference between the original and the reconstructed signal can be denoted by $e_N(t)$ and expressed as:

$$e_N(t) = x(t) - x_N(t) \quad (3.20)$$

As the subinterval length is increased, $x_N(t)$ lies closer to $x(t)$ in the above equation. Thus the MSE level is dependent on the selection of finite number of samples in a subinterval and can be avoided by choosing a longer subinterval.

As pointed out earlier, the first and the last samples are not restored during the iterative procedure. In addition, during the first iteration, the two boundary samples namely, second and $N - 1$ samples of the original sequence are also not restored. Hence the number of samples in the sequence is reduced to $N - 4$ at the end of first iteration. Thus the two boundary samples are not restored during each iteration in the original sequence of N samples.

The second kind of error may also arise during the reconstruction procedure, the jitter error. The deviation of the sampling instants are allowed to vary by the jitter parameter (J) in its sampling interval shown in Fig. 3.2. $(k-1)\Delta t$, $k\Delta t$, and $(k+1)\Delta t$ represent the synchronous positions of $(k-1)$, k and $(k+1)$ th samples, and Δt is the average distance between two samples. For $J = 1$, the unequally spaced samples lie within the region of $(-\Delta t/2, +\Delta t/2)$. When $J = 0$, $t_k = k\Delta t$ and therefore the samples are equally spaced and hence lie exactly at $(k-1)\Delta t$, $k\Delta t$ and $(k+1)\Delta t$ as can be seen in the Fig. 3.2. Thus the jitter parameter determines the deviation of the

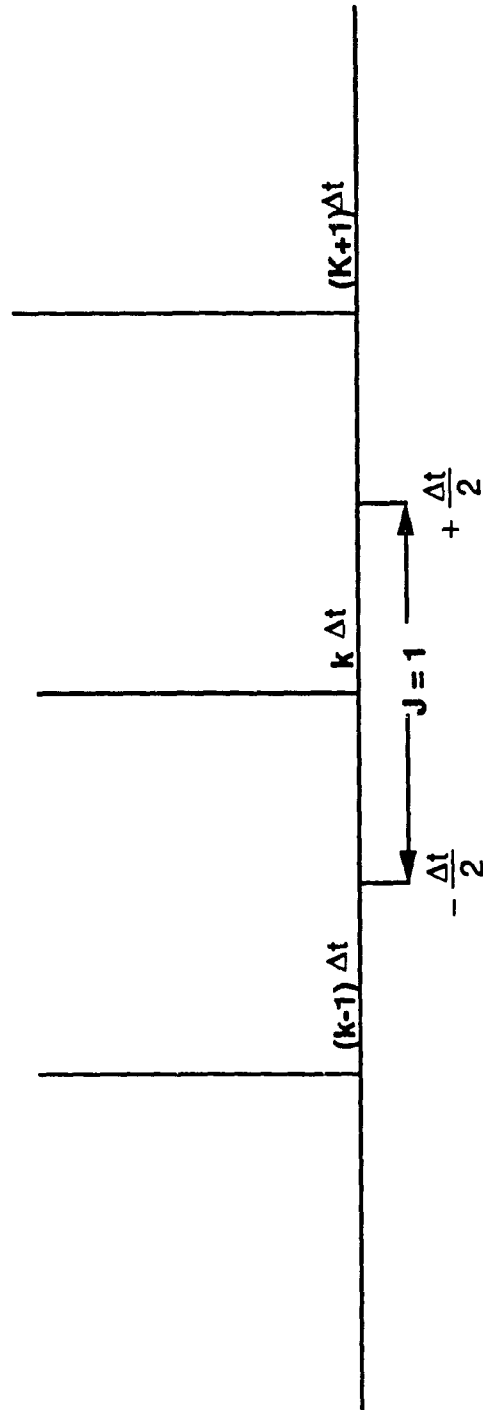


Fig. 3.2 Samples perturbed from their uniform location

unequally spaced samples from their uniform positions. The influence of the jitter parameter is predicted based on the selection of unequally spaced time instants in the simulation procedure. If the deviation of the sampling instants are closer to the synchronous positions $\{k\Delta t\}$, then $x(k\Delta t \pm \Delta_k)$ is closer to $x(k\Delta t)$ and therefore the MSE level computed using Equation (3.14) is reduced.

The inherent details and philosophy of the present simulation methodology is cited along with its mathematical expressions. The principal error, namely the truncation error, that occurs in the simulation procedure is studied using MSE Index. Further, an iterative procedure is suggested and explained to minimize the above error. Small influence of the second kind of error that may occur due to the deviation of sample instants is also discussed.

CHAPTER 4

PRESENT COMPUTER CODE AND SIMULATED RESULTS FOR THE DETERMINISTIC PROCESSES

This chapter presents and discusses the computer code that is developed for the reconstruction of signals. To confirm the simulation results of the developed computer code, the results are compared with those of Plotkin and Swamy (1987) for the same input conditions. In the second section, simulation results are obtained by using sine waves. The simulated results are discussed and compared with a recent iterative adaptive procedure of Further comparisons are also presented for the reconstruction of signals using sum of sine waves. In all the cases, the effect of subinterval length and the variation of the jitter parameter are studied. The calculated MSE is always used as a measure of comparisons for the different methods of signal reconstruction.

4.1 DESCRIPTION OF THE PRESENT COMPUTER CODE

The present computer code is developed using an interactive software tool, MATrix LABoratory abbreviated as MATLAB (Moler et al,1987). MATLAB has extensive applications in solving engineering and mathematical problems in research fields. Typical application includes numerical computation and solving special purpose matrix problems that arise in the discipline of digital signal processing, automatic control and statistics. The sunwork station Graphics Post Processor (GPP) are used for obtaining the device independent MET-files. These metafiles are transformed into image files which are later used to plot on an APPLE laser.

Various steps involved in the present computer code are shown diagrammatically in Fig. 4.1. The variables are initialized first. Secondly, a set of parameters are given as input. They are respectively, the number of samples (N), band-limited frequency (f_m), sampling frequency (f_s), subinterval length (M), Jitter parameter (J), number of iterations ($Iter$) and the number of trials ($Trial$). N determines the number of samples necessary to process the simulation algorithm. f_s is the sampling frequency that determines the sampling time interval of the signal. The number of samples used for the partitioning scheme is determined by M . The extent to which the samples are allowed to migrate in the uniform distribution is established by J .

For example, a particular simulation using deterministic sinusoidal function takes the value of N as 100, f_m and f_s respectively 1100 Hz. and 2400 Hz. The number of samples for the partitioning scheme is chosen as 3. The unequally spaced time instants are distributed uniformly in the range of $(-\Delta t/2, \Delta t/2)$, with J equal to unity (refer Fig. 3.2). This typical simulation takes approximately 34 sec. of CPU time on Vax/8550 under batch mode operation.

With the above mentioned input parameters, the time instants are selected. A statistical model for the unequally spaced samples is developed in the simulation procedure. The unequally spaced sample instants are generated by using PRO-MATLAB random number generator function. The `rand('uniform')` function is used to generate random numbers that are uniformly distributed in the interval (0.0,1.0). The samples are distributed randomly at sampling interval in respective time slot. Having known the sampling instants, it is necessary to generate the input signal. The input signal may be deterministic or random.

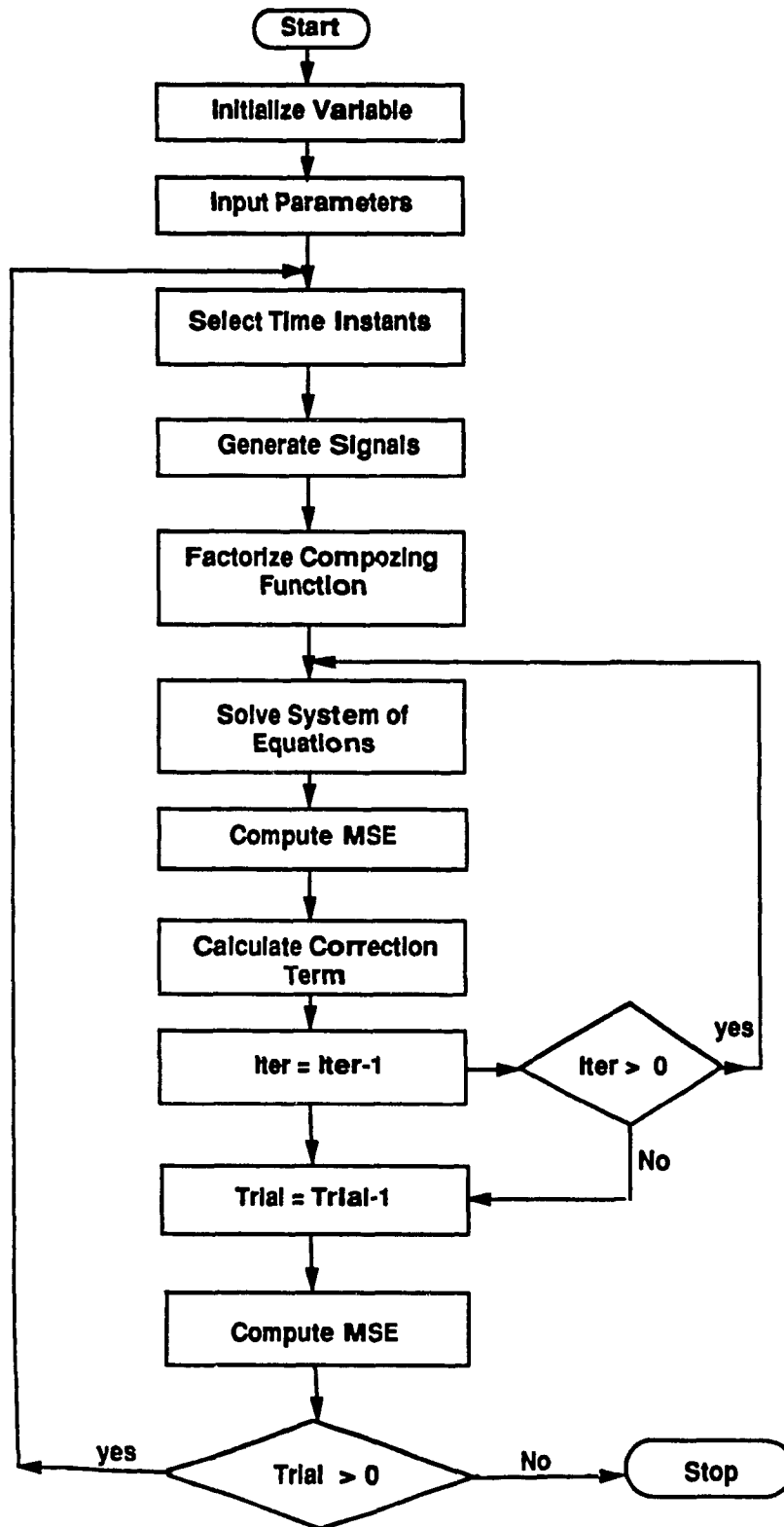


Fig. 4.1: Flow chart of the present computer code

$\text{sinc}\omega_m(t_n - k\Delta t)$ is called the composing function for the sample point $\{t_n\}$ and it possesses different forms for different sampling points. By using Equation (3.8), the coefficients a_{nk} are calculated and stored in a matrix **A**. As discussed in section 3.1, a system of equations are solved using inversion matrix technique (Equation 3.10) and the solution represented by a matrix, **B**. The restored samples in the matrix, **B** are $\hat{x}_c(k\Delta t)$ and differ from $x(k\Delta t)$. The restored samples, $\hat{x}_c(k\Delta t)$ are obtained without implementing the iterative procedure. It can be otherwise called "without iteration". The variation between the restored and the original samples is the main source of the reconstruction error and it can be computed using the Mean Squared Error.

However, to reduce the error level the iterative procedure is used. The restored samples, $\hat{x}_c(k\Delta t)$ are used to reconstruct $x(t)$ as in Equation (3.16). The reconstructed $\hat{x}(t)$ differs from original $x(t)$ and therefore can be denoted as $\hat{x}(t)$. The difference between $x(t)$ and $\hat{x}(t)$ is computed for every subinterval. Let the difference be represented for the l -th subinterval as $\Delta_l x(t)$. Subsequently, $\Delta_l x(t)$ is used to calculate the correction term $\Delta_l x(k\Delta t)$ by using matrix inversion technique (Equation 3.10). The correction term, $\Delta_l x(k\Delta t)$ is added to the previously solved $\hat{x}(k\Delta t)$ to obtain $\hat{x}(k\Delta t)$. This is the result of implementing the iterative procedure once to $\hat{x}(k\Delta t)$ and therefore called first iteration. The restored samples, $\hat{x}(k\Delta T)$ due to the first iteration is substituted instead of $\hat{x}(k\Delta t)$ in Equation (3.14) to obtain the MSE level. During each process the variable Iter is reduced by one and the iterative procedure is terminated based on the number of specified iterations.

The utility function random number generator `rand('uniform')` selects time instants that are different from trial to trial. Therefore the statistical parameters,

namely mean and standard deviation, are calculated. During each cycle the number of Trial is reduced by one and the program terminates depending upon the specified trials. The following paragraph brings a brief description of deterministic and random process used in reconstruction procedure.

In the present study deterministic processes, random processes and deterministic signal in the presence of random noise for various SNR values are considered. A deterministic signal is one that can be represented with instantaneous value as a function of time. This includes all signals whose instantaneous values can be predicted using mathematical equations. It also includes functions that do not have describing equations but can also be represented by graphs. In other words the exact value of a deterministic signal can be predicted at a given time in advance. An example of a deterministic signal is a sine wave. From the viewpoint of design, analysis, testing and operation, it is both necessary and desirable to use sinusoidal signals for predicting system performance. Such signals have well defined properties and are easy to deal with. Hence they will be employed for the reconstruction procedure.

The computer code is also modified for random signals such as noise. A random signal is one whose instantaneous value cannot be predicted exactly at any given time. However, many random signals have certain reasonably well behaved statistical parameters. They are useful in predicting the behaviour of random signals encountered in actual systems. Various statistical functions namely, mean, standard deviation, rms and average value can be determined by statistical analysis.

Two types of random distributions are considered, they are uniform and Gaussian distributions. These two random distributions are obtained by switching the random generators in MATLAB. Note that Gaussian distribution have zero mean and unit variance. The computer code is implemented for the above two random distributions.

A deterministic test signal in the presence of a random noise is also considered for analysis and the Signal to Noise Ratio at the input is defined as:

$$SNR_{IN} = 10 \log_{10} \frac{A_s^2}{2\sigma_n^2} \quad (4.1)$$

A_s represents the amplitude of the deterministic signal and σ_n^2 is the variance of the random noise.

4.2 SIMULATION RESULTS AND DISCUSSION FOR THE DETERMINISTIC PROCESSES

4.2.1 Confirmation of the Present Study

The above discussed computer code is validated by inputting the same parameter as that of Plotkin and Swamy (1987). A sequence of 100 samples at $\{t_k\}$ instants are extracted from a sinusoidal waveform and these instants are taken randomly with uniform density function in the range of $-\Delta t/2$ to $\Delta t/2$ around the corresponding synchronous positions $\{k\Delta t\}$. The average time between any adjacent samples is given as 10^{-4} sec. (10 KHz. sampling rate) and a band-limit frequency of 4.3 KHz is used in the simulation. A subinterval length of 3 is used in the present study; however, 6 samples have been considered by Plotkin and Swamy (1987) for the partitioning scheme.

Fig. 4.2 (a) illustrates the reconstruction of a sinusoidal waveform by using the present computer code and the one proposed by Plotkin and Swamy (1987) without implementing the iterative procedure, whereas Fig. 4.2 (b) compares the results when the iterative procedure is implemented. It can be observed that the restored signal obtained by implementing the iterative procedure lie closer to the original sinusoidal signal. Generally, the agreement between these two studies are quite satisfactory even though variations may be attributed due to the difference in the subintervals used in the two studies.

4.2.2 Reconstruction Using Sine Wave

In this section the reconstructed results using sine waves are discussed. Consider a sequence of 42 samples at $\{t_k\}$ instants which are extracted from a sinusoidal waveform using a random generator. The random generator is a utility function in MATLAB and is used to select $\{t_k\}$ instants. As discussed in Fig. 3.2, the $\{t_k\}$'s are allowed to migrate in uniform distribution depending upon the jitter parameter, J , which is chosen as 0.5 for this case. Therefore the sampling instants are perturbed from their synchronous positions in the region of $(-\Delta t/4, \Delta t/4)$. The sinusoidal waveform is generated for the necessary input parameters. The band-limited frequency, f_m , the sampling frequency, f_s , are respectively chosen as 1100 Hz. and 2400 Hz. The subinterval length, M is chosen as 3. In the present study for every subinterval length only the centre sample is recovered while the boundary samples are excluded. For the above input condition, the solid line in Fig. 4.3 represents the unequally spaced time instants, $\{t_k\}$ and their values $x(t_k)$. These values are used for the signal reconstruction.

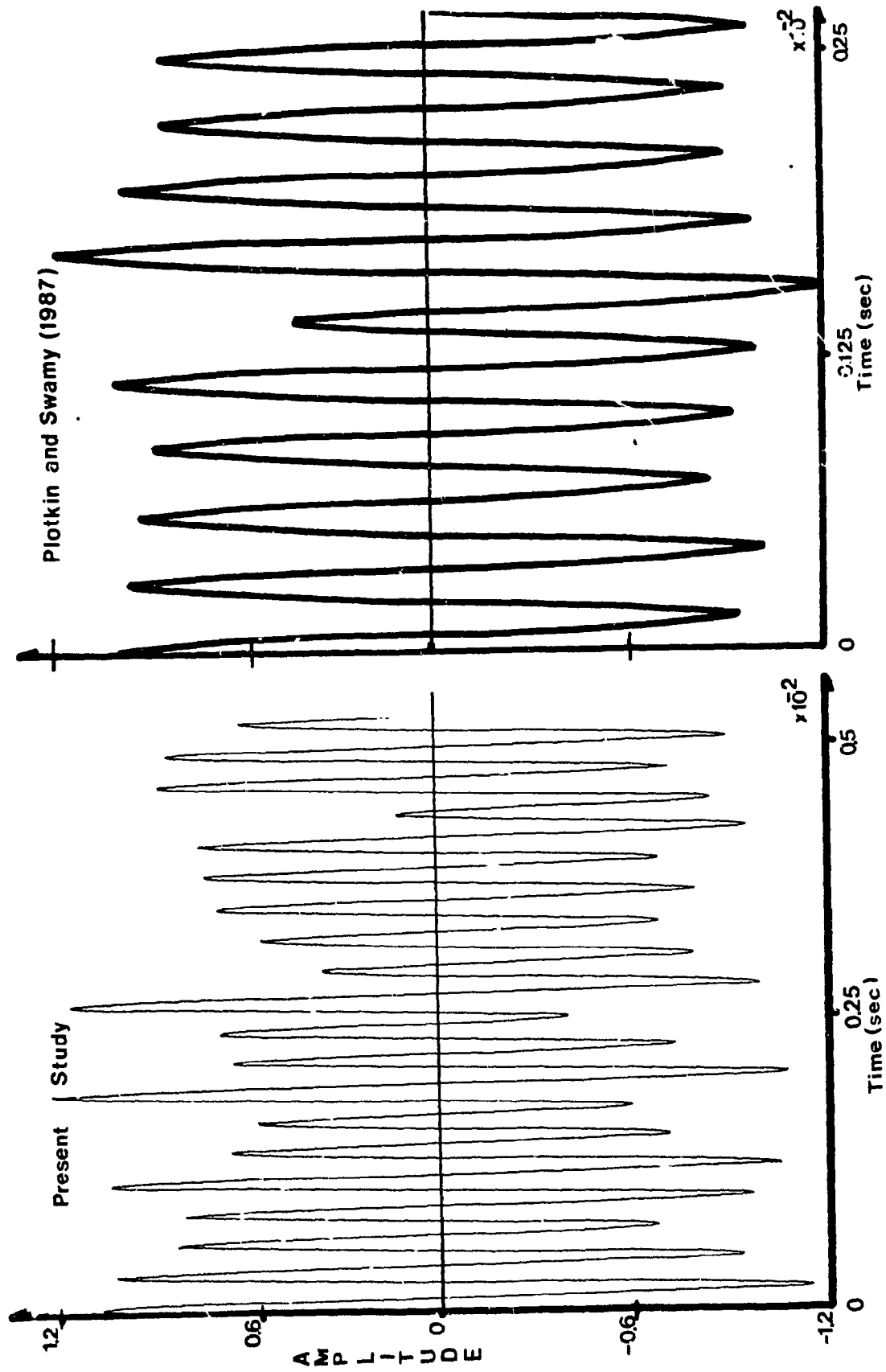


Fig. 4.2(a) Confirmation of the present simulated results for sinusoidal waveform (without iterations).

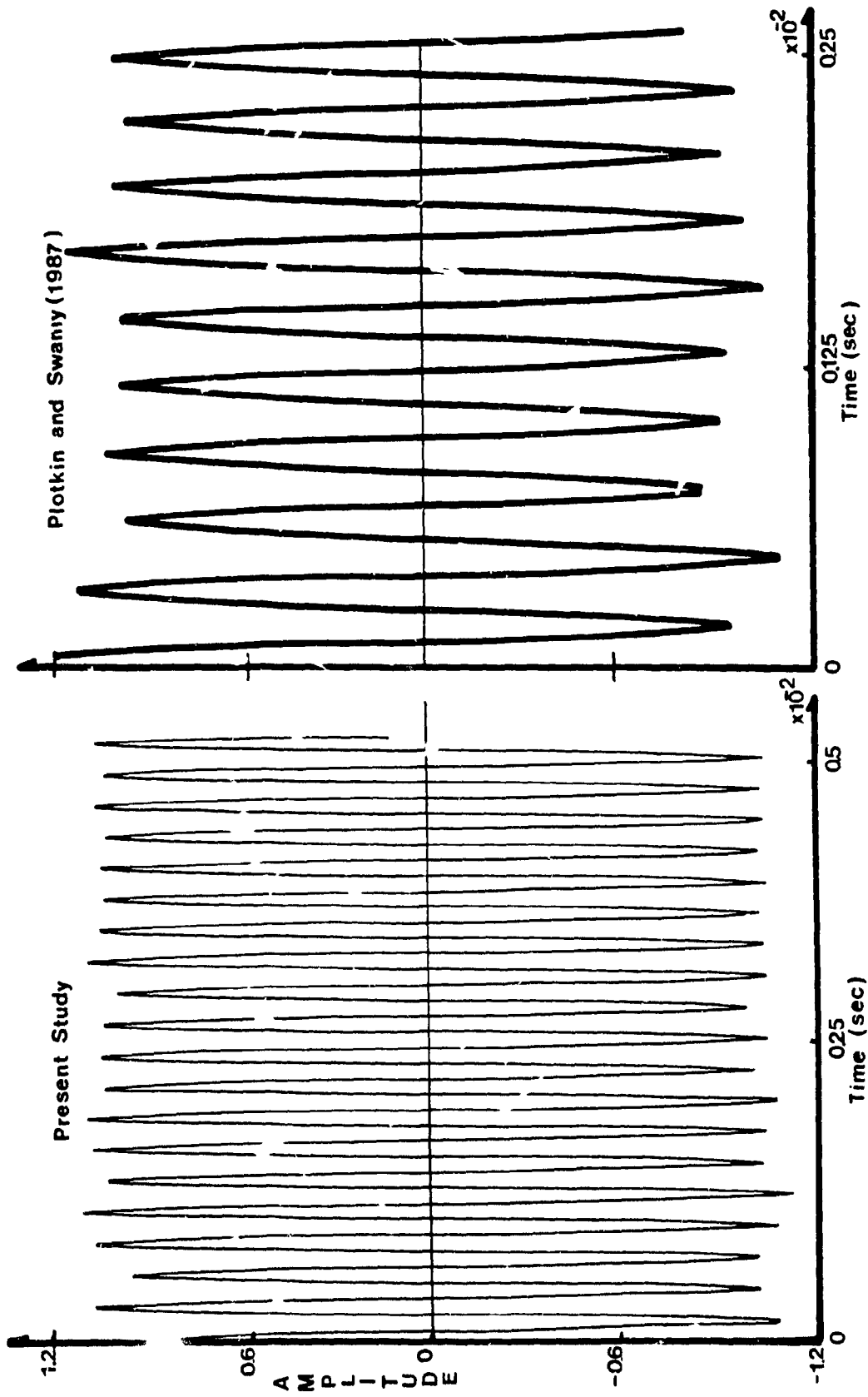


Fig. 4.2(b) Confirmation of the present simulated results for sinusoidal waveform (after two iterations).

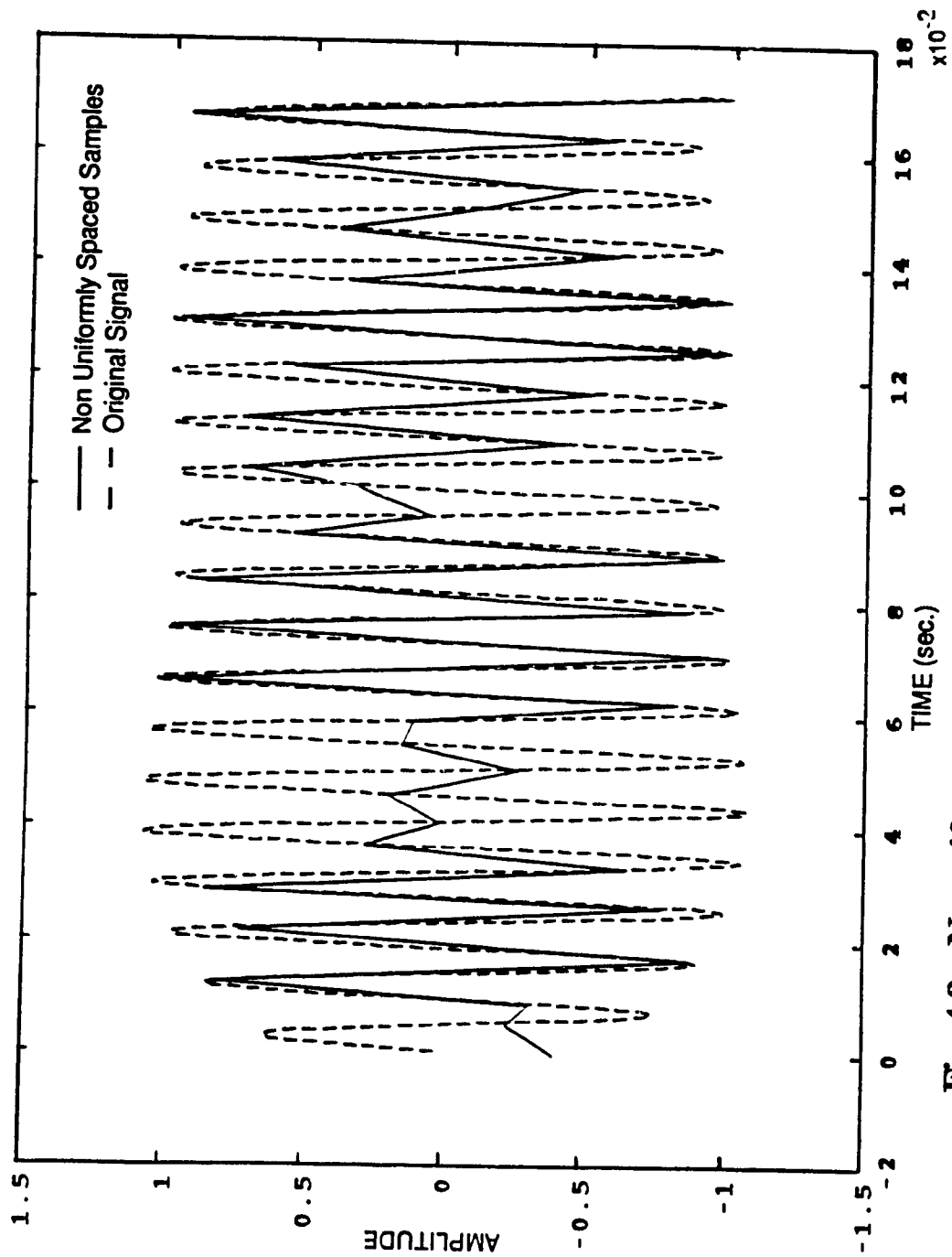


Fig. 4.3: Nonuniform distribution of samples using sinusoidal

waveform ($J=0.5$)

Recalling Equation (3.10):

$$\mathbf{B} = \mathbf{A}^{-1} \mathbf{C} \quad (3.10)$$

The unknown matrix \mathbf{B} in the left hand side of the above equation is calculated by using the known matrices \mathbf{A} and \mathbf{C} . The solved matrix, \mathbf{B} represents the restored samples $\hat{x}_c(k\Delta t)$ and this operation is without implementing the iterative procedure. Therefore $\hat{x}(k\Delta t)$ represents restored samples "without iteration". The restored samples obtained of without iteration are used to reconstruct $\hat{x}(t)$ (Equation 3.16) which in turn differs from original $x(t)$. The difference between $x(t)$ and $\hat{x}(t)$ is used for every subinterval to compute the correction term. The correction term is added to the previously calculated value $\hat{x}(k\Delta t)$. As a result, $\hat{x}(k\Delta t)$ is obtained and it corresponds to the restored samples "after 1 iteration". When the procedure is repeated twice, it represents the restored samples, "after 2 iterations".

Fig. 4.4 (a) shows the status after reconstruction in which the original signal, signal reconstructed without iteration and the reconstructed signal after two iterations are displayed. They are respectively marked by solid, dash and star lines. It is clear that the star line is closer to the solid line. Recall Equation (3.14) used to compute Mean Squared Error (MSE):

$$\bar{e}_0^2 = \frac{\sum_{k=1}^N [x(k\Delta t) - \hat{x}(k\Delta t)]^2}{\sum_{k=1}^N x^2(k\Delta t)} \quad (3.14)$$

In the above Equation, $x(k\Delta t)$ and $\hat{x}(k\Delta t)$ are respectively the original uniform samples and the restored samples without iteration. Then the calculated \bar{e}_0^2 represents the error without iteration. $\hat{\hat{x}}(k\Delta t)$ are the restored samples "after two iterations" and can

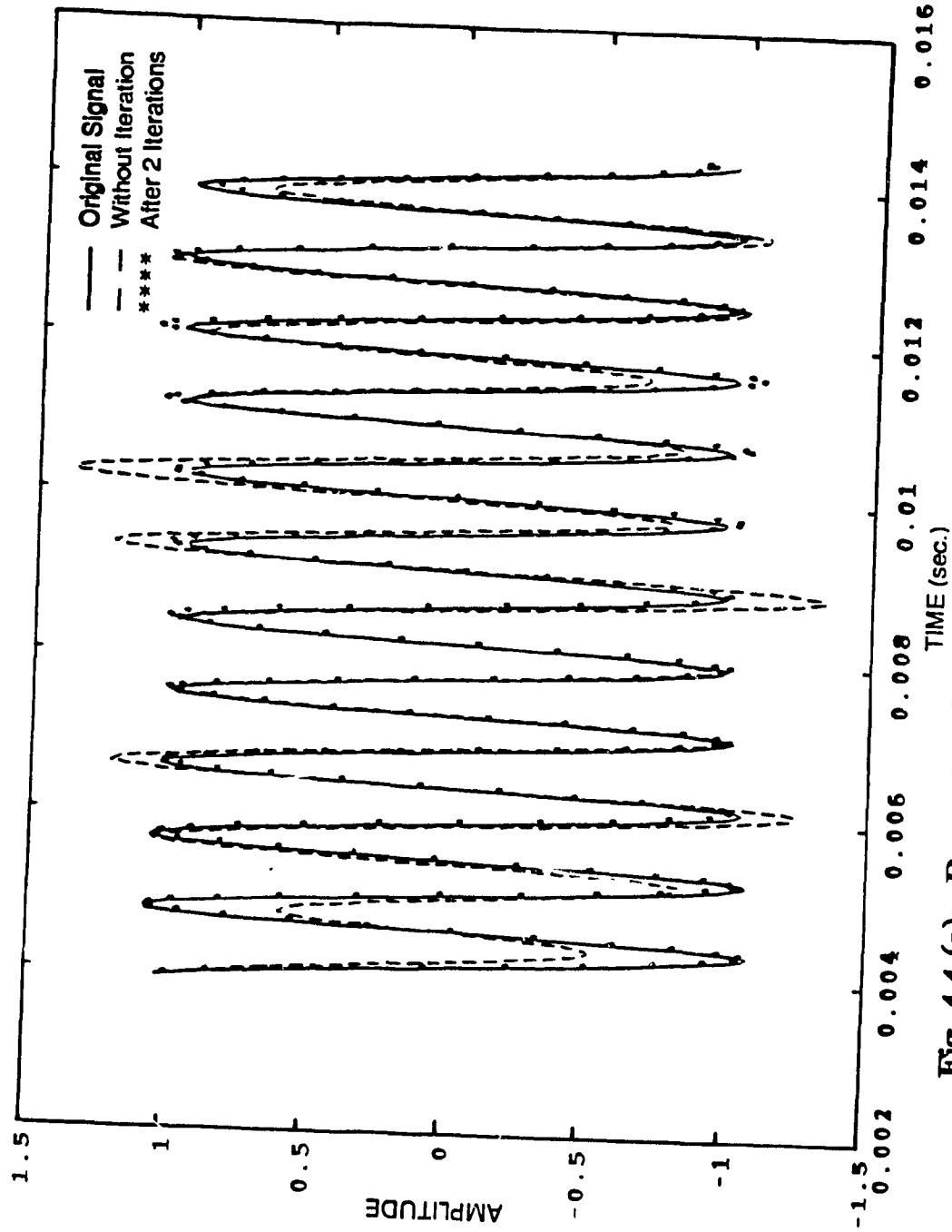


Fig. 4.4 (a): Reconstruction from nonuniformly distributed samples using sine waveform, ($J=0.5, PS$)

be substituted instead of $\hat{x}(k\Delta t)$ in Equation (3.14) and thus MSE can be estimated corresponding to two iterations. From the above Equation it is evident that the MSE value reduces when the restored samples lie very close to the original samples.

For the above reconstruction process the computed MSE are respectively 9.6% and 0.12% for the cases of "without iteration" and "after two iterations". This implies that the deviation of the reconstructed signal is reduced significantly in its second iteration. For the first iteration, $\hat{x}(k\Delta t)$ is obtained by adding $\hat{x}(k\Delta t)$ with $\Delta x(k\Delta t)$. $\Delta x(k\Delta t)$ is the gradient of first difference (first derivative), which is further used in the second iteration. Thus the MSE level is reduced significantly in the second iteration.

The same input conditions are given to the algorithm of Marvasti and Analoui (1989) (-hereafter abbreviated as MA) and compared with the Present Study (-hereafter abbreviated as PS) to evaluate the performance. Only the essential features of MA are discussed here whereas further details can be found in section 2.1.4. The band-limited finite energy signal $x_{k+1}(t)$ can be recovered from its nonuniform samples $x(t)$ as follows:

$$x_{k+1}(t) = \lambda P_1 S_1 x(t) + (1 - \lambda P_1 S_1) x_k(t) \quad (4.2)$$

where $x_{k+1}(t)$ is the signal recovered after $k+1$ iterations. λ is the convergence constant and $P_1 S_1 x(t)$ is the low pass filtered version of the $x(t)$. For example, the following expressions are obtained when k is given values 0 and 1 respectively in the above Equation.

$$x_1(t) = \lambda P_1 S_1 x(t)$$

and

$$x_2(t) = \lambda P_1 S_1 x(t) + x_1(t) - \lambda P_1 S_1 x_1(t) \quad (4.3)$$

The above $x_1(t)$ and $x_2(t)$ are the signals recovered after one and two iterations, respectively. When k is as 9 in Equation (4.2), the recovered signal $x_{10}(t)$ corresponds to the simulated result after 10 iterations.

The simulation results based on MA algorithm are shown in Fig. 4.4 (b). The three curves are respectively the original signal, signal reconstructed after one iteration and ten iterations. Even though the original signal is the same as before, it is included in the figure for the sake of comparison. It is evident from the figure that the signal is reconstructed poorly even after 10 iterations. Consider a typical sampling time 0.01 sec. In X axis, the dashed line deviates much from the solid line. However, the star line is also not close to the solid line. With the same input conditions in the PS, the MSE is 0.12% after two iterations whereas in MA the error is reduced to only 10% after 10 iterations. Not much reduction in MSE is evident even after 10 iterations and that is why it is decided to present the simulation results with 10 iterations.

The instant $\{t_k\}$ instant is now allowed to migrate in the uniform distribution for a longer interval from its synchronous position such that it ranges from $-\Delta t/2$ to $\Delta t/2$ (Jitter parameter = 1.0). Fig. 4.5 shows two curves namely, unequally spaced samples and the original signal. Consider a sequence of 42 samples with f_m and f_s as 1100 Hz. and 2400 Hz. respectively. The unequally spaced data are used to reconstruct the original signal. It can be observed that the solid line is much distorted in comparison to Fig. 4.3 due to the increase in J from 0.5 to 1.0.

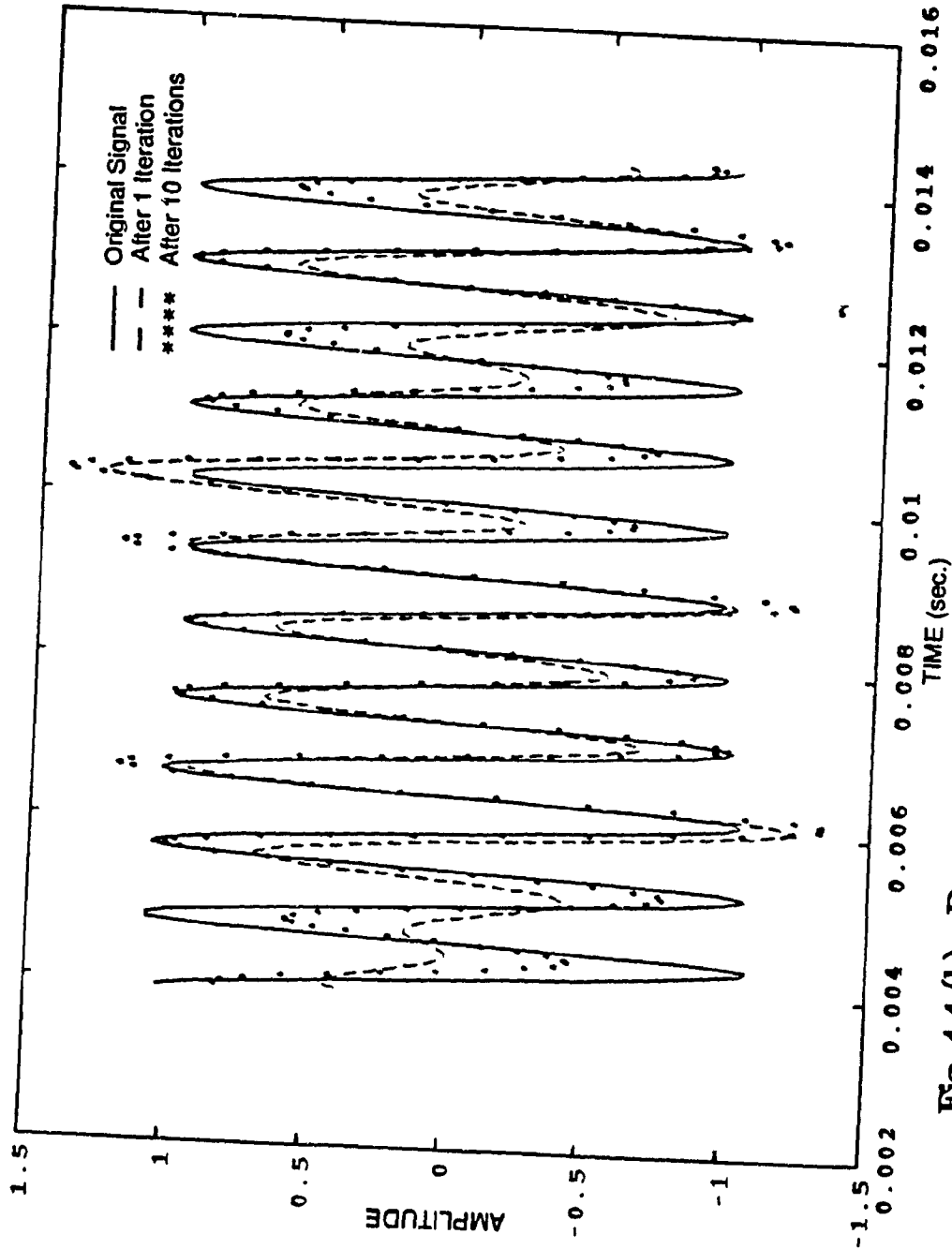


Fig. 4.4 (b): Reconstruction from nonuniformly distributed samples
using sine waveform, ($J=0.5, MA$)

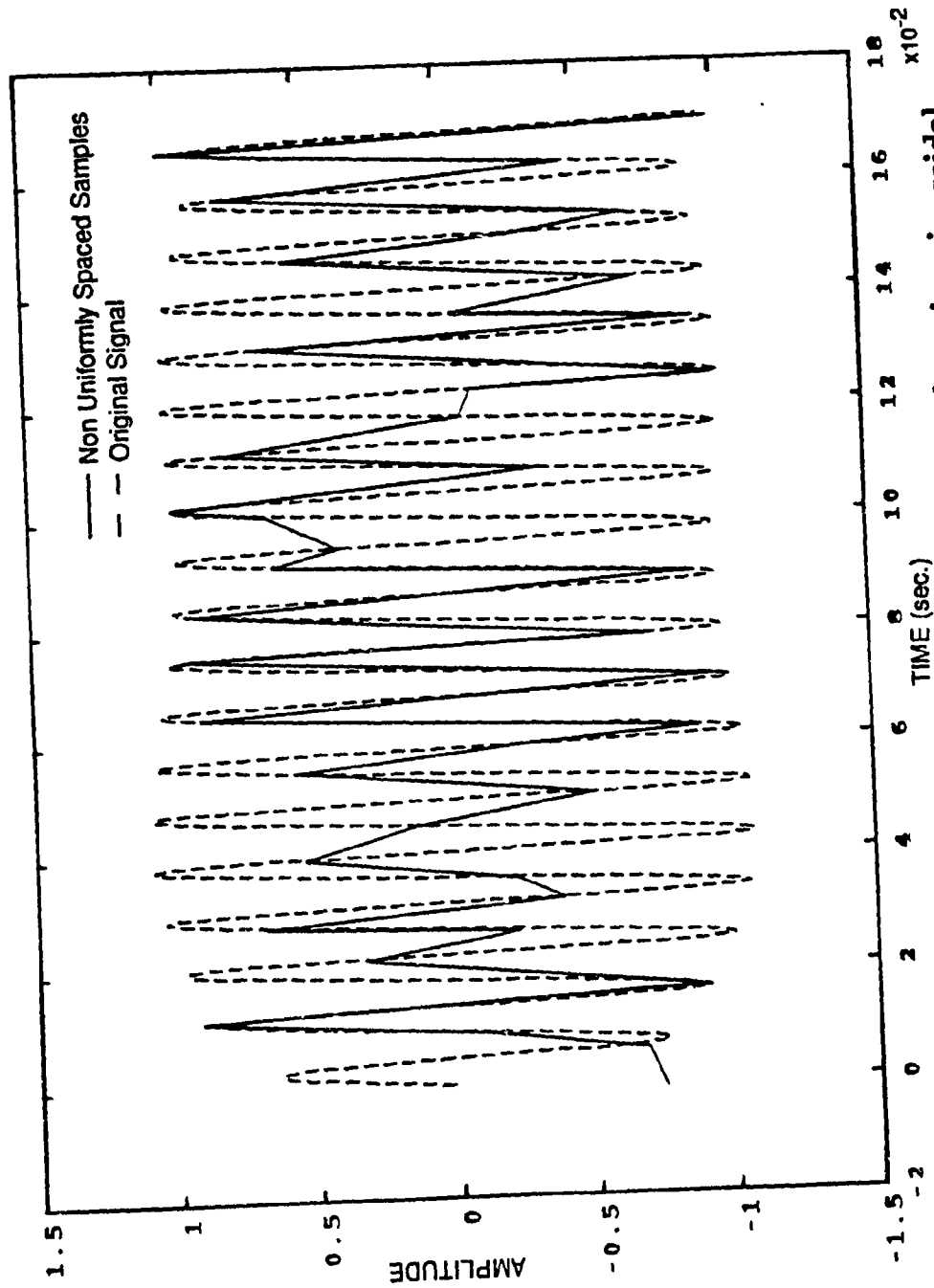


Fig. 4.5: Nonuniform distribution of samples using sinusoidal waveform ($J=1.0$)

Fig. 4.6 (a) shows the reconstructed signal using PS in same format as that of Fig. 4.4 (a). It is evident from the figure that the reconstructed signal without iteration lies farther away from that of the original signal, whereas the reconstructed signal after two iterations lies very close to the original signal. Thus it is seen that the iterative procedure can be very effective in signal reconstruction. The MSE are estimated as 48.3% for without iteration and 0.71% after two iterations for PS. Therefore, the third curve lies very close to the first curve.

Fig. 4.6 (b) illustrates the simulation results obtained for the same input parameters for the MA method. Two curves, namely the original signal and the reconstructed signal after 10 iterations, are shown in the figure. It can be observed that the dashed line lies farther away from the solid line with an estimated MSE of 52%. Since there is no significant reduction in the error, the iterative procedure is terminated and the results plotted.

From the above discussion it is clear that the MSE is reduced to only 52% even after 10 iterations when the MA method is employed. On the otherhand, the reconstruction using the PS reduces the MSE level significantly to 0.71% within 2 iterations. Thus the method of MA is not feasible for larger deviation of samples and therefore the analysis is restricted to the PS only.

To show the superiority of the PS, J is further increased to 2.75 and therefore $\{t_k\}$ instants can deviate in a larger range of $(-1.375\Delta t/1.375\Delta t)$. A sequence of 100 samples are extracted at $\{t_k\}$ instants from the sinusoidal waveform. These $\{t_k\}$ instants are taken randomly with uniform density functions for the above range around

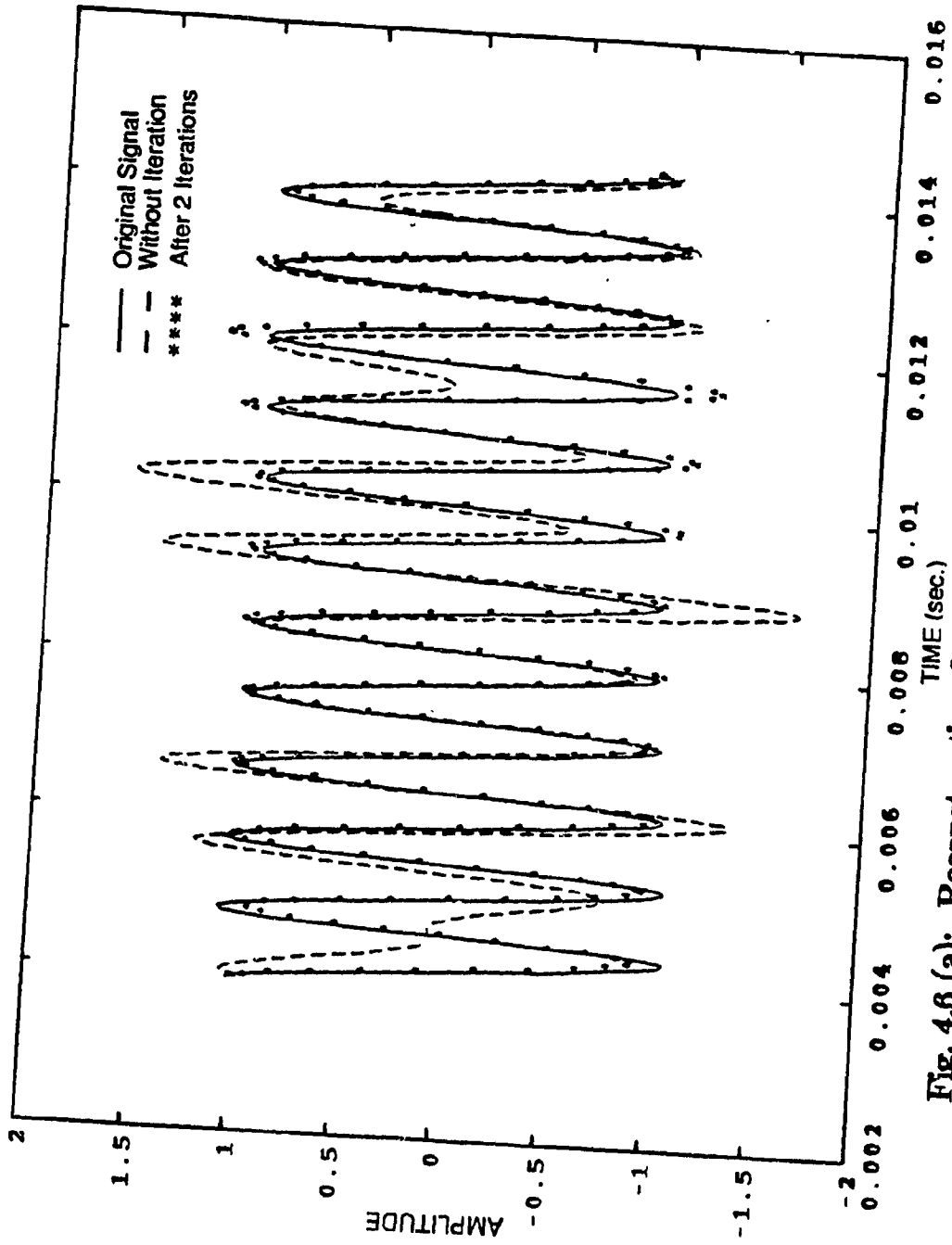


Fig. 4.6 (a): Reconstruction from nonuniformly distributed samples
using sine waveform, ($J = 1.0, PS$)

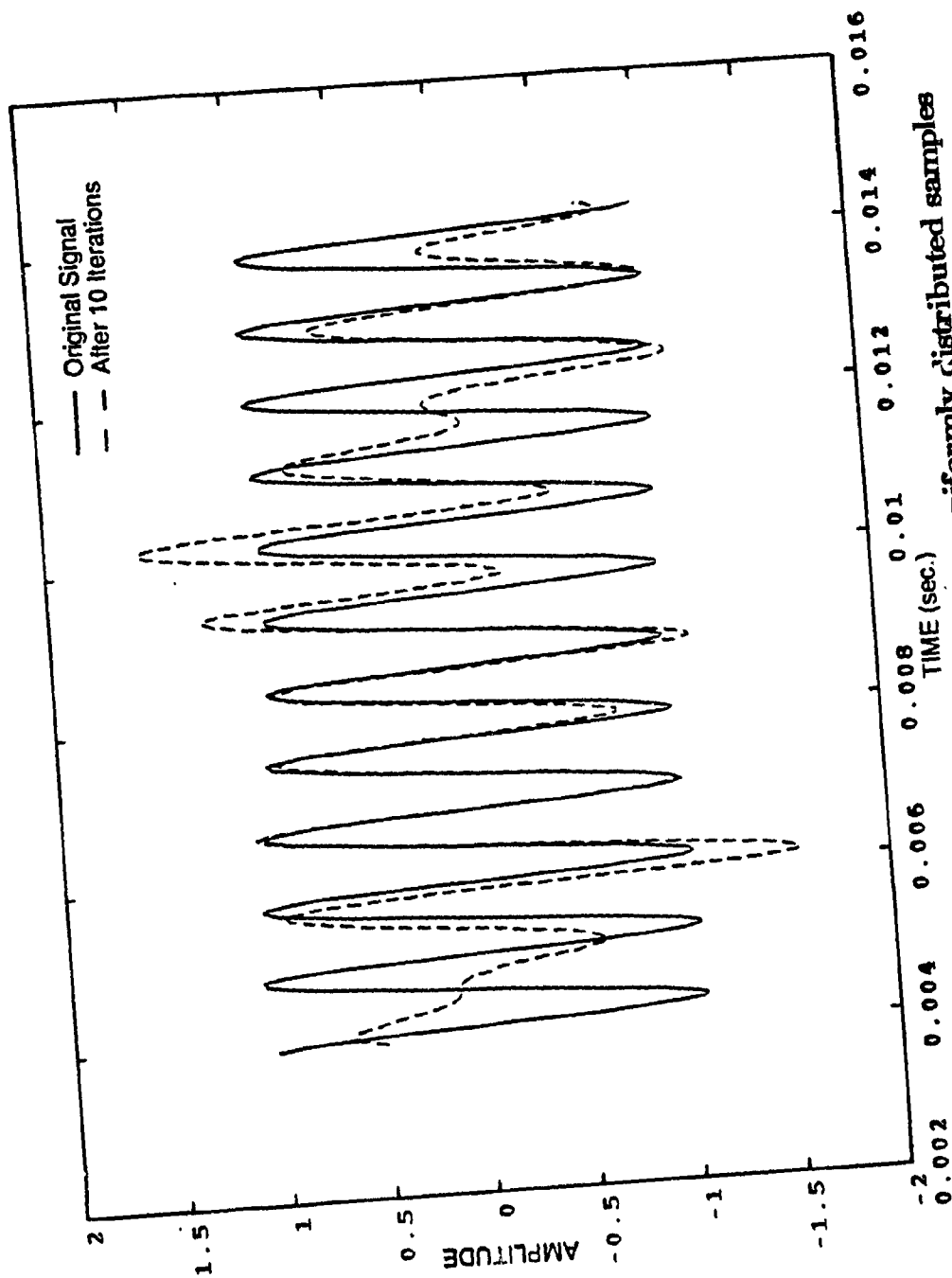


Fig. 4.6 (b): Reconstruction from nonuniformly distributed samples
using sine waveform, ($J=1.0, MA$)

the synchronous positions $k\Delta t$. The f_m (1100 Hz.) and f_s (2400 Hz.) are selected to be the same as before. A subinterval length of 9 is chosen in order to perform the partitioning scheme. Therefore, only the centre sample is recovered and the four boundary samples on either side are excluded.

Fig. 4.7 shows the original and the reconstructed signals after three iterations by solid and dash lines respectively. Again, using Equation (3.14), MSE is estimated as only 1.35% after 3 iterations and it can be easily observed from the figure that the reconstructed signal lies very close to the original signal. It is worth mentioning again that for a larger deviation of $\{t_k\}$ instants, the MA method is not feasible and therefore the simulation results are not compared.

To compare the efficiency of the PS with that of the MA method, simulations are performed for various jitter parameters. The MSE for the different cases are calculated and grouped in Fig. 4.8. For all the simulations a sequence of 100 samples at $\{t_k\}$ instants are extracted from the sinusoidal waveform and they are randomly distributed with uniform density functions. The frequencies f_m and f_s are chosen as 1100 Hz. and 2400 Hz respectively.

Fig. 4.8 compares the performance of PS and MA. There is only one curve corresponding to MA whereas there are three curves for PS respectively for subinterval 3, 5 and 7. The range of Y axis is reduced in order to show clearly the data points corresponding to $M = 5$ and 7. The results presented for MA correspond to 10 iterations; however, only two iterations are used for the PS to recover the signal from its unequally spaced data. From the figure it is clear that the MSE of the PS is always

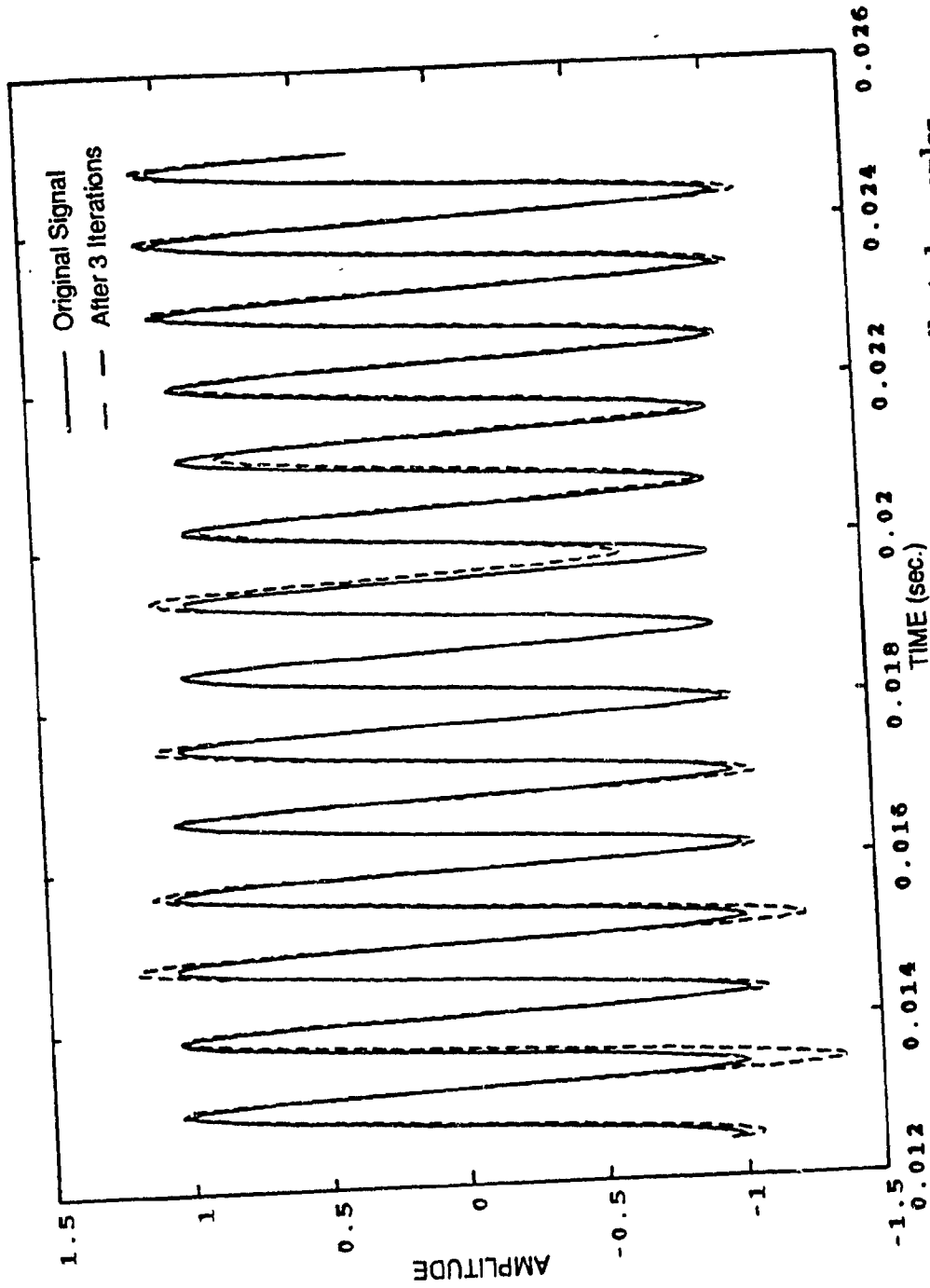


Fig. 4.7: Reconstruction from nonuniformly distributed samples
using sine waveform ($J=2.75$)

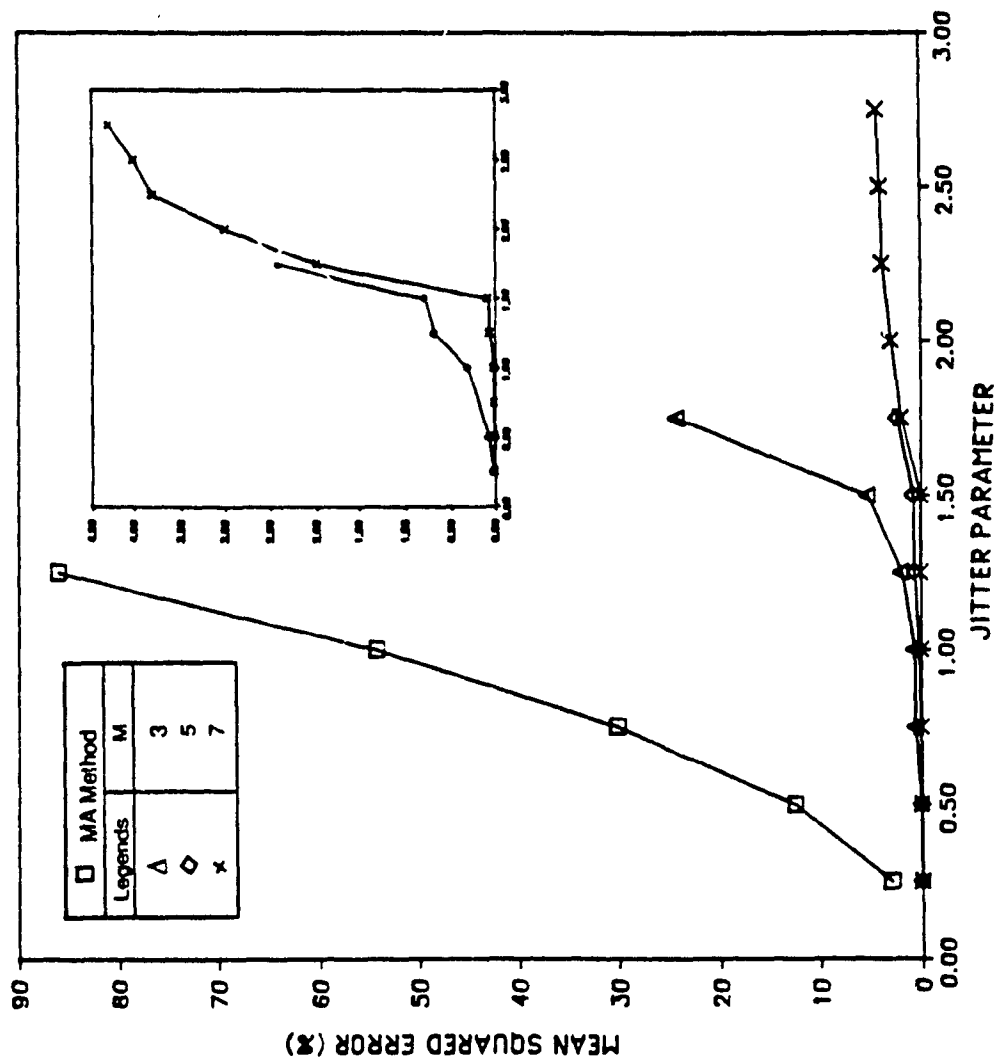


Fig. 4.8: A comparative study for the MSE between PS and MA

lower than the MA method irrespective of the jitter value, and the MSE of the PS is found to decrease with an increase in the subinterval length. For example, when $J = 0.5$, the MSE of MA is 10% whereas it is found to be 0.12%, 0.07% and 0.009% for $M = 3, 5$ and 7 respectively. Thus the errors are reduced significantly when the PS is applied. As explained before, the calculated MSF for the MA method is found to be very high when J takes a value more than 1.0 and it is not included in the figure.

Reconstruction procedure is repeated with $J = 1.75$, by taking M as 5 or 7. For this deviation, MSE are estimated as 2.41% and 2.0% for $M = 5$ and $M = 7$ respectively and thus the PS is found to perform better by increasing the value of M to 7. Also from Fig. 4.8, the estimated MSE is 4.2% when $J = 2.5$. From the above discussion, the requirements of M over a range of J can be formulated as follows:

$$\begin{aligned} &\text{-For } 0.0 < J \leq 1.00; M = 3 \\ &\text{-For } 1.0 < J \leq 2.00; M = 5 \\ &\text{-For } 2.0 < J \leq 2.75; M = 7 \end{aligned} \tag{4.4}$$

When the above relationship is employed in the PS, it is feasible to reconstruct a signal within 5% of MSE.

To understand the influence of number of iterations performed on the MSE, consider a sequence of 100 samples extracted at $\{t_k\}$ instants from a sinusoidal waveform. The $\{t_k\}$ instants are randomly chosen with uniform density functions in the range of $(-\Delta/2, \Delta/2)$. The simulation is performed only by implementing the PS. M is varied as 3, 5, 7, 9 and 11 for implementing the partitioning scheme and the MSE are estimated in % using Equation (3.14).

Fig. 4.9 shows the influence of MSE on various subinterval lengths with different number of iterations. These curves correspond to the signal reconstructed without any iteration, after 1 iteration and after 2 iterations. When $M = 3$, the MSE are estimated as 48%, 5.2% and 1%, respectively for the cases of without iteration, one iteration and two iteration. When M is increased to 5, the corresponding MSE are computed to be 32%, 1.97% and 0.66%. Further an increase in M to 7 reduces the MSE to 20%, 0.63% and 0.075% respectively.

From the above results it is very clear that an increase in the number of iterations decreases the MSE. Moreover, the MSE can also be reduced by increasing the M value. This unique characteristic provides two options for the reconstruction process. They are respectively, selecting the subinterval length or fixing the number of iterations. This can be implemented depending upon the MSE requirement.

The truncation error plays a major role in the MSE for various subinterval lengths. Recall Fig. 1.4 where the number of samples necessary for a fixed reconstruction error bound is studied. For perfect reconstruction, the cardinal series needs at least 100 samples. If M is chosen as 100 for the partitioning scheme, then the matrix operation becomes more complicated. In other words, it is not possible to solve vector \mathbf{B} in Equation (3.10). For $R \geq 2$, the number of samples is still greater than 20 and it is again complicated to perform matrix multiplication. On the other hand, even with a short subinterval length the MSE is reduced considerably when PS is used, and thus computational complexity is minimized.

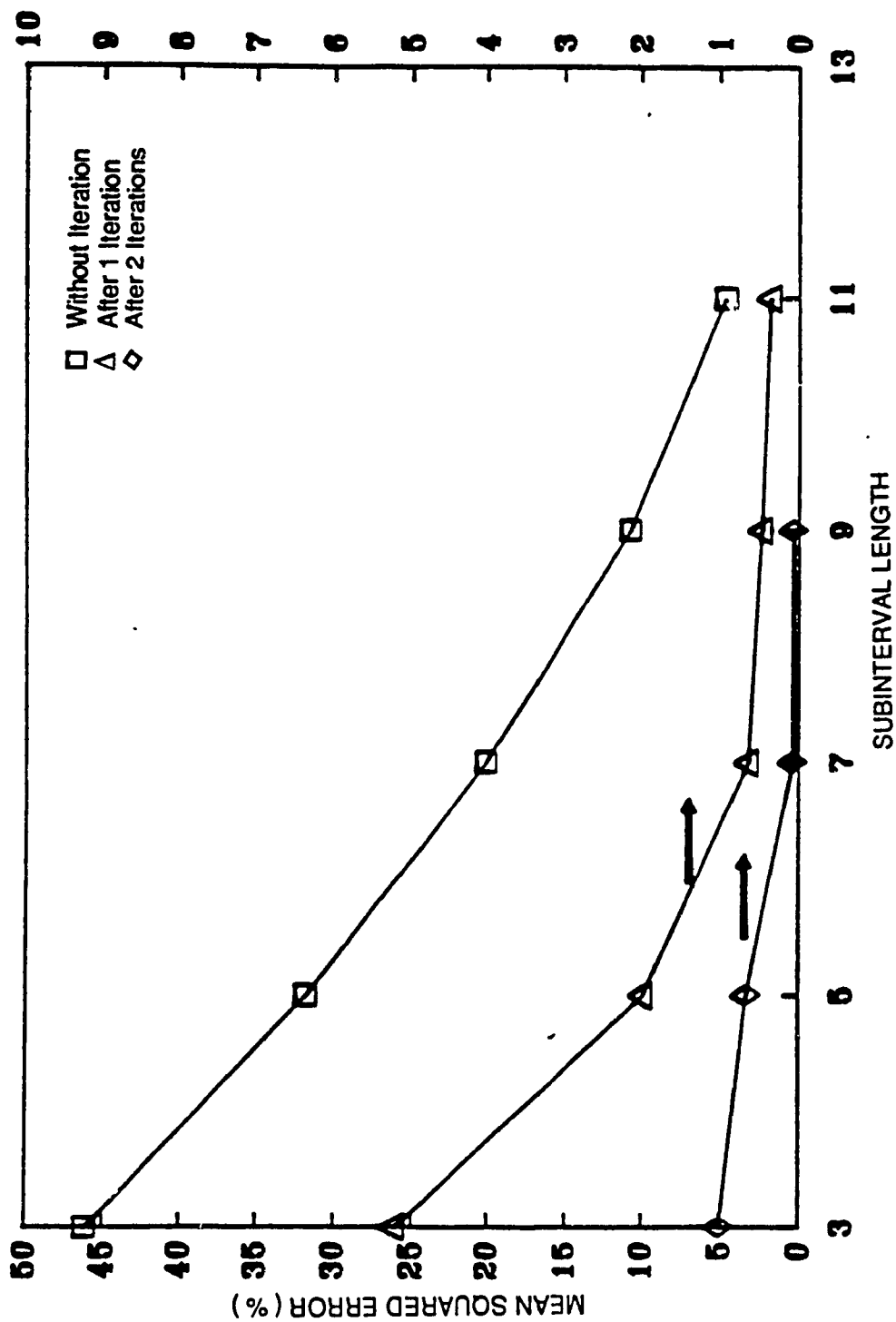


Fig. 4.9: Effect of subinterval length on MSE

The number of mathematical operations will directly influence the required CPU time. By considering a sequence of 100 samples in an observation interval with $J = 1$ the effect of M as well as the number of iterations on CPU time are studied. Again f_m and f_s are taken as 1100 Hz. and 2400 Hz respectively. The CPU time are obtained under batch mode operation in Vax/8550 (6.3 MIPS).

For $M = 3$, in the selected observation interval the required CPU times are observed as 24 sec., 28 sec. and 34 sec. respectively for the three cases without iteration, one iteration and two iterations; the CPU time increases to 27 sec., 36 sec. and 45 sec., respectively when $M = 5$. Thus it is clear that either an increase in M or the number of iterations increases the CPU time. However, with the recent advancement in computer technology, computational cost is not a major criterion. Moreover, considering the reduction in MSE due to PS, the additional cost is negligible.

For all the results discussed above, f_m is chosen approximately half of the sampling frequency. According to the WKS sampling theorem, this is the minimum required sampling frequency for the reconstruction of a band-limited signal. The influence of f_m on the PS performance is also studied. Consider the factor, R , which can be mathematically expressed as:

$$R = \frac{f_s}{f_m} \quad (4.5)$$

Sankur and Gerhardt (1975) studied the effect of R on the Signal to Noise Ratio (SNR). They considered a deterministic signal for the analysis and therefore the SNR is the ratio of original samples to the error in the restored samples. In the PS, a different terminology is used. The sum of a deterministic sinusoidal signal and a ran-

dom noise is considered for analysis, and therefore SNR is termed as Reconstruction Error (RER) and defined as follows:

$$RER = 10 \log_{10} \left\{ \frac{\sum_{k=1}^N x^2(k \Delta t)}{\sum_{k=1}^N [x(k \Delta t) - \hat{x}(k \Delta t)]^2} \right\} \quad (4.6)$$

where

$x(k \Delta t)$ is the original sample;

$\hat{x}(k \Delta t)$ is the restored sample;

Δt is the sampling interval; and

N is the number of samples;

RER is used as the index of performance to evaluate the reconstruction method which estimates the output in db.

To calculate RER the following data have been used: $N = 42$, $M = 3$ and $J = 1$. The X and Y axis of Fig. 4.10 represents respectively R and RER . The RER is found to increase with R up to a value of 8.0 and then remain constant for any further increase in R . For example when R increases from 2 to 4, RER increases from 18.3 db. to 31 db. However, even when $R = 24$, RER is estimated only as 36.5 db. Thus the results indicate that the performance of the PS even at higher sampling rates is satisfactory. The most rapid change in RER occurs only around the Nyquist rate. More about the applications of the criterion (Equation 4.6) may be found in chapter 6, which is devoted to the stability problem of the proposed method.

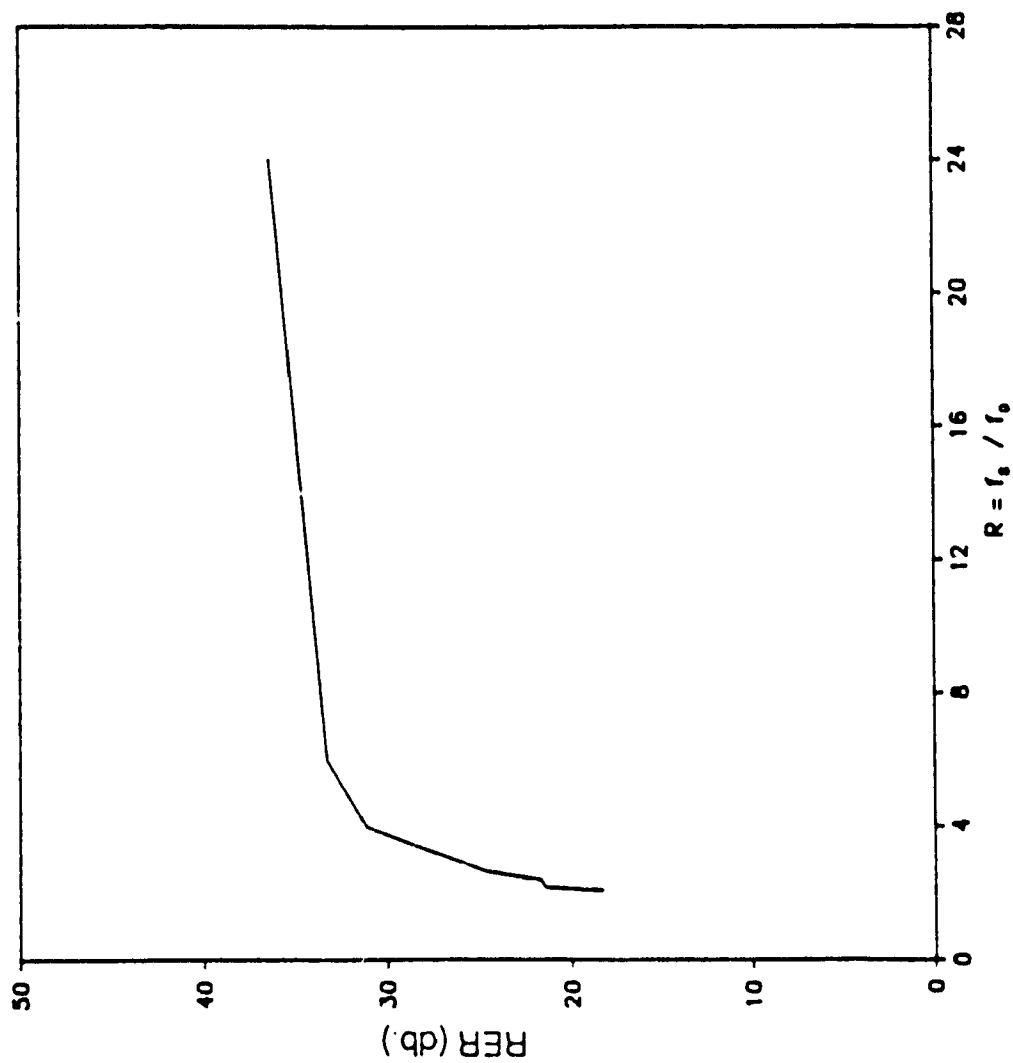


Fig. 4.10: Influence of the frequency ratio on the RER (db.)

4.2.3 Reconstruction Using Sum of Sine Waves

This section compares the simulation results of the PS and MA using a sum of two sine waves, which is also a deterministic signal. The sequence of unequally spaced samples are extracted from the summation of sinusoids given by:

$$x(t) = 0.75 \sin \omega_m t + 0.25 \sin \frac{\omega_m}{3} t \quad (4.7)$$

where

$$\omega_m = 2\pi f_m \quad (4.8)$$

Equation (4.7) is a complex waveform with two operating frequencies, one at f_m and other at $f_m/3$.

A sequence of 42 samples at $\{t_k\}$ instants are extracted from the above equation. They are distributed with uniform density function in the range of $(-\Delta/4, \Delta/4)$ or having $J = 0.5$. f_m and f_s are chosen respectively as 1100 Hz. and 2400 Hz. The subinterval (M) is chosen as 3 for the partitioning scheme in reconstructing the uniform samples. The solid line indicates the unequally spaced samples and the dashed line the original signal in Fig. 4.11.

The above unequally spaced samples are used for reconstructing the signal and Fig. 4.12 (a) displays the simulation results obtained by the PS. The three curves correspond to the original signal, signal reconstructed without iteration and reconstructed signal after 2 iterations. Consider a typical sampling time, 0.006 sec. The reconstructed signal without iteration (dashed line) lies further away from the original signal (solid line), whereas the signal reconstructed after two iterations (star line) lies

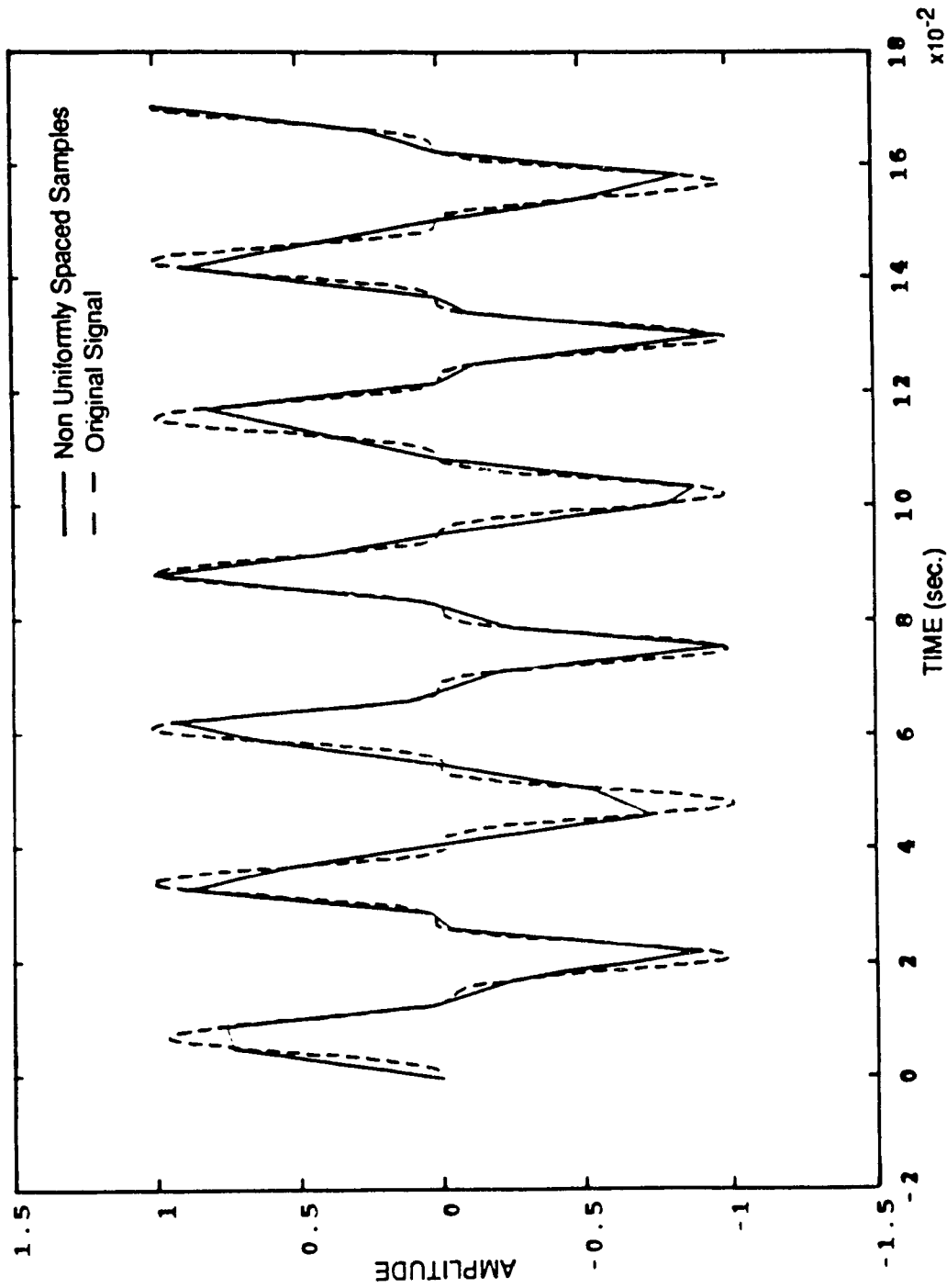


Fig. 4.11: Nonuniformly distributed samples using sum of sine waves

($J = 0.5$)

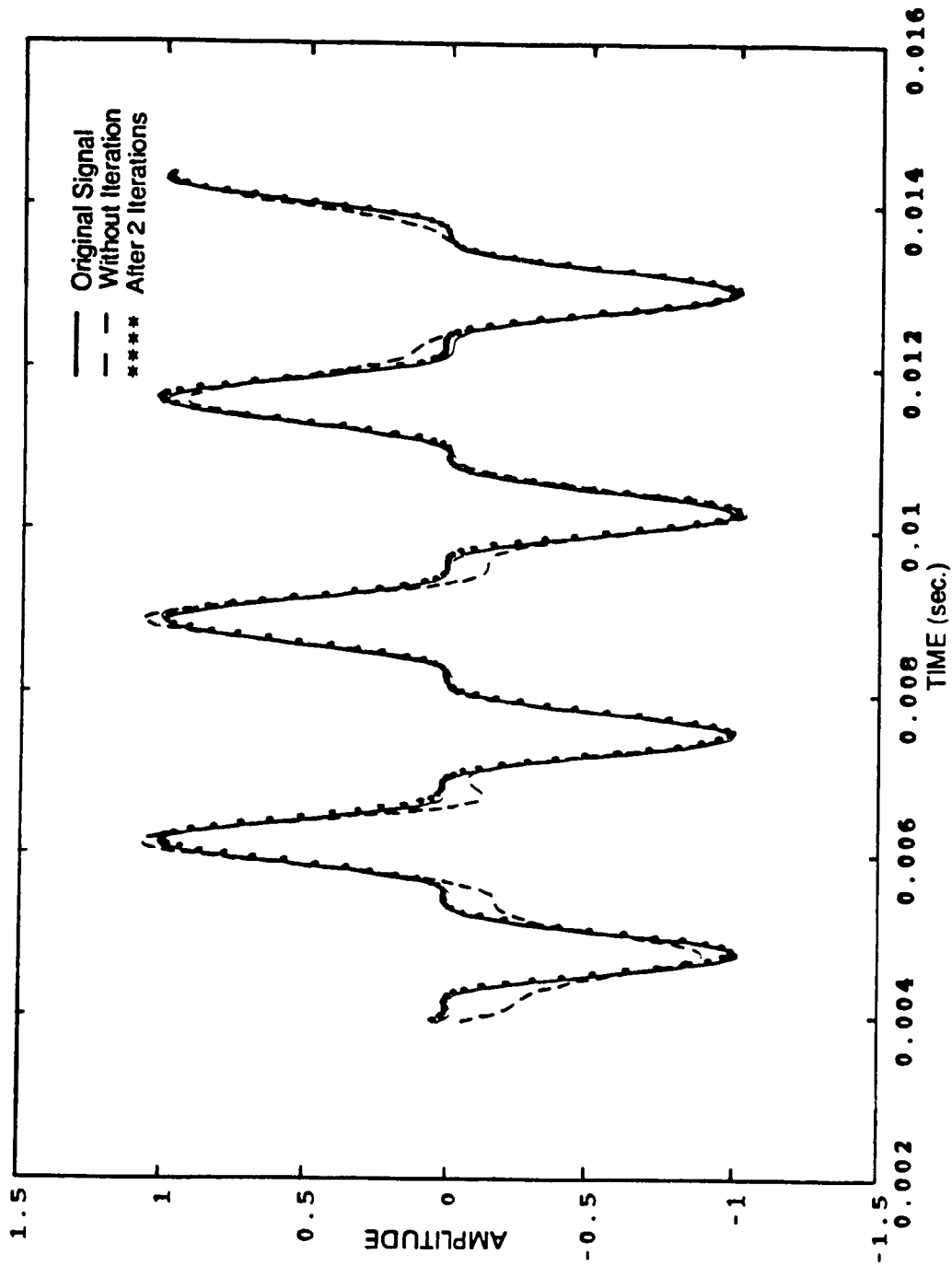


Fig. 4.12 (a): Reconstruction from nonuniformly distributed samples
using sum of sine waves ($J=0.5, PS$)

very close to the solid line. Thus it can be observed that the restored signal lies very close to the original one. The iterative adaptive method of MA is also applied for the same input condition and the simulation results are shown in Fig. 4.12 (b). The curves correspond to the original signal, reconstructed signal after 1 iteration and 10 iterations. For example, consider a sampling time of 0.012 sec. Both the dashed line and the star line are far away from the solid line. This confirms the better performance of PS compared to MA. The MSE are estimated both for PS and MA to scrutinize the performance of reconstruction. The MSE are calculated for the reconstruction using Equation (3.14) as before. They are respectively 1.62% and 0.09% for without iteration and after 2 iterations for PS, whereas 8.6% and 1.9% after one and 10 iterations for MA. For the latter case there is no considerable reduction in MSE even after 10 iterations and therefore, the figure displays only after one and ten iterations.

From the above discussion it is clear that the performance of the PS is not only better than that of MA, but also the MSE is reduced considerably in the reconstructed signal within two iterations. However, it is worth mentioning that the above simulation is performed for $J = 0.5$ and therefore the effect of these two reconstruction methods are further studied by increasing J to 1.0. Now $\{t_k\}$ instants are distributed uniformly in the range of $(-\Delta/2, \Delta/2)$ and the number of samples are kept constant at 42. The above input conditions are shown in Fig. 4.13 for unequally spaced samples and for the original signal.

Fig. 4.14 (a) presents the simulation results of the PS. The curves represent respectively the original signal, reconstructed signal without iteration and after 2 iterations. The third curve is closer to the first curve and therefore perfect reconstruction

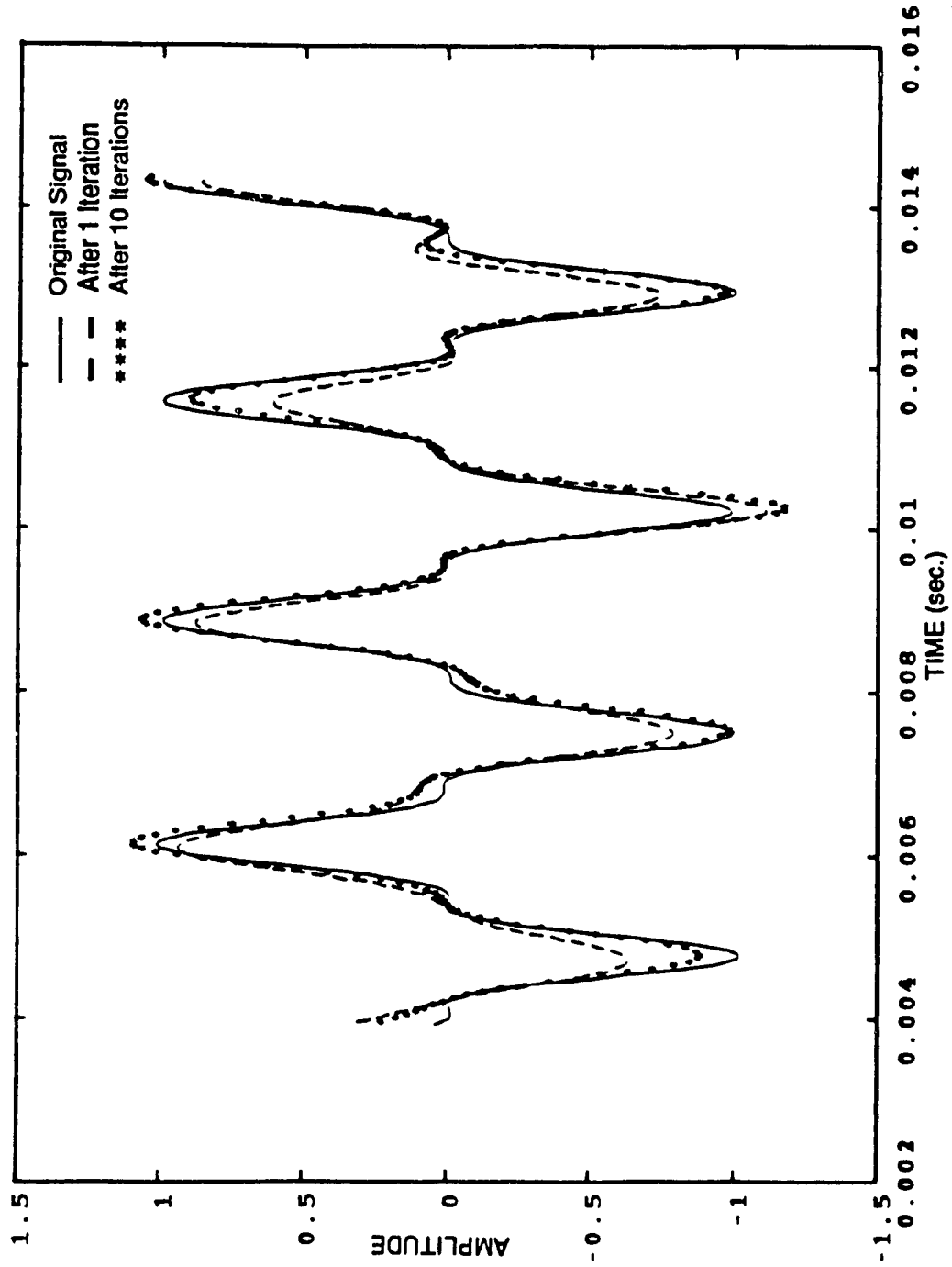


Fig. 4.12 (b): Reconstruction from nonuniformly distributed samples
using sum of two sine waves ($J = 0.5, MA$)

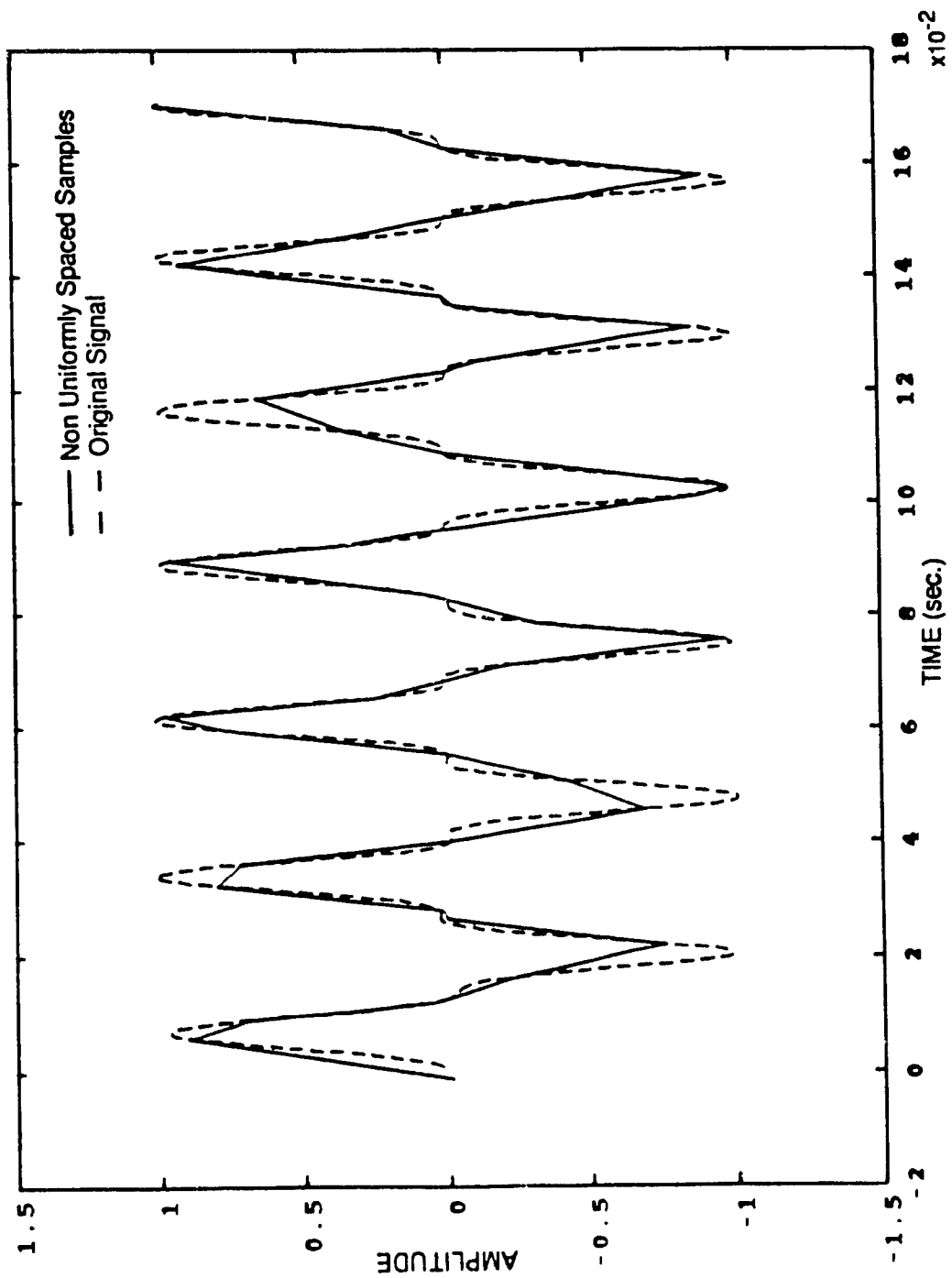


Fig. 4.13: Nonuniformly distributed samples using sum of sine waves

($J = 1.0$)

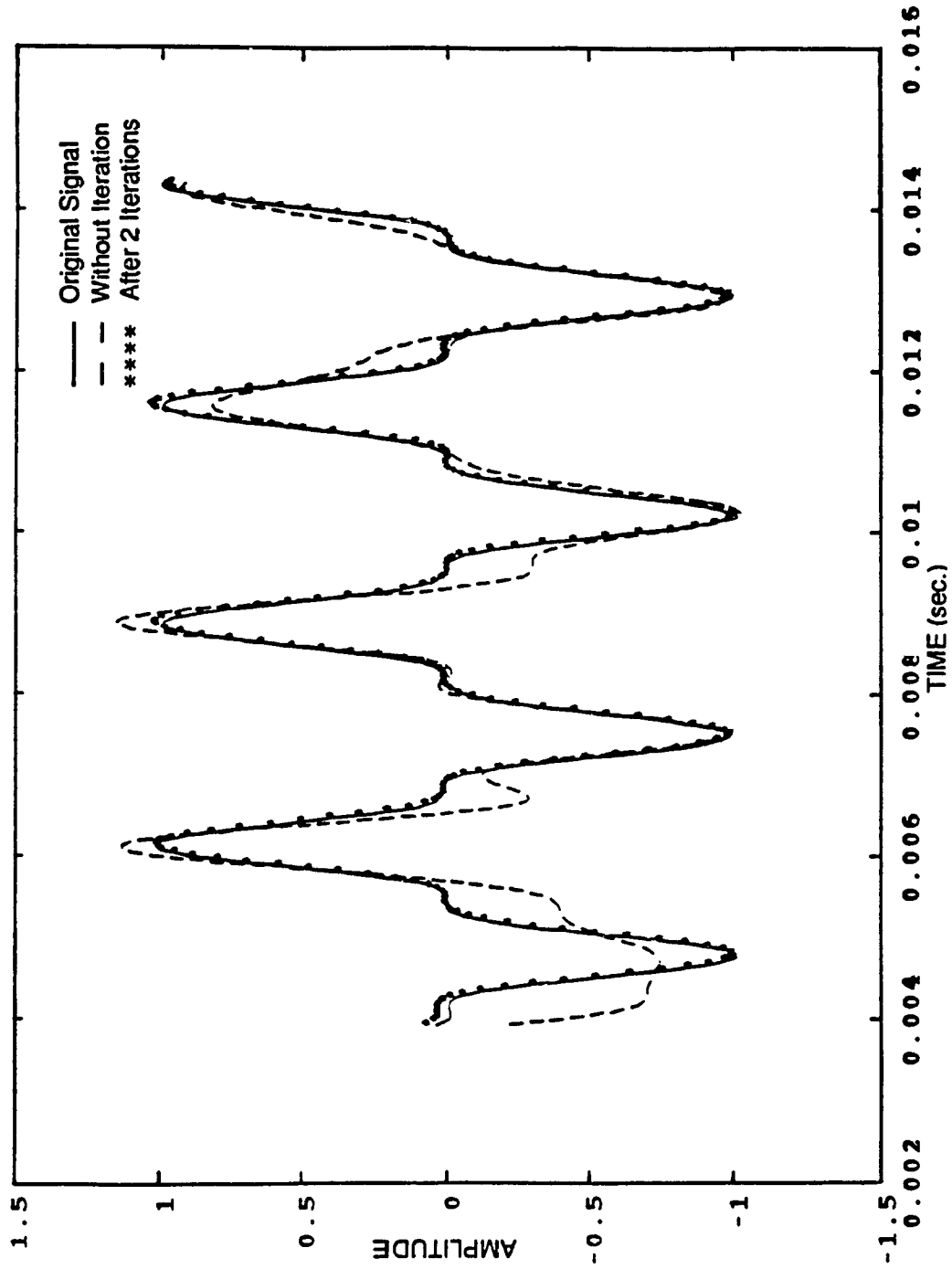


Fig. 4.14 (a): Reconstruction from nonuniformly distributed samples
using sum of two sine waves ($J = 1.0, PS$)

is feasible by the PS. Thus it is clear that the PS performs better even with an increase in J value for the sum of sine waves. The MSE are estimated to be 8% and 0.018% respectively for the cases of without iteration and after 2 iterations. The third curve lies almost exactly on the first curve and therefore perfect reconstruction is obtained.

Fig. 4.14 (b) shows the simulation results for MA. The original signal and the reconstructed signal after 4 iterations are shown in the figure. Calculated MSE after 4 iterations are found to be unfavourable and thus the iterative process is terminated. As discussed above, the MA method fails to reconstruct the original signal for jitter values more than 0.5.

To demonstrate the superiority of the PS, a complex deterministic signal is considered and can be generated as follows:

$$x(t) = 0.75\sin\omega_1 t + 2\cos\omega_2 t - 0.25\sin\omega_3 t - 4\cos\omega_4 t + 3.0 \quad (4.9)$$

The frequencies f_1 , f_2 , f_3 and f_4 are respectively 300 Hz., 400 Hz., 500 Hz. and 1100 Hz. J and M are chosen as 1.0 and 3 respectively. Fig. 4.15 illustrates three curves with same format as in Fig. 4.14 (a). The reconstructed signal without iteration lies farther away from the original signal, whereas the signal reconstructed after two iterations lies very close to the original signal. The calculated MSE are respectively 19% and 0.39% for the case of without iteration and after two iterations.

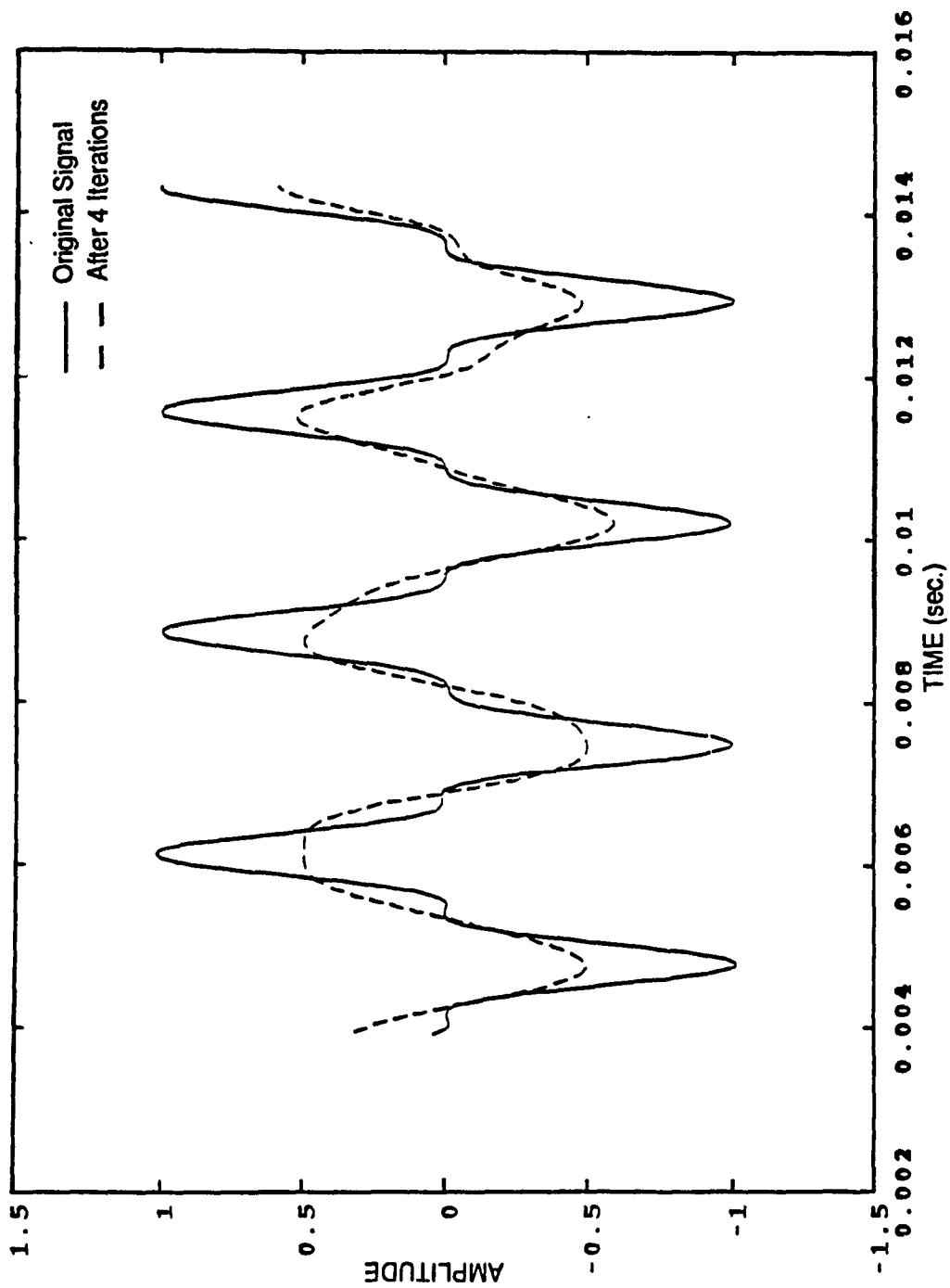


Fig. 4.14 (b): Reconstruction from nonuniformly distributed samples
using sum of two sine waves ($J = 1.0, MA$)

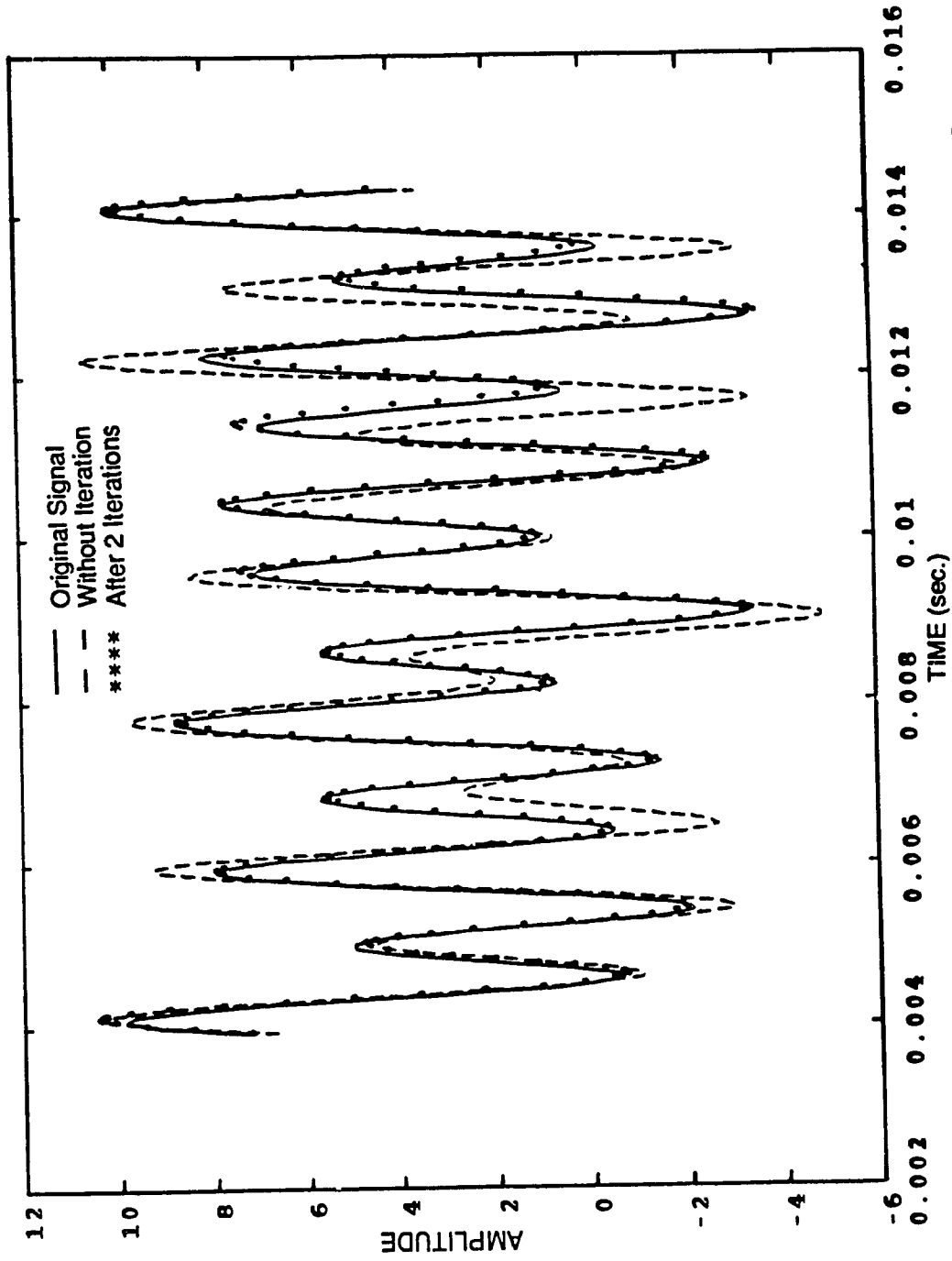


Fig. 4.15: Reconstruction from nonuniformly distributed samples
using a complex waveform

4.3 CONCLUSION

A user friendly computer code is developed by implementing the iterative technique. This uses a partitioning scheme for selecting the number of samples in a subinterval length. This chapter has presented the simulation results for a deterministic signal. The superiority of the present study is illustrated throughout the chapter by comparing it to a recent iterative algorithm by Marvasti and Analoul (1989). Based on the calculated MSE, it can be concluded that the present study can be applied not only for larger deviation of samples but also for various band-limited frequencies. The method of Marvasti and Analoul (1989) fails to reconstruct the signal when J is greater than 0.5. This has been found true even for the case of sum of sine waves.

A relationship is formulated between the jitter parameter and the subinterval length such that it is always feasible to obtain the MSE level less than 5%. A complex test signal is also reconstructed by the present study with minimum MSE level.

CHAPTER 5

RECONSTRUCTION OF RANDOM PROCESSES FROM UNEQUALLY SPACED SAMPLES

A generalized computer code (-refer Fig. 4.1) for reconstructing a band-limited signal from unequally spaced samples has been presented in the previous chapter. Various interesting simulations have also been performed for the deterministic processes which are analyzed and discussed. Reconstruction of band-limited random processes from the unequally spaced samples is the objective of this chapter and it is addressed under five sections. The first section discusses the details involved in generating a random process. Its reconstruction procedure from unequally spaced samples is presented in the second section. The third section elaborates the reconstruction procedure for sum of deterministic and random signals. Statistical analysis of the computed results are performed in the fourth section. Two parameters, mean and standard deviation, are obtained by calculating "Mean Squared Error" of the repeated procedure i.e., by studying an ensemble of randomly taken realizations of the same process. The fifth section brings an overall conclusion of the chapter itself.

5.1 GENERATION OF A RANDOM PROCESS

For generating a random process, the MATLAB utility function "rand" is used. The random process obtained is not band-limited to a given frequency whereas the simulation can be performed for only band-limited processes by using the present computer code. To obtain the band-limited process, a practical realizable filter has to be designed. For the present study, a Low Pass Filter (LPF) is used to meet the

specifications of 1200 Hz. of cut-off frequency (f_c) and 2400 Hz. of sampling frequency (f_s). These specifications can be implemented by using either an analog or digital filter. A digital filter namely, Butterworth filter is implemented to obtain the flat frequency response within the passband range.

By inputting a random process (x), a filtered output (y) can be obtained when the MATLAB function "filter" is used. Then x and y can be related as follows:

$$y = \text{filter}(b, a, x) \quad (5.1)$$

where a and b are the design coefficients of the filter. The design coefficients are related with the input and output of the filter in both the time and frequency domains, which are given by Equations (5.2) and (5.3) respectively (Rabiner and Gold, 1975).

$$y(n) = b(1)x(n) + \dots + b(nb)x(n-nb+1) - a(2)y(n-1) - \dots - a(na)y(n-na+1) \quad (5.2)$$

$$Y(z) = \frac{b(1) + b(2)z^{-1} + \dots + b(nb)z^{-(nb-1)}}{1 + a(2)z^{-1} + \dots + a(na)z^{-(na-1)}} X(z) \quad (5.3)$$

Note that Equation (5.2) is in difference form whereas Equation (5.3) is obtained by using Z transformation.

To obtain the coefficients a and b the MATLAB utility function "Butter (N, ω_n)" is used. This will design an N -th order low pass Butterworth filter with filter coefficients for a and b . The input ω_n is the cut-off frequency which takes a value between $0.0 < \omega_n < 1.0$. The upper limit 1.0 corresponds to half of the sampling rate. For the present design specifications the input value of ω_n and N are respectively chosen as 0.6391 and 6.

The transfer function $H(z)$ defined as:

$$H(z) = \frac{Y(z)}{X(z)} = \frac{b(1) + b(2)z^{-1} + \dots + b(nb)z^{-(nb-1)}}{1 + a(2)z^{-1} + \dots + a(na)z^{-(na-1)}} \quad (5.4)$$

have been determined and the corresponding frequency responses are shown in Fig. 5.1 which displays two curves, namely simulated and theoretical. From the frequency response plots, it is obvious that a cut-off frequency of 1200 Hz. is met for the designed filter. The above discussion provides confirmation for the designed filter and the generated random process can be band-limited by using it. The details involved for the reconstruction procedure are presented in the next section.

5.2 RECONSTRUCTION FROM UNEQUALLY SPACED SAMPLES FOR RANDOM PROCESSES

This section presents the result of reconstruction as applied to unequally spaced samples of random processes. There are different statistical distributions for a random process; however, only Gaussian and uniform distributions are considered in the present study. The reconstruction of Gaussian process is discussed first, whereas the uniform process is presented later. To obtain a band-limited process, filtering is performed by using Equation (5.1). The filtered output is used for further study. It is worth mentioning that the distribution of sample locations within the observation interval is uniform and independent of the input signal.

For the Gaussian process the following input parameters are considered. A sequence of 42 samples are taken at $\{t_k\}$ instants which are in the range of $-\Delta t/2$ to $\Delta t/2$ from the corresponding synchronous positions $\{k \Delta t\}$. Therefore the jitter parameter (J) can be calculated as unity. Note that the sampling frequency is 2400 Hz. and

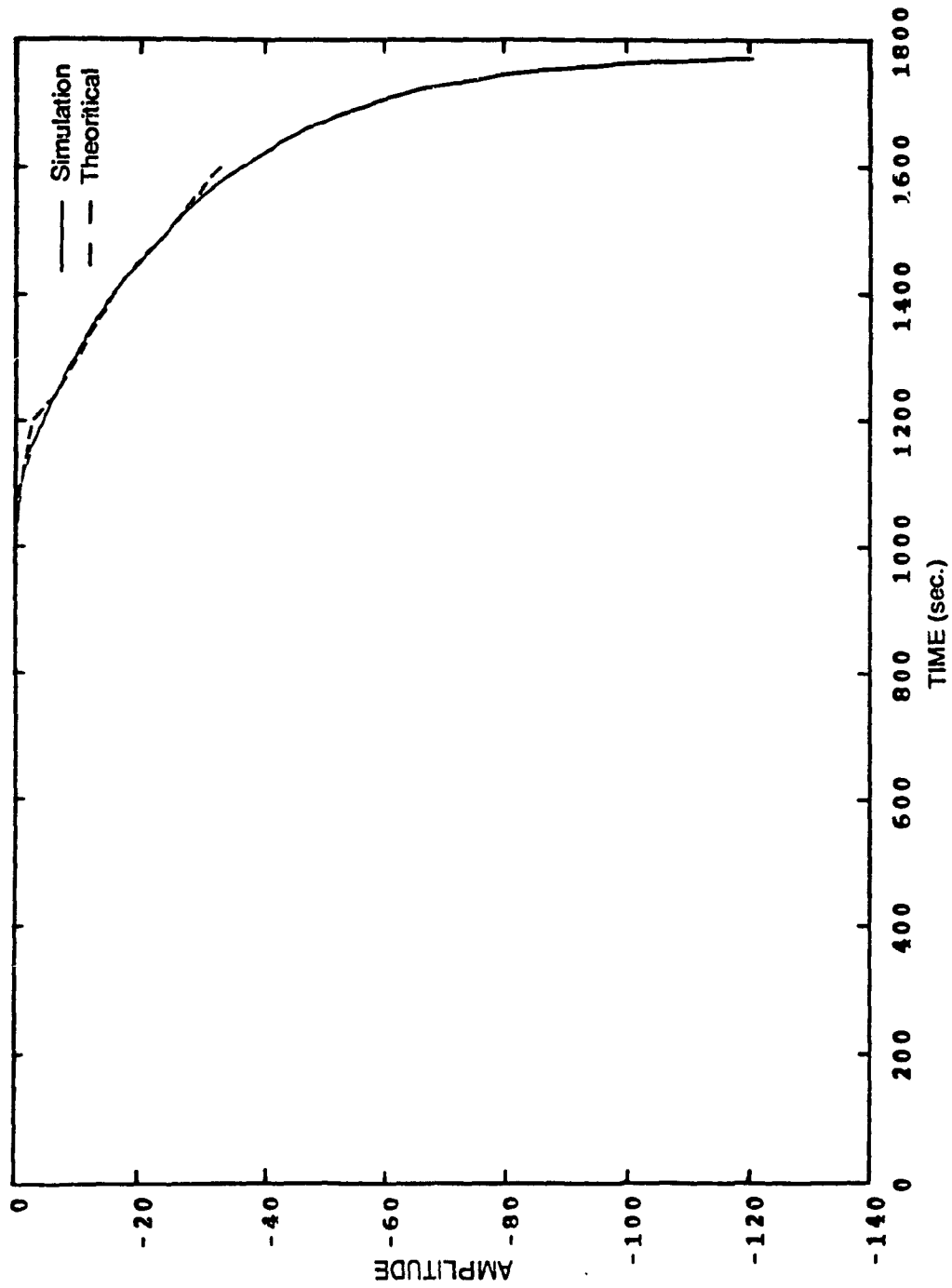


Fig. 5.1: Magnitude response of a Butterworth lowpass filter

the subinterval length (M) is chosen as 3 for the partitioning scheme (-refer Fig. 3.1). As explained in the previous chapter the developed iterative algorithm is implemented during the reconstruction procedure.

Fig. 5.2 shows the reconstructed Gaussian process from unequally spaced samples. The figure contains three curves namely the original process, reconstructed process without iteration and with 3 iterations. These three curves are represented respectively by solid, dash and star lines. From the figure, it is clear that the dashed line lies farther away from the solid line whereas there is no significant difference between the solid and the star line. The MSE of the reconstructed signals are also calculated as explained in the section 3.2 by using Equation (3.14). Only 2% of error is computed after the reconstruction and it has been found to diminish further when the iterative procedure is implemented. It is also evident that the errors are found to be negligible after 3 iterations and hence the iterative procedure is terminated.

Having the same input parameters, an uniform random process has been generated. This process is also filtered and the reconstruction results are presented in Fig. 5.3. It has three curves namely, the original signal and the reconstructed signals without iterations and with 2 iterations and they are respectively represented by solid, dash and star lines. Since from the previous study the MSE after 3 iterations is found to be negligible, only 2 iterations are performed for this case.

There are some deviations between the original and the reconstructed process without any iteration. On the otherhand, the iterative process effectively improves the reconstruction and thus the reconstructed signal after 2 iterations lies closer to the

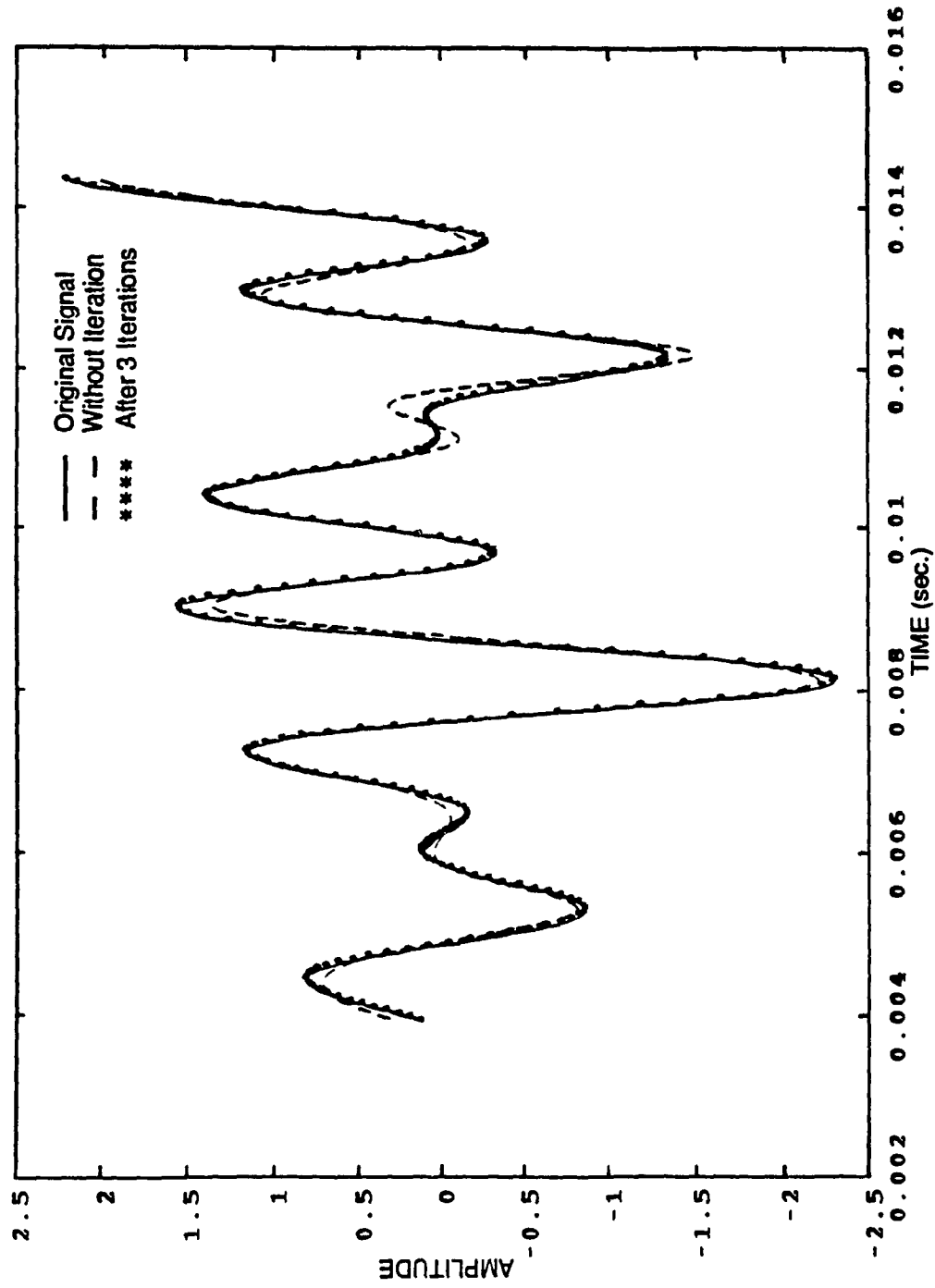


Fig. 5.2: Reconstruction from nonuniform samples using

Gaussian distribution

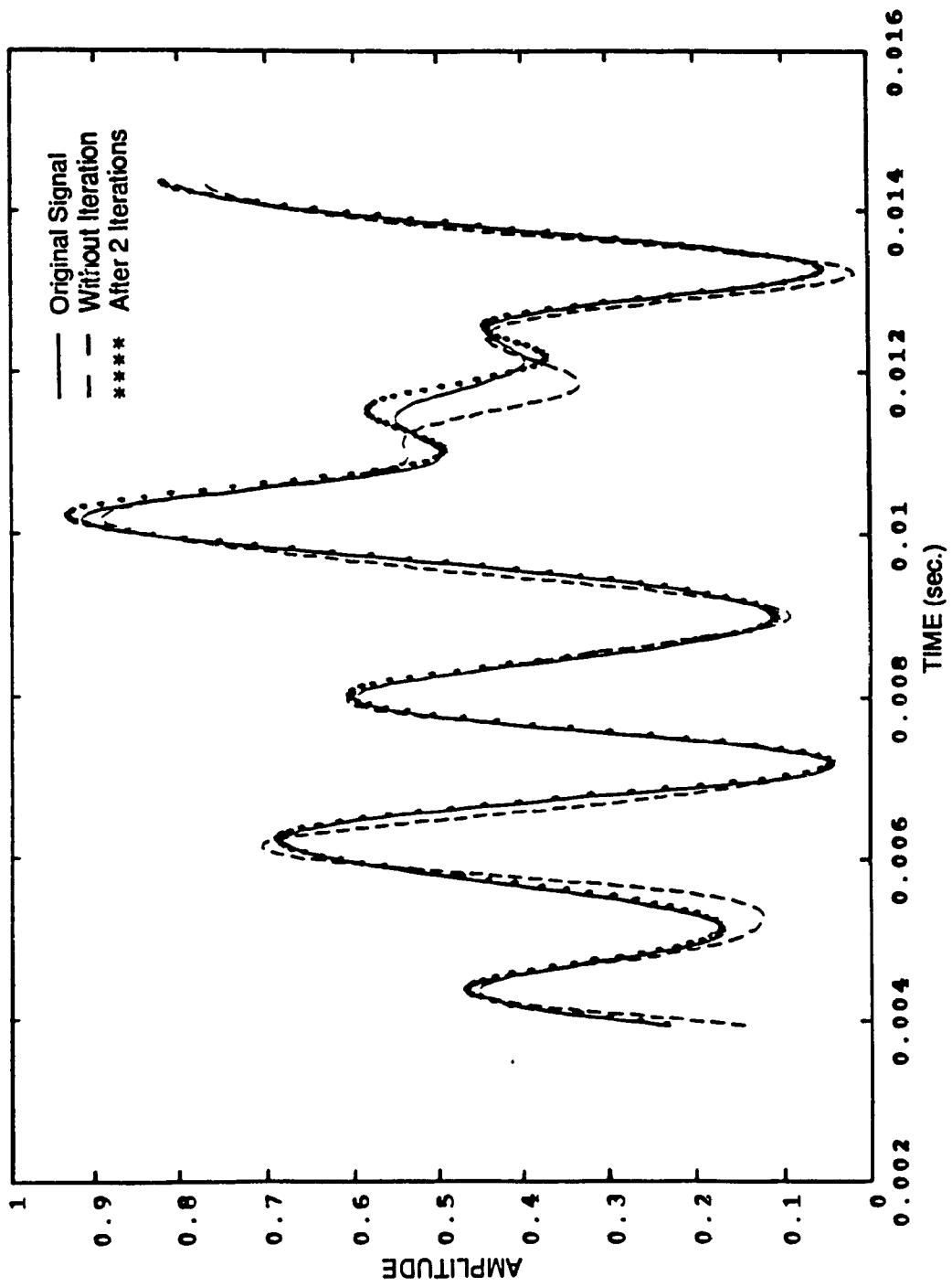


Fig. 5.3: Reconstruction from nonuniform samples using random uniform distribution

original signal. The MSE are computed as 1.5% - without iteration and 0.07% - after 2 iterations. These discussions reveal that the computer code is capable of reconstructing a random process from unequally spaced data.

5.3 RECONSTRUCTION FROM UNEQUALLY SPACED SAMPLES FOR THE SUM OF DETERMINISTIC AND RANDOM PROCESSES

From the previous sections, It is evident that a reconstruction of a random process given by its unequally spaced samples can be effectively accomplished by the proposed method. It is also observed that the error in the reconstruction of a random process is much less than that of the deterministic signal, particularly a sinusoidal signal with operating frequency close to half of the sampling frequency. In this section, the research is further extended to perform the reconstruction from nonequally spaced samples for the summation of deterministic and random signals. The deterministic signal is added to a random processes which itself is classified as either Gaussian or uniform. Before initiating the reconstruction procedure, It is necessary to generate the necessary reference signals which will be discussed below.

Consider a band-limited deterministic (sinusoidal) signal $x_1(t)$ and a random process, $x_2(t)$. As discussed in section 5.1, the $x_2(t)$ is band-limited to 1200 Hz. Then the summation of $x_1(t)$ and $x_2(t)$ is mathematically expressed as:

$$x(t) = x_1(t) + x_2(t) \quad (5.5)$$

The above obtained $x(t)$ is a band-limited signal with a summation of the deterministic sinusoidal function and a random noise. Let " A_s " and " σ_n^2 " be the two parameters used to denote the amplitude of the sinusoidal function and the variance of a random

noise, respectively. Then $x(t)$ can be expressed in terms of these two parameters which can be represented by the Index Signal to Noise Ratio (SNR). Since $x(t)$ is used as the input to the computer code, SNR is suffixed by the term "IN" (SNR_{IN}) and expressed as follows:

$$SNR_{IN} = 10 \log_{10} \frac{A_s^2}{2\sigma_n^2} \quad (5.6)$$

As pointed out earlier, $x_2(t)$ in Equation (5.5) can be classified either as Gaussian or uniform distribution. Thus this section comprises two subsections describing the reconstruction procedure dealing with Gaussian and uniform distributions. Moreover, the reconstructions for these cases are also performed by using the iterative procedure of Marvasti and Analoui (1989). Various interesting comparisons are made for the simulated results between the Present Study (PS) and those of Marvasti and Analoui (1989) (MA).

5.3.1 Gaussian Distribution

Under this subsection three different cases are studied by for the SNR_{IN} of -10 db., 0 db. and +10 db. The obtained results are presented and discussed. These three cases are considered typically to measure the performance of the two iterative methods (PS and MA).

For $SNR_{IN} = -10db.$, the calculated A_s and σ_n are respectively 0.1 and 0.2236. A sequence of 42 samples are extracted at $\{t_k\}$ instants in Equation (5.5). The time instants are randomly distributed with uniform density functions in the range of $-\Delta/2$

to $\Delta t/2$ for its corresponding synchronous positions $\{k\Delta t\}$. Therefore J is calculated as unity (-refer Fig. 3.2). f_m and f_s are chosen as 1100 Hz. and 2400 Hz. respectively.

The PS is applied for a subinterval length (M) of 3 samples and iterative procedure is repeated twice during the reconstruction. Fig. 5.4 (a) displays three curves namely, the original signal, reconstructed signal without iteration and signal reconstructed after 2 iterations, which are respectively represented by solid, dash and star lines. It is clear from the figure that the dashed line lies farther away from the solid line whereas the star line lies very close to it. The MSE of the reconstructed signals are also computed using Equation (3.14) and they are respectively 5% and 0.1% for without and with 2 iterations. Thus a substantial reduction of about 4.5% in MSE level is obtained when the iterative procedure is used.

By inputting the same parameters, the iterative adaptive algorithm of MA is used for reconstruction. Fig. 5.4 (b) shows three curves of MA, in the same format as that of Fig. 5.4 (a). However it is worth mentioning that the dashed and the star lines are respectively obtained as a result of 3 and 10 iterations. Figure shows much deviation between the dashed line and the original signal. Only little improvement is observed even after 10 iterations as shown by the star line of the figure. For the MA procedure, the MSE are also computed and they are respectively 10.4% and 7% for 3 and 10 iterations. Even by repeating the procedure for 10 iterations, the MSE is still found to be high and only a reduction of approximately 3% is obtained for the additional iterations.

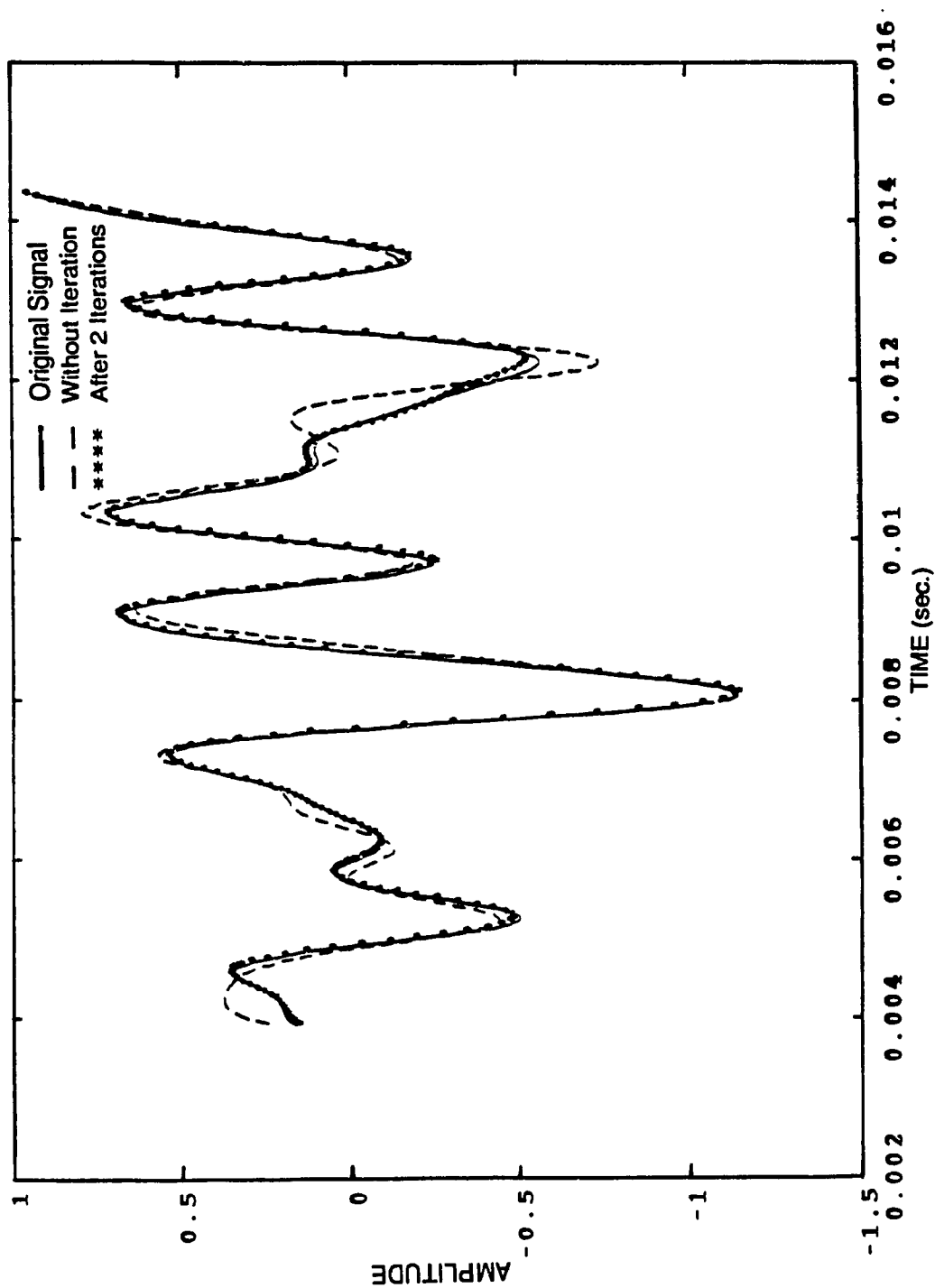


Fig. 5.4 (a): Reconstruction from nonuniformly spaced samples
($\text{SNR}_{\text{IN}} = -10\text{db.}$; random Gaussian noise; PS)

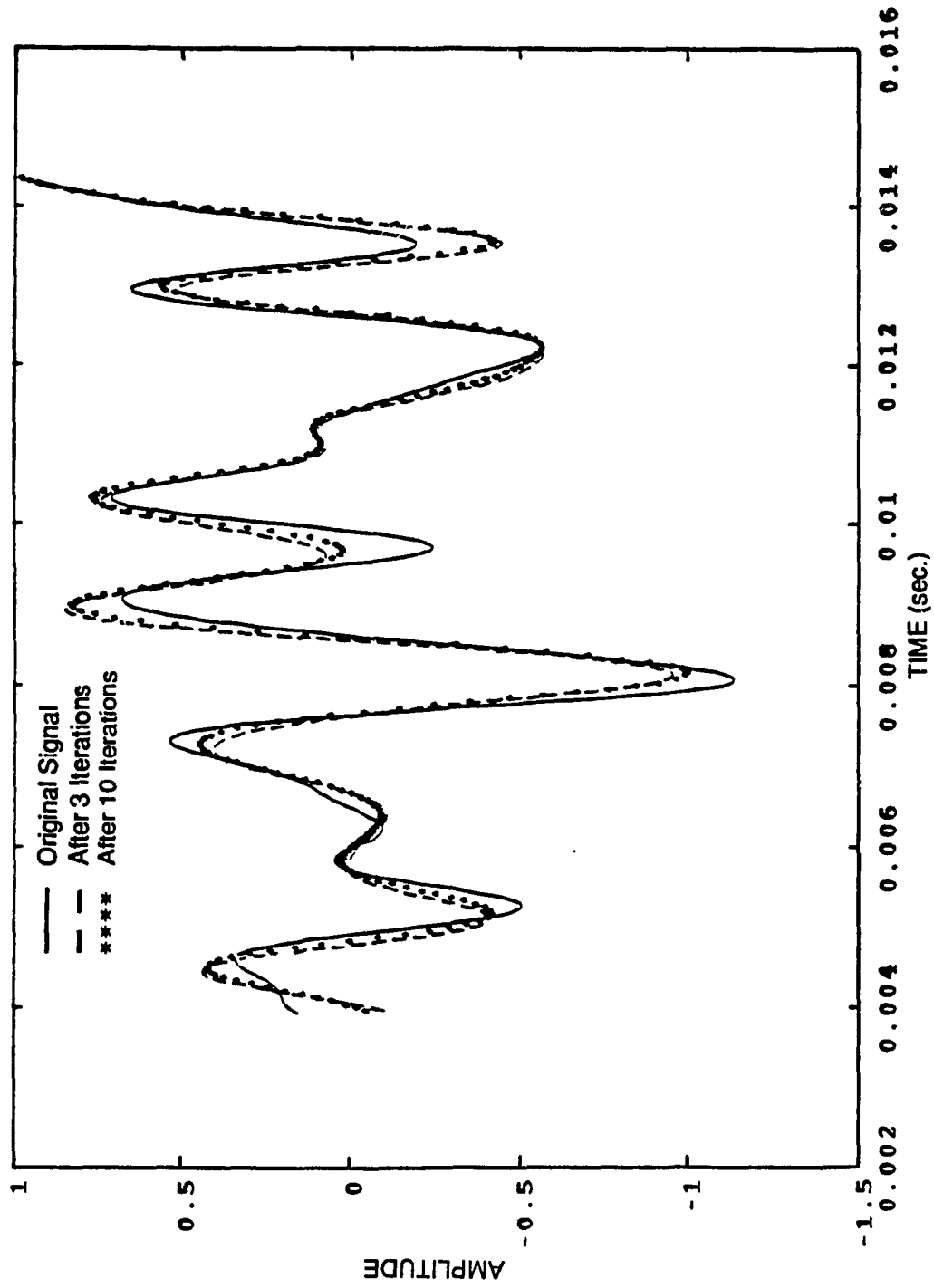


Fig. 5.4 (b): Reconstruction from nonuniformly spaced samples
($\text{SNR}_{\text{IN}} = -10\text{db.}$; random Gaussian noise; MA)

Comparing these MSE levels with those of the previous figure, it is evident that the PS method performs considerably better than the MA method. Since there is no significant reduction obtained after 2 iterations for the MA method, it has been decided to continue up to 10 iterations. The above observations reveal that the PS can perform better than MA with limited number of iterations. Comparisons between these two methods are further extended by increasing SNR_{IN} from - 10 db. to 0 db.

Fig. 5.5 (a) and Fig. 5.5 (b) illustrate the results obtained by using the PS and MA for the case of $SNR_{IN} = 0db.$. These two figures are plotted in the same fashion as before, however with a different range of the amplitude. The increase in amplitude is not surprising because there is an increase in SNR_{IN} . As shown in Equation (5.6), SNR_{IN} is directly related to A_s and inversely proportional to σ_n . Thus either an increase in A_s or reduction in σ_n will increase the SNR_{IN} .

For both figures the dashed lines are totally distorted and lie farther away from the solid line when $t = 0.004sec$. It is worth mentioning that the number of iterations for the PS is only limited to 2 whereas up to 10 iterations are performed for MA. By applying the iterative procedure in the PS remarkable improvements are obtained, while for the MA method still significant difference of the reconstructed signal from the original signal is observed. Reconstructed signals with and without iterations are also obtained by increasing the $SNR_{IN} = +10db.$, and Fig 5.6 (a) and (b) respectively illustrate the results obtained by applying the PS and MA methods. The observations of Fig. 5.5 are also equally applicable for these figures. The MSE for the above three cases are also calculated and compared to derive some observations with regard to the increase in SNR_{IN} .

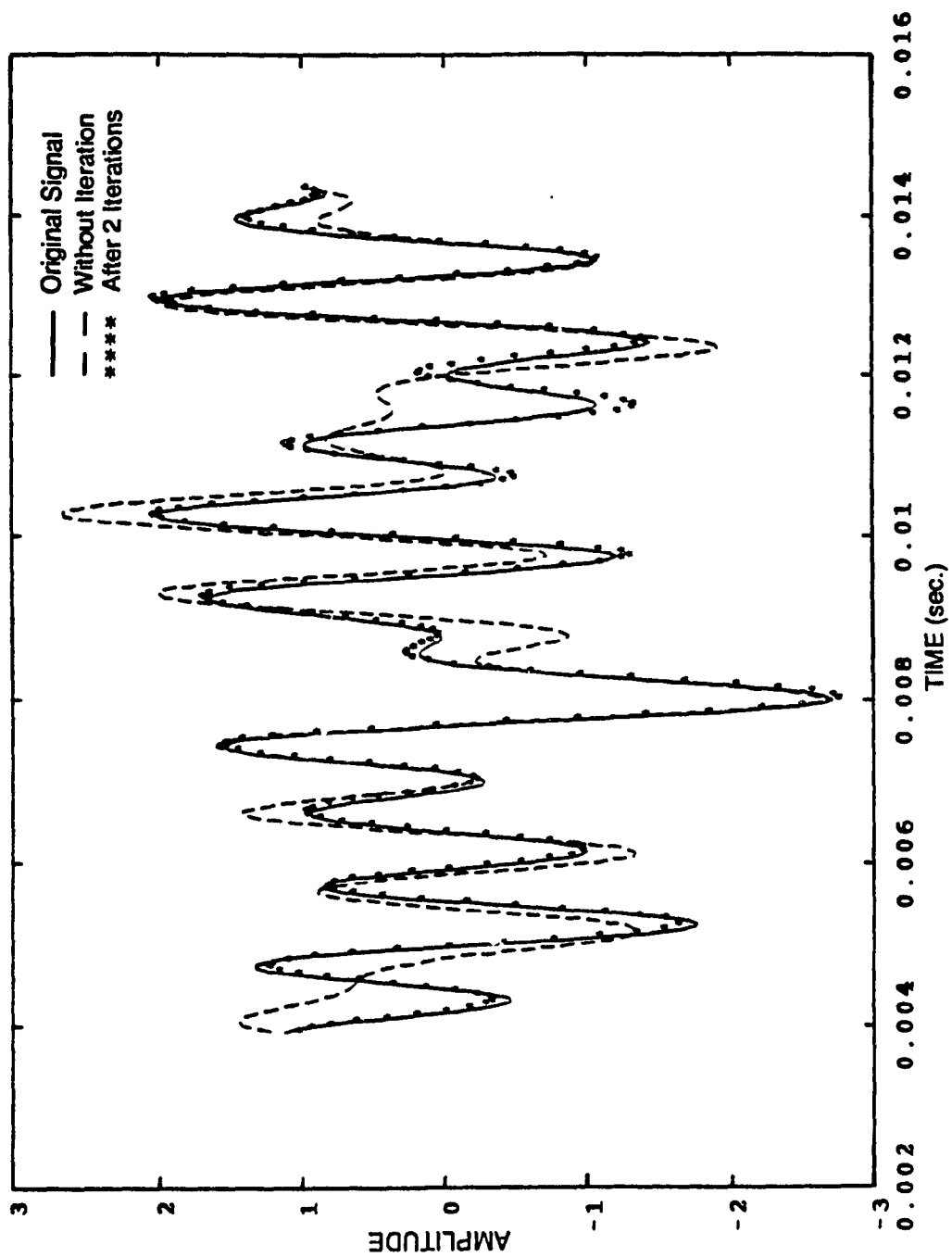


Fig. 5.5 (a): Reconstruction from nonuniformly spaced samples

($\text{SNR}_{\text{IN}} = 0\text{db.}$; random Gaussian noise; PS)

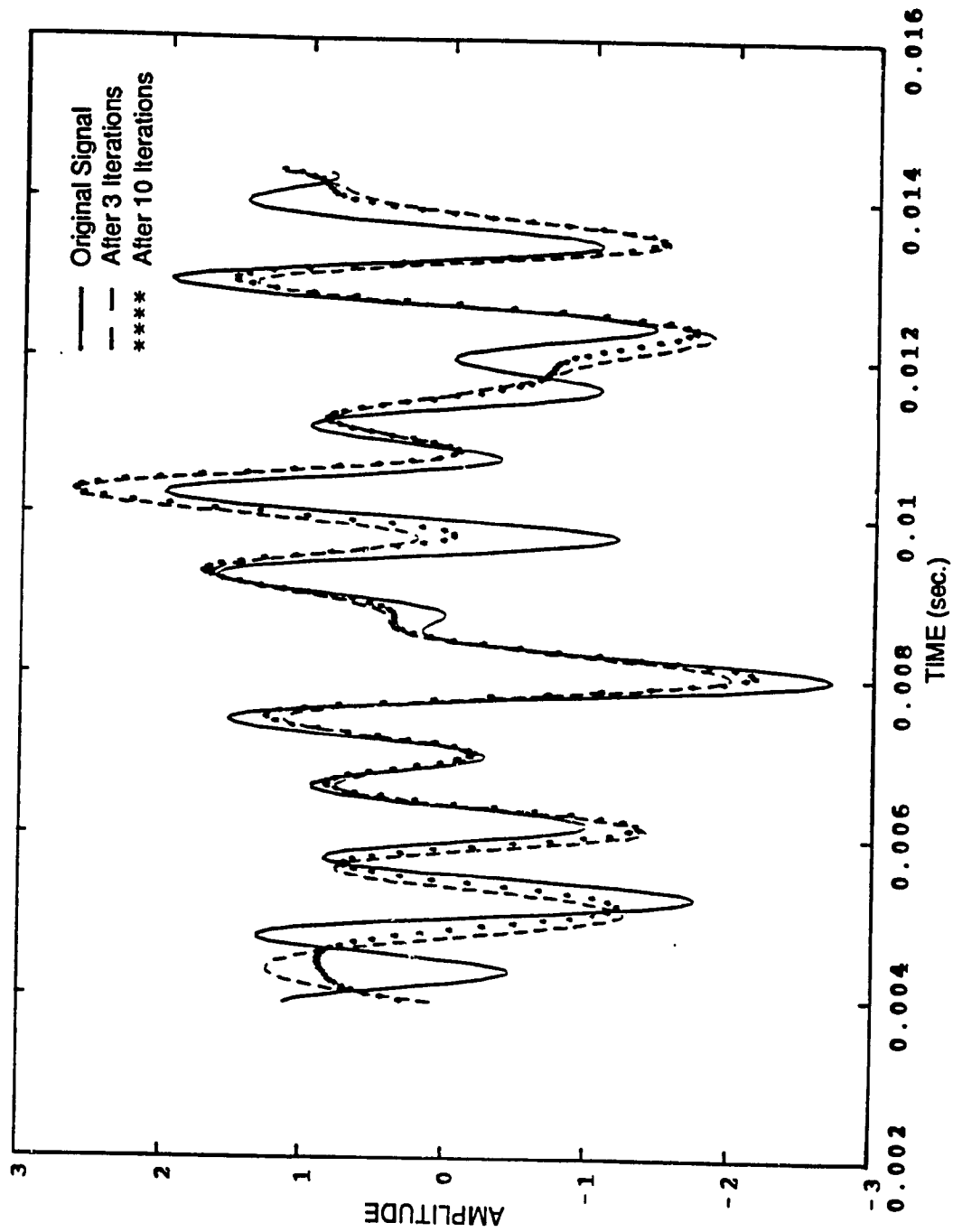


Fig. 5.5 (b): Reconstruction from nonuniformly spaced samples

($\text{SNR}_{\text{IN}} = 0\text{db.}$; random Gaussian noise; MA)

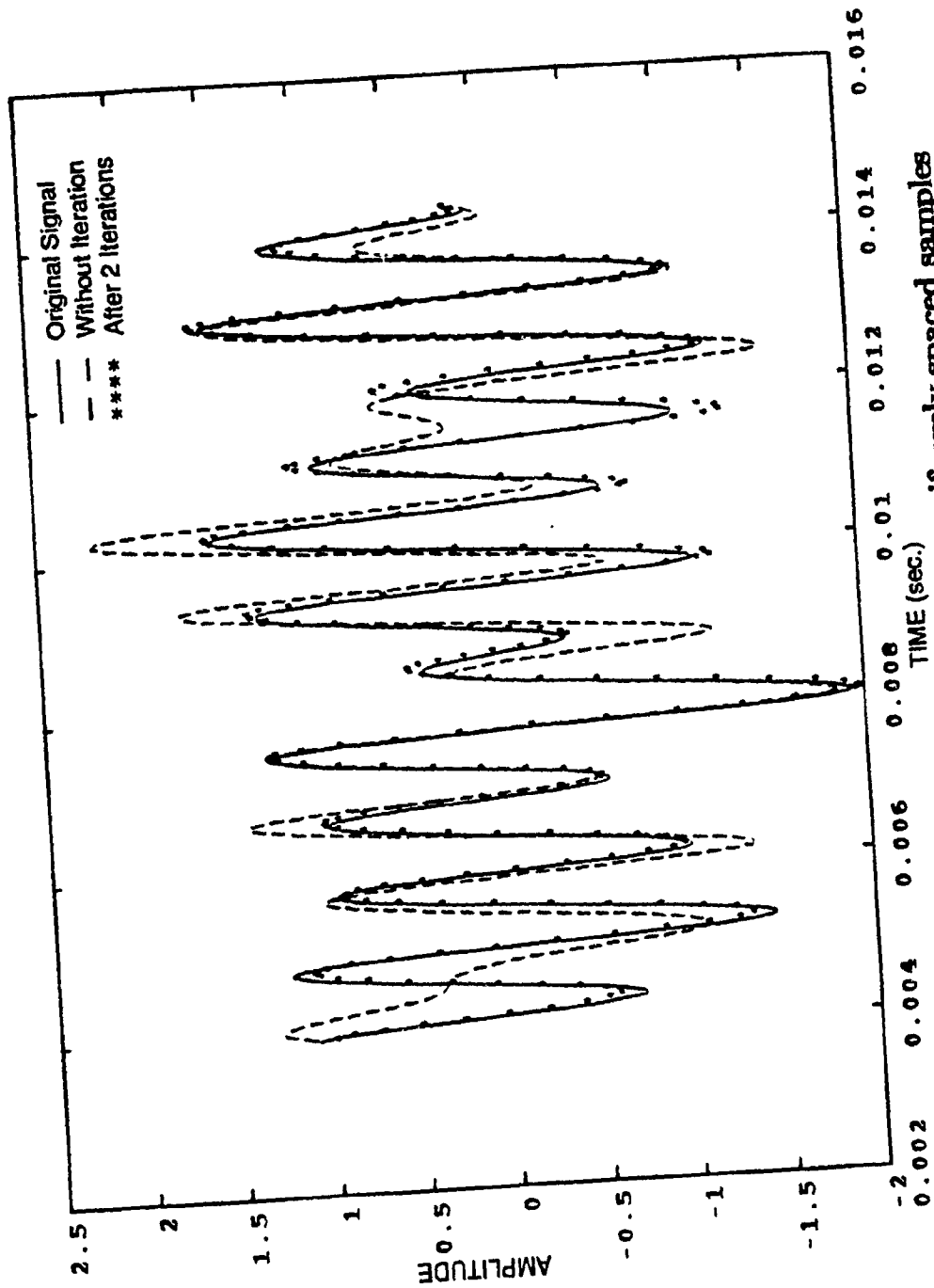


Fig. 5.6 (a): Reconstruction from nonuniformly spaced samples
($\text{SNR}_{\text{IN}} = +10\text{db.}$; random Gaussian noise; PS)

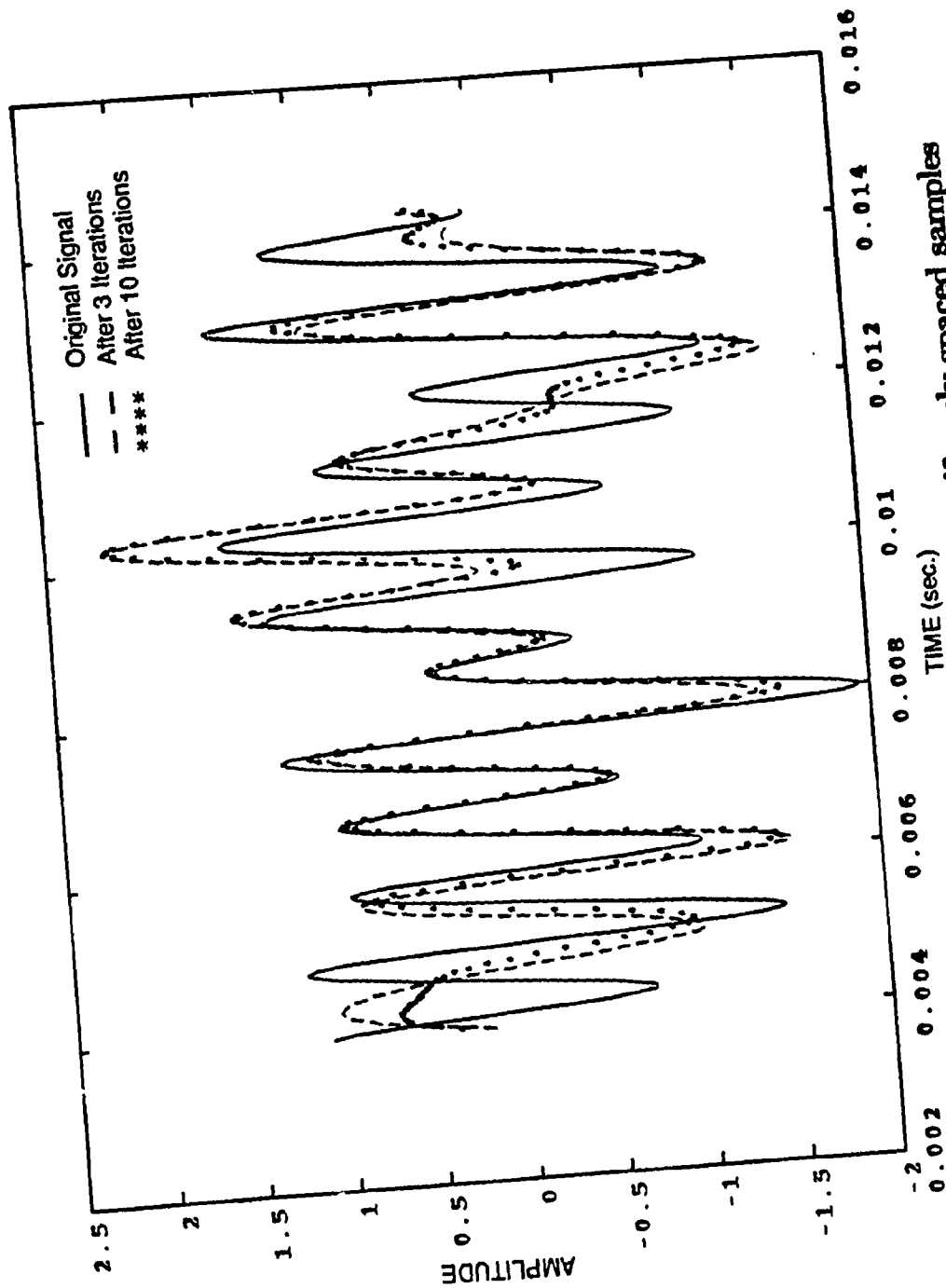


Fig. 5.6 (b): Reconstruction from nonuniformly spaced samples
($\text{SNR}_{\text{IN}} = +10\text{db.}$; random Gaussian noise; MA)

Fig. 5.7 compares the performance of the two methods PS and MA for all the three cases studied. X and Y axes corresponds to SNR_{IN} and the calculated MSE. It has four curves representing two curves for each method. It is evident from this study that for an increase in SNR_{IN} causes an increase in MSE. For a weak signal to noise ratio ($SNR_{IN} = -10db.$), all the four curves have a MSE value below 10% and this trend breaks down when the SNR_{IN} ratio is increased to 0 db. and 10 db. When the iterative algorithm is implemented, irrespective of the SNR_{IN} ratio, MSE is reduced for the PS method. Fig. 5.7 also shows that for MA, the MSE after 10 iterations is approximately the same as that without iteration. Typically considering $SNR_{IN} = 0db.$, the MSE are respectively calculated as 30% and 0.5% for without and with 2 iterations by applying the PS, whereas they are respectively 39% and 30% for 3 and 10 iterations by implementing the iterative scheme of MA. From these discussion it is clear that the MSE of the PS decreases rapidly from 30% to 0.5% while the rate of decrease of MSE is very low for the MA method.

From the above analysis it is evident that the reconstruction of a deterministic signal in the presence of random noise, can not only be performed by the present computer code, but also the performance is found to be better than the MA method. It should be noted that even by increasing the number of iterations for the MA method, the reduction in error is not well pronounced, whereas the PS performs better with limited computational efforts. It can be concluded that the performance of PS is superior to that of MA.

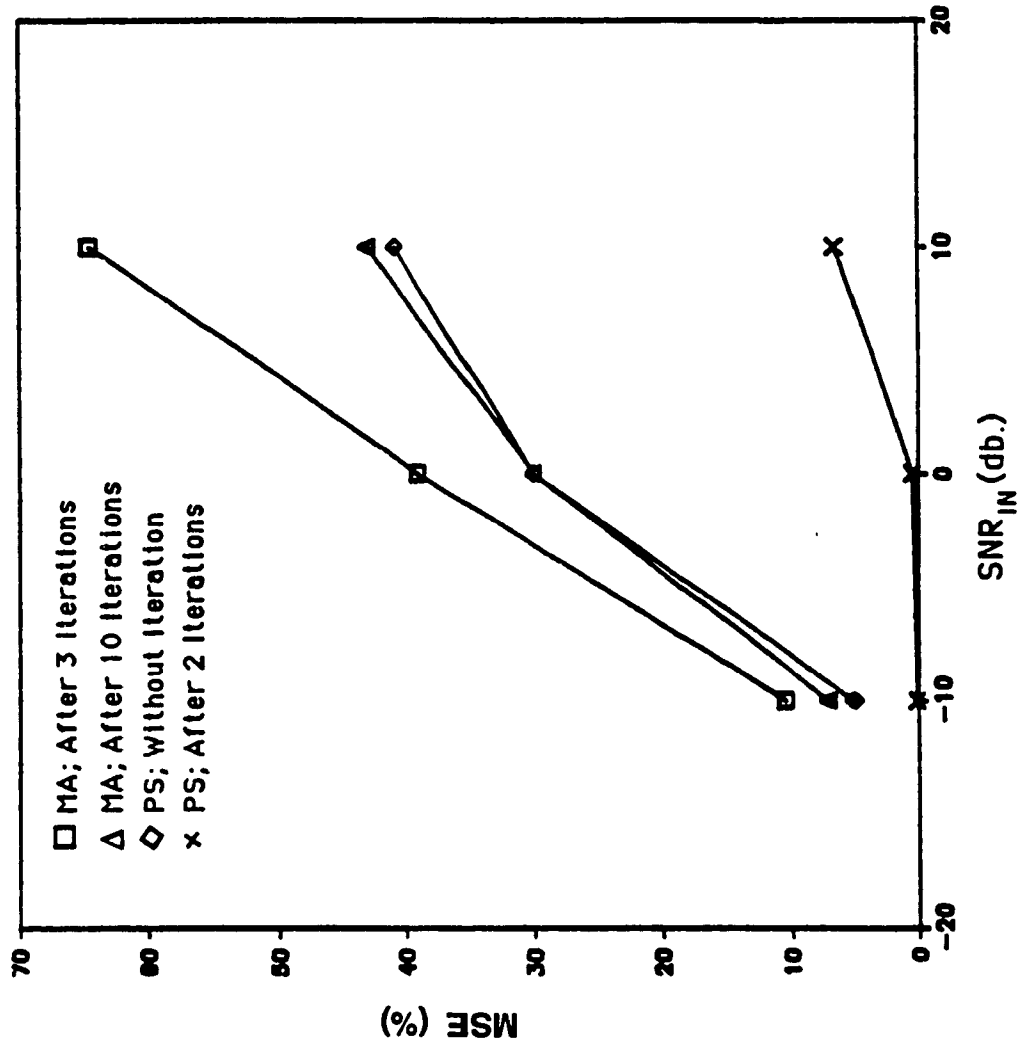


Fig. 5.7: Comparative study of MSE between PS and MA

5.3.2 Uniform Distribution

In order to shed some further light on the stability of the reconstruction procedure, the results are repeated for the case of uniformly distributed background noise. Consider a sequence of 42 samples that are extracted at $\{t_k\}$ instants using Equation (5.5). These time instants are distributed with uniform density function in the range of $-\Delta t/2$ to $\Delta t/2$ around its corresponding synchronous positions $\{k\Delta t\}$. f_m and f_s are respectively chosen as 1100 Hz. and 2400 Hz. For the PS, M is chosen as 3 and the iterative procedure is repeated twice.

Refer Fig. 5.8 (a) and (b), where the simulated results are plotted by applying PS and MA respectively. Fig. 5.8 (a) emphasizes that the amplitude of the reconstructed signal, without iteration (dash line) differs from the original signal (solid line) whereas the agreements are improved after 2 iterations. In contrast, Fig. 5.8 (b) reveals that there is no considerable improvement even after 10 iterations. Note the departure in the reconstructed signals from the solid line for both 0.004 sec. and 0.012 sec. The above figures correspond to $SNR_{IN} = 0\text{db}$. and the same arguments are also found to be valid when the SNR_{IN} is increased to 10 db., for which the results are displayed in Fig. 5.9 (a) and (b) respectively for PS and MA. From Fig. 5.9, it is found that the reconstructed signals (dash lines) are more distorted than the previous case (Fig. 5.8). In the PS method, one might attain better results even with limited number of iterations.

For both PS and MA the MSE are calculated and found to be less than the Gaussian distribution. In fact the MSE levels for the PS are only 7.5% and 0.04% when

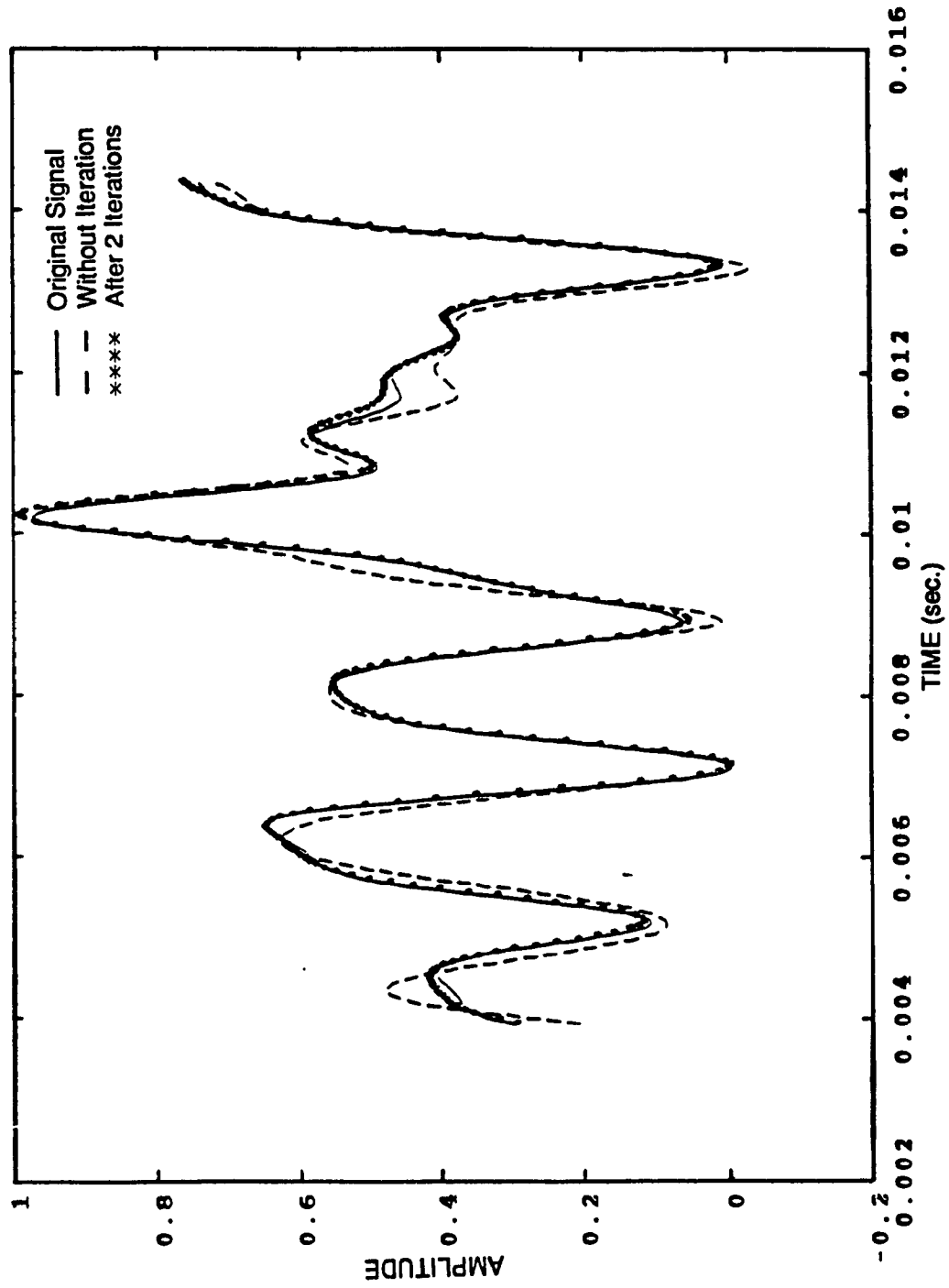


Fig. 5.8 (a): Reconstruction from nonuniformly spaced samples
($\text{SNR}_N = 0\text{db.}$; random uniform noise; PS)

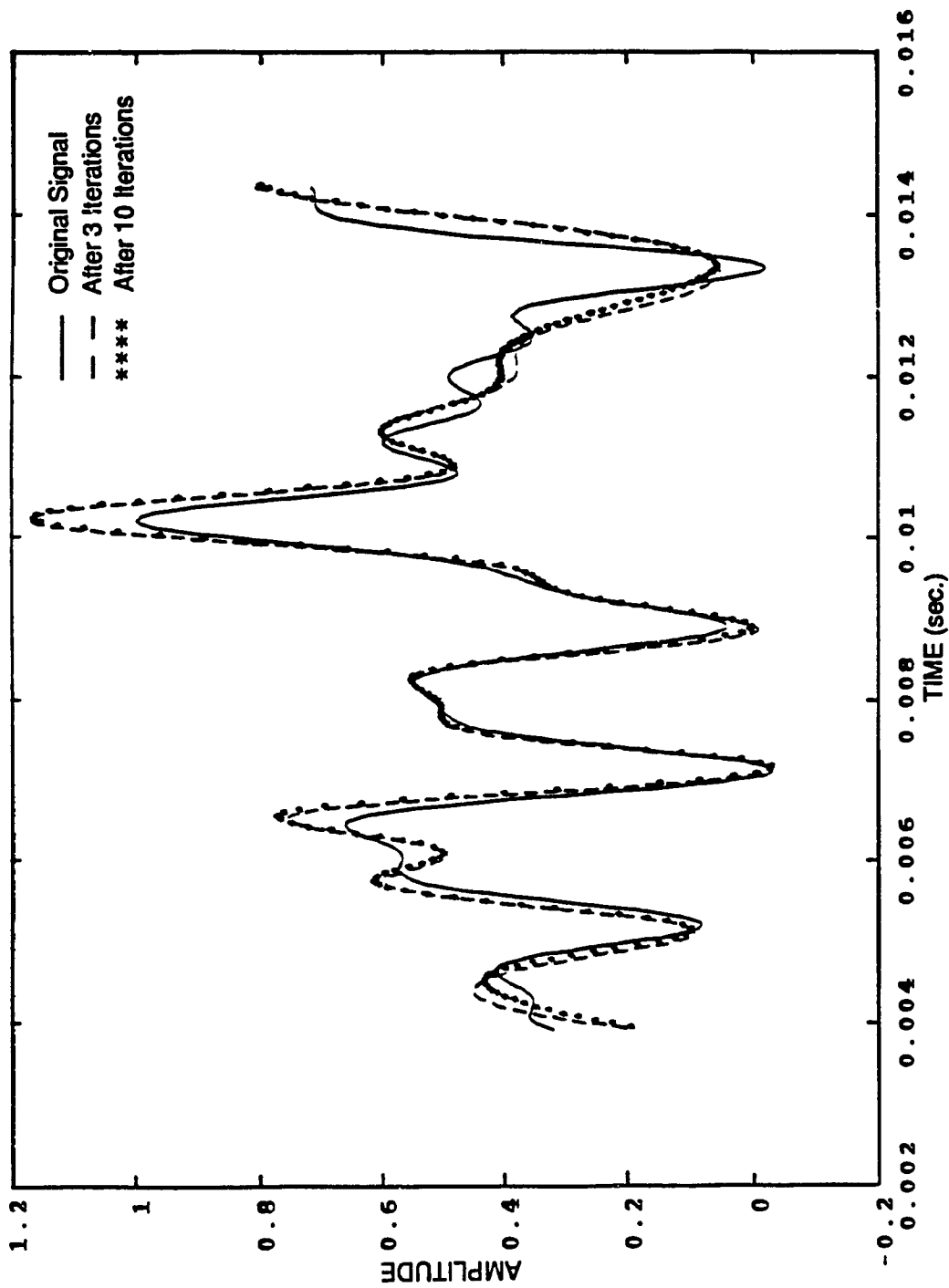


Fig. 5.8 (b): Reconstruction from nonuniformly spaced samples

($\text{SNR}_{\text{IN}} = 0\text{db.}$; random uniform noise; MA)

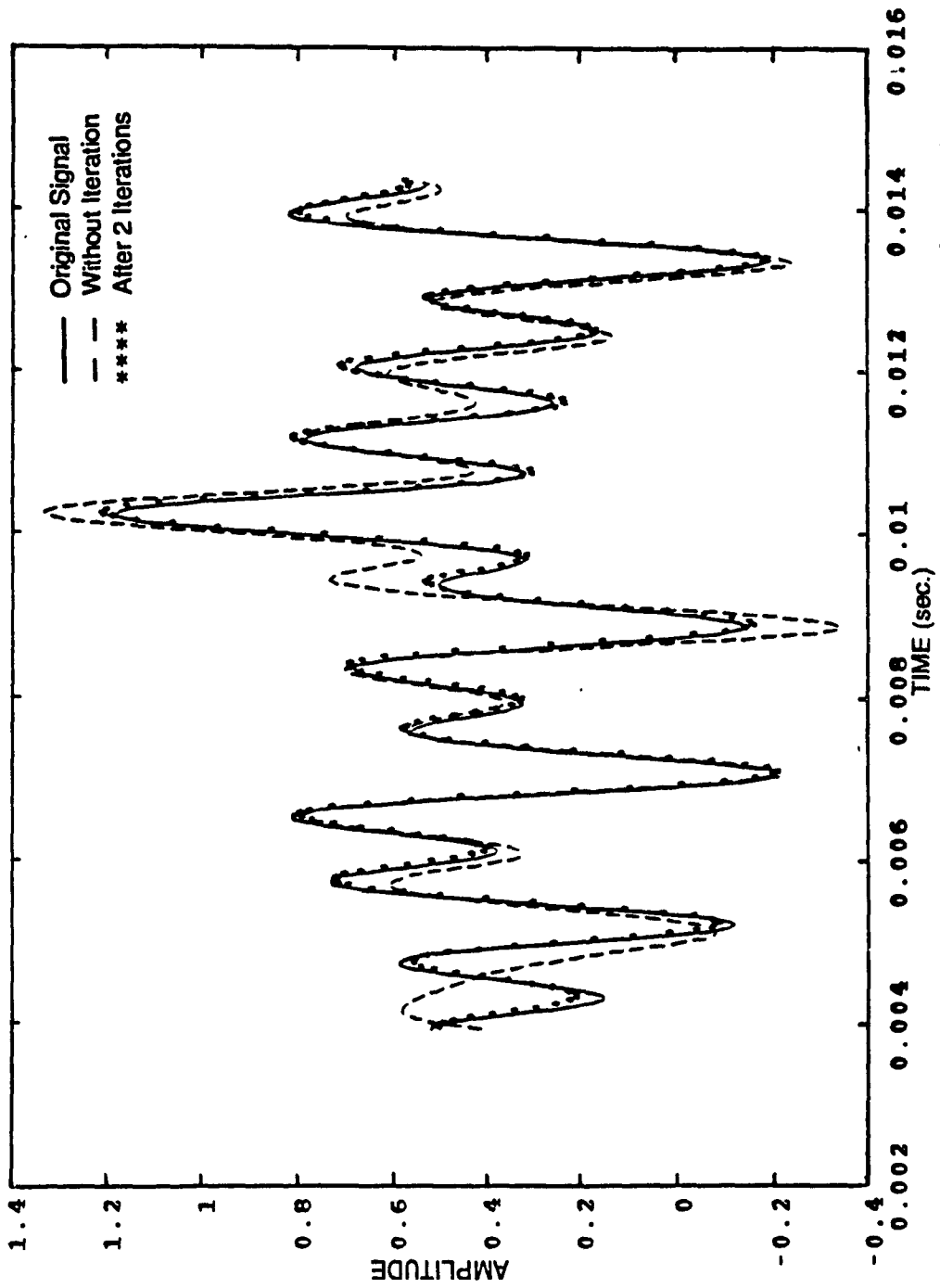


Fig. 5.9 (a): Reconstruction from nonuniformly spaced samples

($\text{SNR}_{\text{IN}} = +10\text{db.}$; random uniform noise; PS)

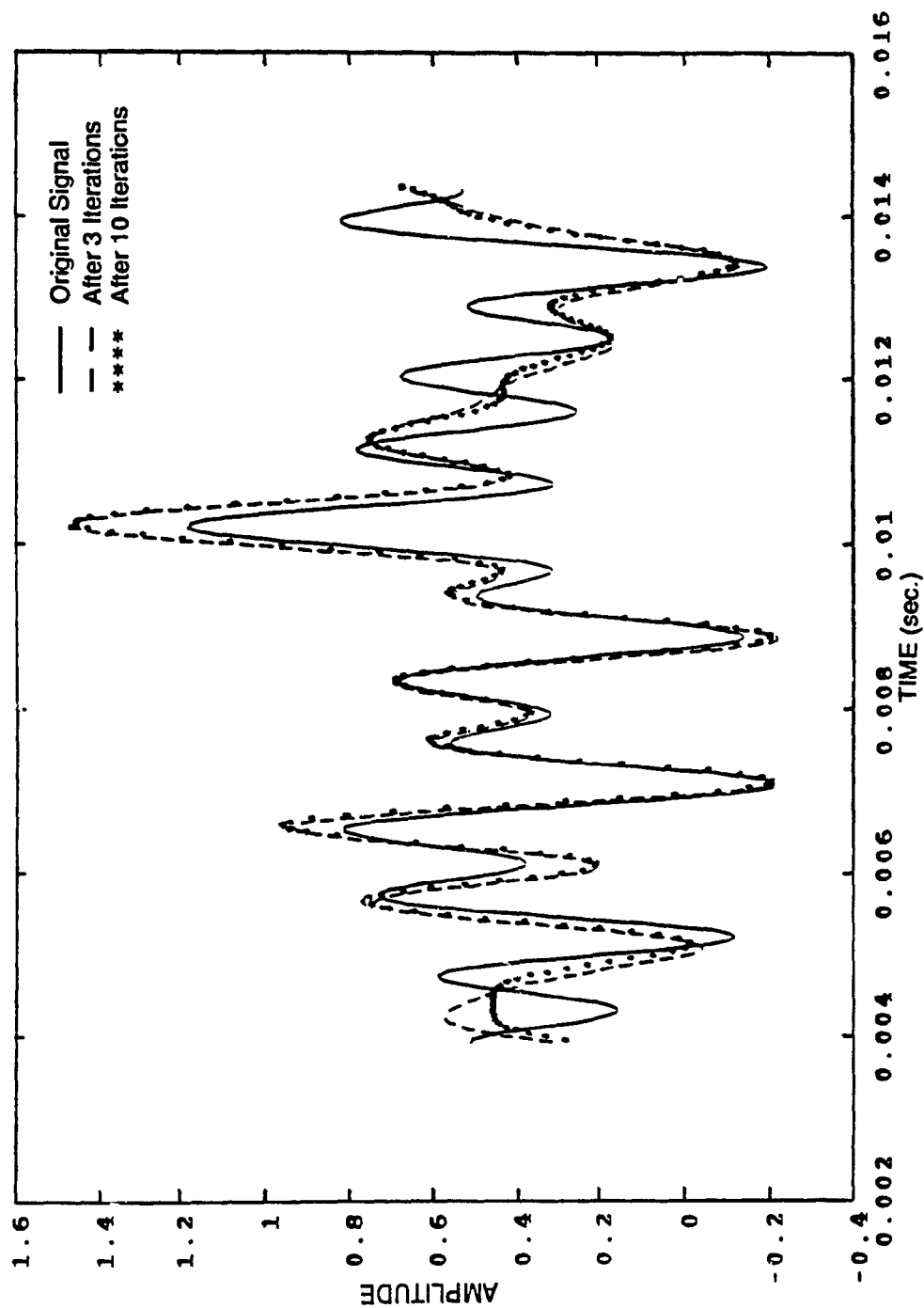


Fig. 5.9 (b): Reconstruction from nonuniformly spaced samples

($\text{SNR}_{\text{IN}} = +10\text{db.}$; random uniform noise; MA)

$SNR_{IN} = +10db$. They are reduced further to 1.7% and 0.03%, when SNR_{IN} considered is 0 db. By using MA method also the MSE (3.8% and 2.8% for $SNR_{IN} = 0db$; 13% and 10% for $SNR_{IN} = +10db$.) are calculated. In the case of random distribution (-ref: Fig. 5.2 and Fig. 5.3), the calculated MSE level is low in comparison to the deterministic sinusoidal wave (-ref: Fig. 4.3), for the same power. From this it is evident that an increase in noise or when the signal is weak, it will reduce the MSE level. In all the above discussion the performance of the PS is found to be better than that of the MA method.

5.4 STATISTICAL ANALYSIS OF THE COMPUTED ERRORS

All the results discussed in the above section as well as in the previous chapter are obtained by fixing the number of trial as 1 (-refer the computer code Fig. 4.1). During this trial, 42 samples are extracted at $\{t_k\}$ instants. These instants are uniformly distributed within the range of $-\Delta t/2$ to $\Delta t/2$ from their corresponding synchronous positions $\{k\Delta t\}$. If "NT" trials are performed then one should calculate, "NT" number of MSE values. The results and observations were presented for a stochastic signal, under the assumption of a stationary ergodic process and MSE were computed for the considered trial. However to validate the assumption of the stationarity and ergodicity of the process, for the considered observation interval, the MSE are also computed for different realizations of the same process. This section consists of three subsections discussing two statistical parameters, mean and standard deviation. First investigation for the above parameters is on the reconstruction of a sinusoidal function with uniformly distributed initial phase from its unequally spaced samples. Secondly, the uniformly distributed random process will be considered as a signal under analysis. The

summation of a sinusoidal function and a random uniformly distributed process is considered in the third subdivision.

The MSE are computed for without iteration, with 1 and 2 iterations for a particular realization, say, at the first trial. During the second trial also a set of MSE are computed. By performing "NT" trials the mean of MSE can be estimated as:

$$\overline{MSE} = \frac{\sum_{i=1}^{NT} MSE_i}{NT} \quad (5.7)$$

Note that "NT" is the number of trials and for the present study it is 100. Similar calculation for the mean values of MSE for without, with 1 and 2 iterations can be performed and they are respectively denoted by \overline{MSE}_0 , \overline{MSE}_1 and \overline{MSE}_2 .

The second statistical parameter, 'standard deviation', is calculated as follows. Let the standard deviation of MSE for the case without iteration be denoted as " $\bar{\sigma}_0$ ". It can be mathematically expressed as follows:

$$\bar{\sigma}_0 = \frac{\sqrt{\sum_{i=1}^{NT} MSE_i^2 - \overline{MSE}_0^2}}{NT - 1} \quad (5.8)$$

where \overline{MSE}_0 is already computed using Equation (5.7). By following the same steps, $\bar{\sigma}_1$ and $\bar{\sigma}_2$ are computed based on the previously calculated \overline{MSE}_1 and \overline{MSE}_2 values respectively. Effect of the trials on these two parameters for various cases will be discussed in the following subsections.

5.4.1 Sinusoidal Function With Uniformly Distributed Initial Phase

Consider a sequence of 42 samples are extracted at $\{t_k\}$ instants. They are uniformly distributed in the specified range of their corresponding synchronous positions $\{k\Delta t\}$. The other input conditions remain the same as before namely, $f_m = 1100\text{Hz}$, $f_s = 2400\text{Hz}$ and $M = 3$, $Iter = 2$ and $NT = 100$ and $0 < J < 2.0$.

The sinusoidal function with uniformly distributed initial phase can be obtained as follows. Let $x_1(t)$ be the generated function for the first trial.

$$x_1(t) = A_1 \sin(\omega_1 t + \Psi_1) \quad (5.9)$$

where A_1 and Ψ_1 are the amplitude and the phase of the sinusoidal function respectively and $\omega_1 = 2\pi f_m$. During the m-th trial, the random realization of the process will be different and as a result, the generated $x_m(t)$ can be expressed as:

$$x_m(t) = A_m \sin(\omega_m t + \Psi_m) \quad (5.10)$$

The amplitude and the band-limiting frequency remain the same for the two trials i.e.,

$$A_m = A_1, \quad \omega_m = \omega_1$$

while the initial phase Ψ_m is uniformly distributed

$$0 < \Psi_i < 2\pi$$

within the range $(0, 2\pi)$.

Fig. 5.10 (a) illustrates the variation of jitter by considering a sinusoidal function with uniformly distributed initial phase. It displays three curves corresponding to without, with 1 and 2 iterations. The X and Y axis are respectively the jitter parameter (J) and the mean of Mean Squared Error (\overline{MSE}). When the iterative procedure is implemented, the second and the third curves lie very close to each other. In order to show clearly the data points for these curves, they are also displayed in the same

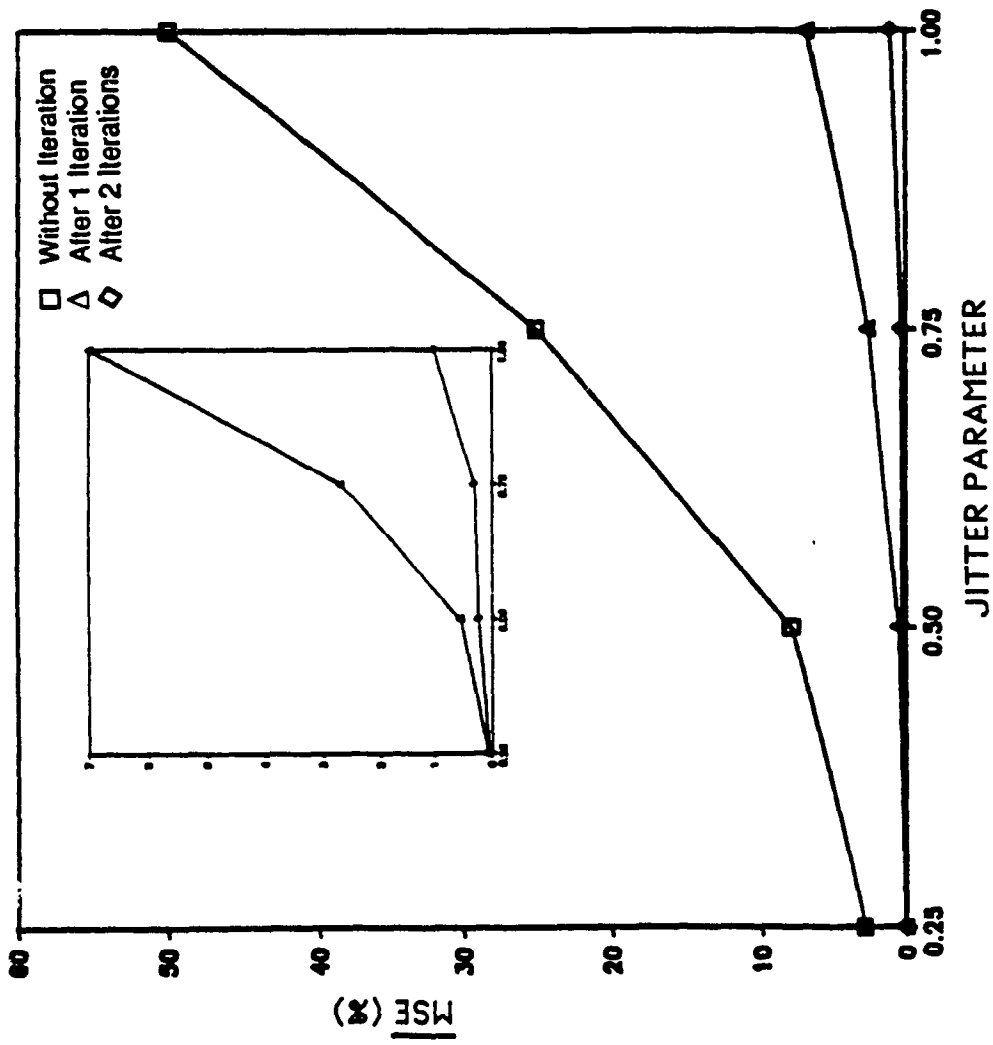


Fig. 5.10 (a): Mean of MSE for sinusoidal function with uniformly distributed initial phase ($M = 3$)

figure by selecting a different scale for the vertical axis. It is worth mentioning that the results for this figure is obtained after running the program for 400 trials, on the basis of 100 trials for each jitter. For each trial a set of MSE are calculated respectively for without, with 1 and 2 iterations and then the mean value of the errors are obtained by using the Equation (5.7).

It is evident from Fig. 5.10 (a) that the value of jitter error ($e_j(t)$) increases with an increase in J , which in turns causes an increase in the \overline{MSE} levels. This has been found to be true for the all three curves. For $J = 0.5$, the computed \overline{MSE}_0 and \overline{MSE}_2 are 8% and 0.2% respectively. Recall that for Fig. 4.3 (a) which shows the results of the first realization, the respective MSE levels are 9.6% and 0.12%. Similarly consider $J = 1$, the \overline{MSE}_0 and \overline{MSE}_2 are estimated to be 50% and 1% respectively which compares with its counterpart 48.3% and 0.71% for without and with 2 iterations respectively (-refer Fig. 4.5 a). Thus irrespective of the variation of J , the \overline{MSE} (mean of MSE) after 100 trials lies closer to the first realization.

The standard deviation is also computed using Equation (5.8), and Fig. 5.10 (b) shows the three curves for without, with 1 and 2 iterations respectively. The X and Y axis are respectively J and the standard deviation of MSE. It is evident that the standard deviations $\bar{\sigma}_0$, $\bar{\sigma}_1$ and $\bar{\sigma}_2$ all increase with J . In Equation (5.8), $\bar{\sigma}_0$ is directly proportional to the difference between MSE_i and \overline{MSE}_0 . If MSE_i lies closer to \overline{MSE}_0 then $\bar{\sigma}_0$ is minimum; that is the standard deviation of MSE is minimum. For $J = 0.5$, $\bar{\sigma}_0$ and $\bar{\sigma}_2$ are 1.52 and 0.05 respectively. Similarly, when $J = 1.0$, $\bar{\sigma}_0$ and $\bar{\sigma}_2$ are 9 and 0.9. From the presented discussion three features are evident. First feature is that the calculated \overline{MSE} 's and $\bar{\sigma}$'s are minimum, and the second is that when the iterative

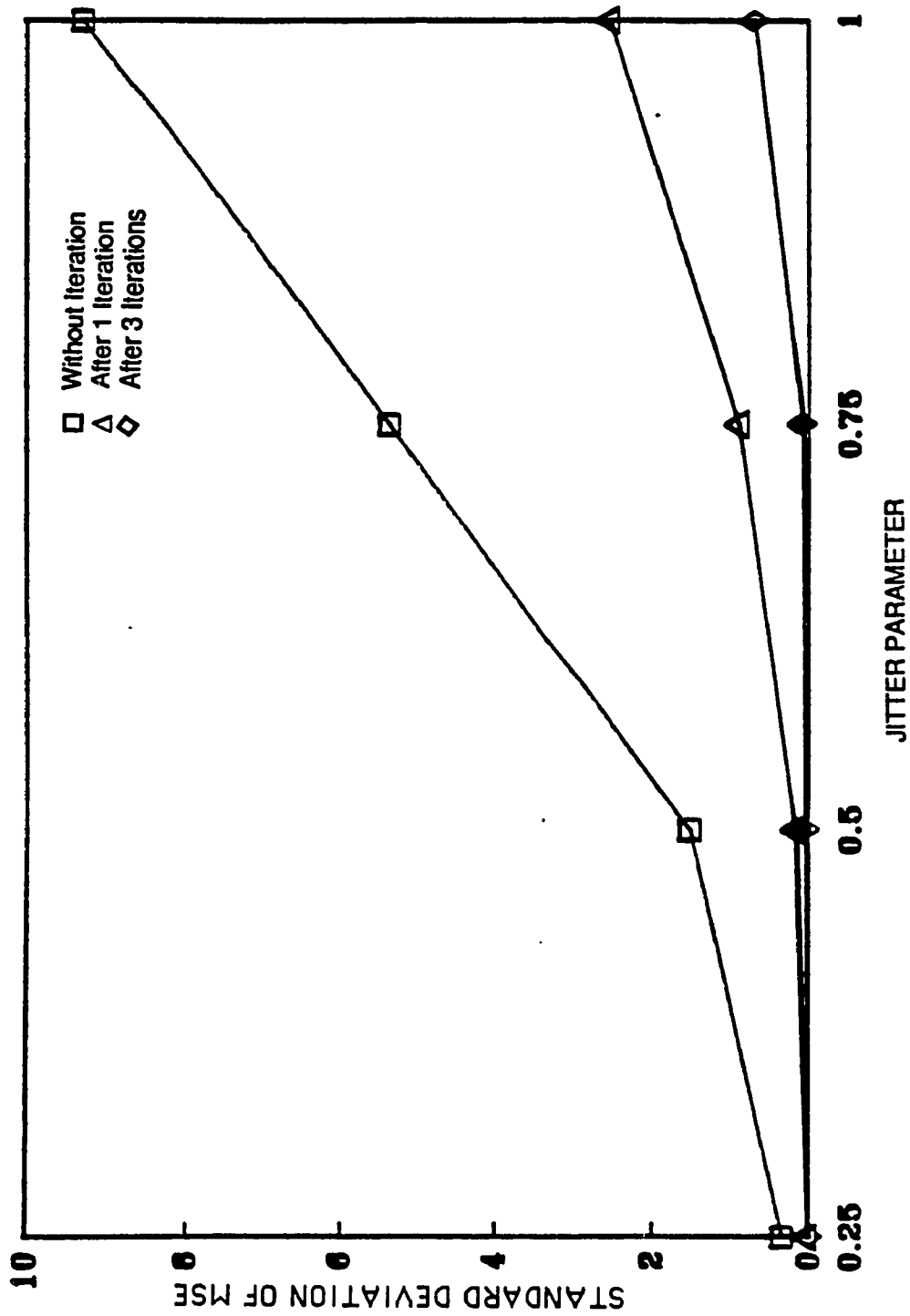


Fig. 5.10 (b): Standard deviation of MSE for sinusoidal function with uniformly distributed initial phase ($M = 3$)

procedure is implemented the differences due to trials are further reduced. Thirdly, the assumption of stationary ergodicity is found to be true when the process is repeated for many trials, by studying the random realization of the samples in an observation interval.

In the above figures mentioned, J is varied from 0.25 to 1.0 and thus the value of M for partitioning scheme is 3. J is further increased and statistical parameters are also compared. When J is increased, M has to be increased in accordance with the partitioning scheme. Recalling Equation (4.4) which provides the requirement of M for the ranges of J , we have

$$\begin{aligned} 0.0 < J \leq 1.0; \quad M &= 3 \\ 1.0 < J \leq 2.0; \quad M &= 5 \end{aligned} \tag{4.4}$$

The value of M chosen to study the effect of J variation from 1.25 to 2.0 is 5.

Having the same input conditions as: $N = 42$, $f_m = 1100\text{Hz.}$, $f_s = 2400\text{Hz.}$, $Iter = 2$ and $NT = 100$, simulations are performed and Fig. 5.11 (a) illustrates the results in the same fashion as Fig. 5.10 (a), however with a different scale for Y axis. For this range of J the number of trials does not affect the mean of the MSE and thus the MSE of the first trial is approximately the same as that of the mean of the MSE from 100 trials. Fig. 5.11 (b) shows the analysis of standard deviation. It is found that the standard deviation has a very small value, implying MSE will vary only marginally from \overline{MSE} . An increase in the value of the standard deviation is also observed with an increase in J .

From the above analysis it is clear that an increase in J causes a direct increase

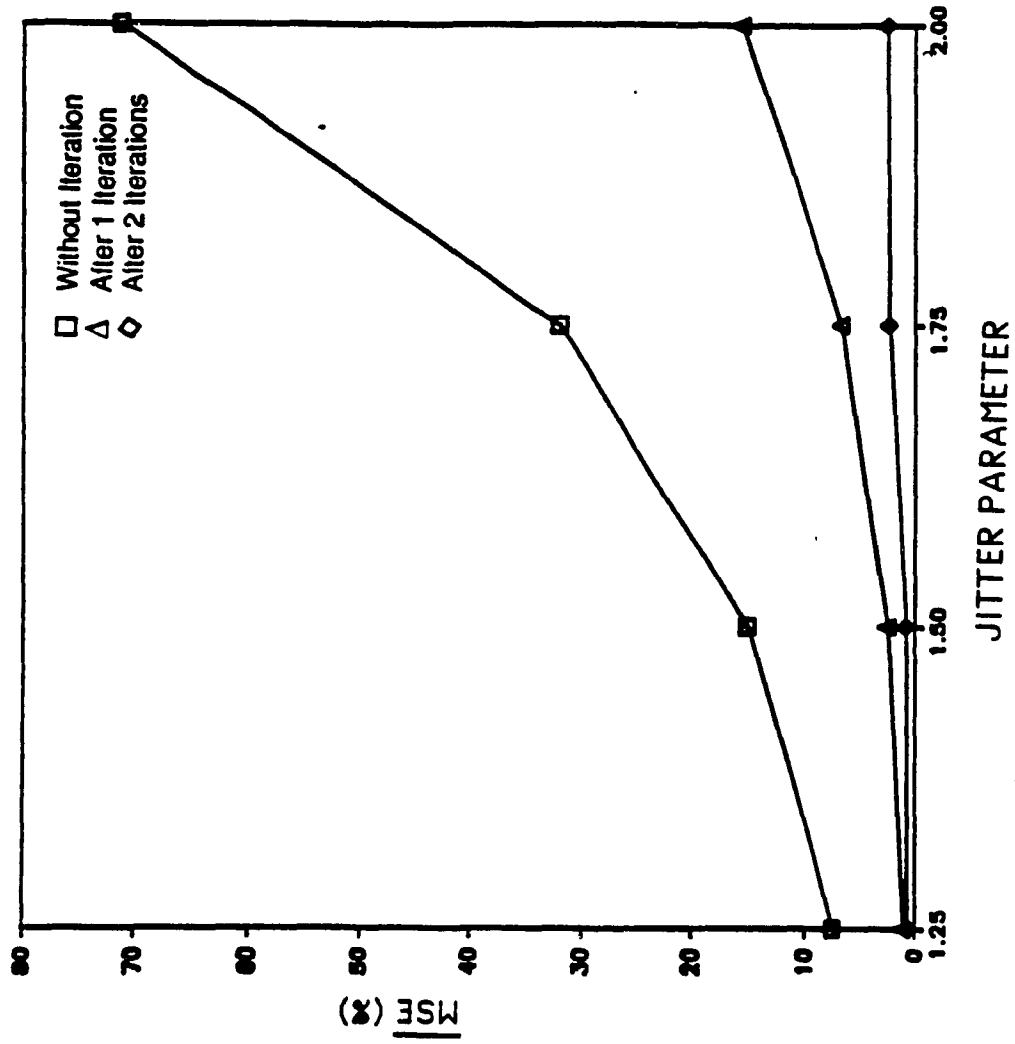


Fig. 5.11 (a): Mean of MSE for sinusoidal function with uniformly distributed initial phase ($M = 5$)

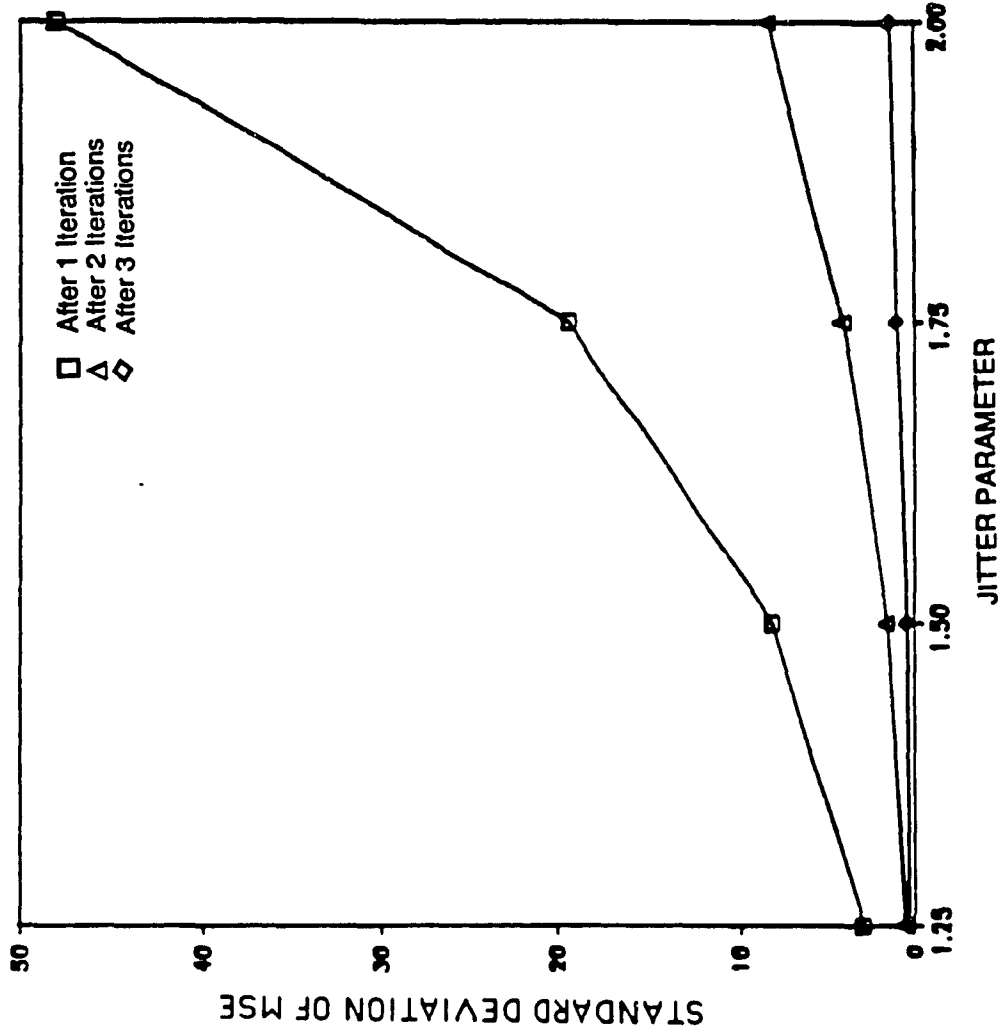


Fig. 5.11 (b): Standard deviation of MSE for sinusoidal function with uniformly distributed initial phase ($M = 5$)

both in the mean and the standard deviation values. It is also equally clear that the MSE for the first trial and the mean value from 100 trials has the same trend. If \overline{MSE} is almost same as that of MSE of the first trial, it means that the considered process may be a first order stationary ergodic process. This can be further confirmed from the analysis of the standard deviation which itself has only a small variation from the first realization to the 100th. Thus it can be formulated that the present code can reconstruct a sinusoidal function with uniformly distributed phase and the simulated results are not affected due to the number of trials performed.

5.4.2 Uniformly Distributed Random Processes

In this subsection the statistical parameters are analyzed with respect to a uniformly distributed random process. The reconstruction for the first trial is presented in the section 5.2 by considering a set of 42 samples which are extracted at $\{t_k\}$ instants and these instants are uniformly distributed in range of $-\Delta t/2$ to $\Delta t/2$ over their corresponding synchronous positions. The time instants are generated as either a Gaussian or uniform distribution by using Equation (5.5). These time instants may vary from trial to trial, and thus it may change the generated random signal. To identify these changes on the simulated results, the MSE's are calculated and analyzed. As before, 100 such MSE's are obtained and the mean of the MSE (\overline{MSE}) and its standard deviation ($\overline{\sigma}$) are presented in the following discussion. The other input parameters are $f_m = 1100\text{Hz}$, $f_s = 2400\text{Hz}$ and $M = 3$.

The calculated MSE are displayed in Fig. 5.12 (a). This figure clearly demonstrates a sufficient reduction in the mean error levels once the iterative procedure is implemented. An increase in the J value causes a considerable increase in \overline{MSE}

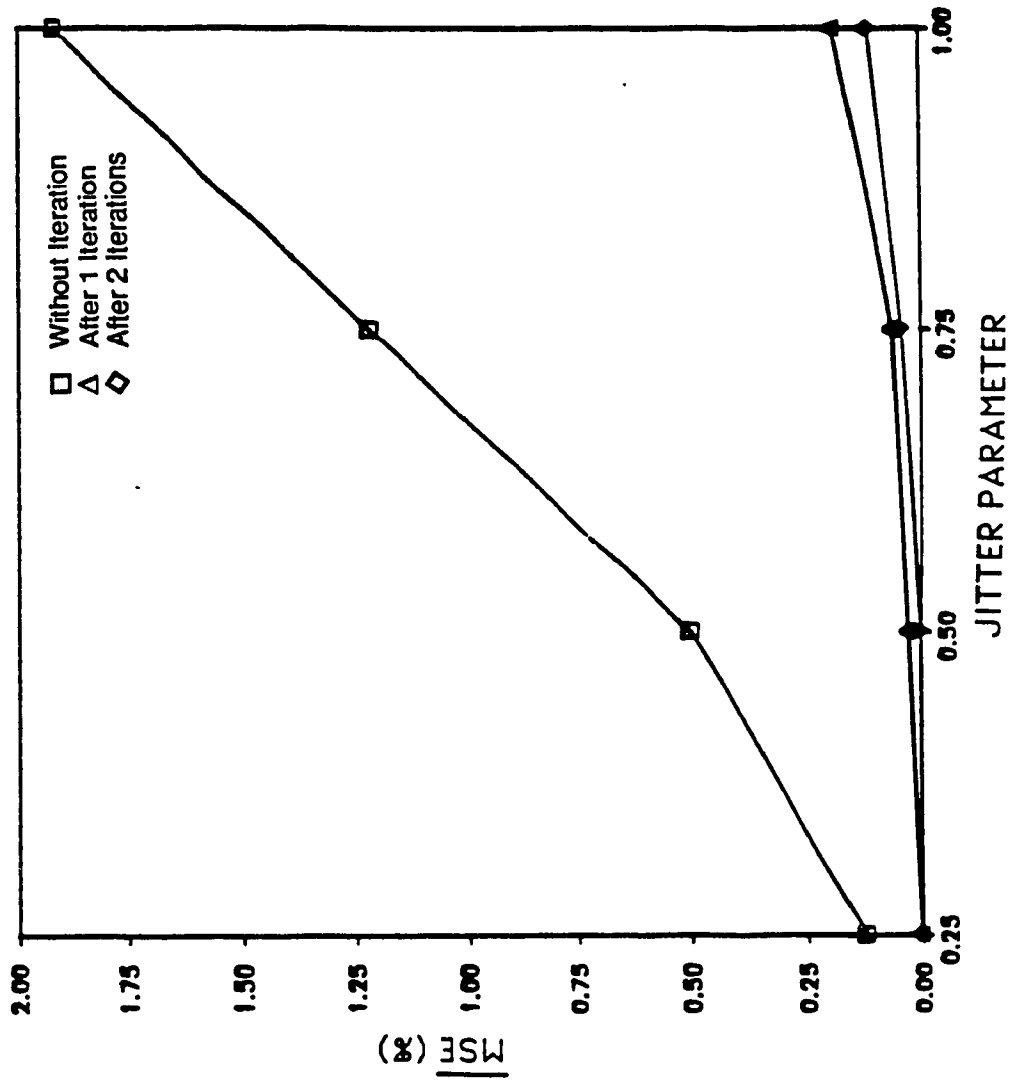


Fig. 5.12 (a): Mean of MSE for uniformly distributed random processes ($M = 3$)

values. Analysing a typical point $J = 0.5$, the computed \overline{MSE}_0 and \overline{MSE}_2 are respectively 0.5% and close to 0%. When comparing these values by increasing $J = 1.0$ the respective increase in values are 2% and 0.1%. It is interesting to realize that these computed MSE values agree well with these computed based on the first realization and discussed in Fig. 5.3. The mean for 100 trials are calculated as only 0.3% and 0.02% respectively for without and with 2 iterations. When $J = 0.5$, it is found that the number of trials do not influence the calculated MSE levels. Moreover, it is also clear that the difference in value diminishes, when the iterative procedure is implemented.

The standard deviation of the random uniform distribution for 100 trials is also studied. Fig. 5.12 (b) shows the observations in the same fashion as before. Since the standard deviation is very small after iterations compared to the without iteration values, they are displayed by using a different scale in the same figure. From this it is clear that the iterative procedure not only decreases the error but also minimizes the uncertainty involved in the generation of time instants. The above observation is true for the case of uniform distribution having a subinterval length $M = 3$ and the performance is further studied by increasing the subinterval length to 5.

The analysed results are presented in Fig. 5.13 (a) and (b) respectively for mean and standard deviation. The iterative procedure is repeated and MSE are computed for 1, 2 and 3 iterations. From the figure it is clear that \overline{MSE} is increased almost linearly with respect to J . When $J = 2.0$, \overline{MSE}_1 is relatively high. This is due to the selected M value for the partitioning scheme and the error can be easily reduced if one increases M from 5 to 7. Smaller magnitude values for the standard deviation are

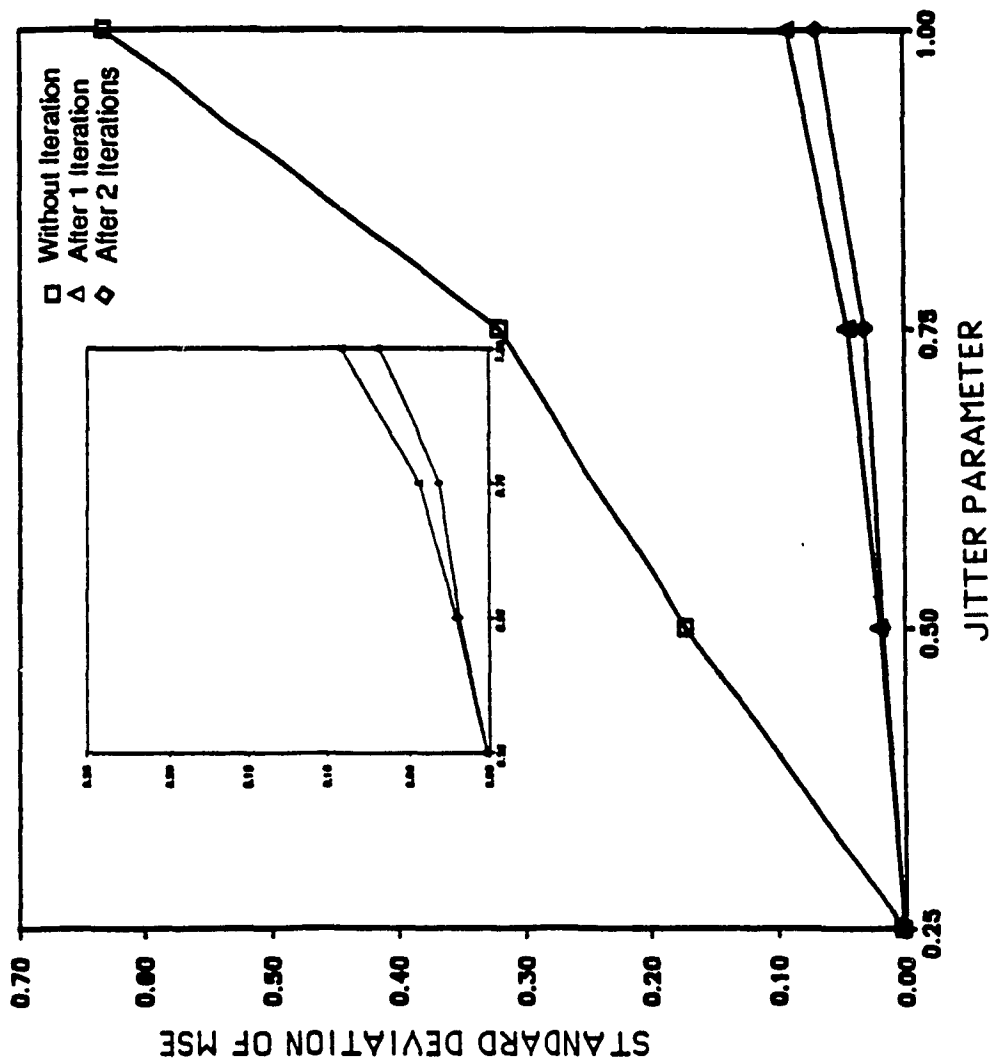


Fig. 5.12 (b): Standard deviation of MSE for uniformly distributed random processes ($M = 3$)

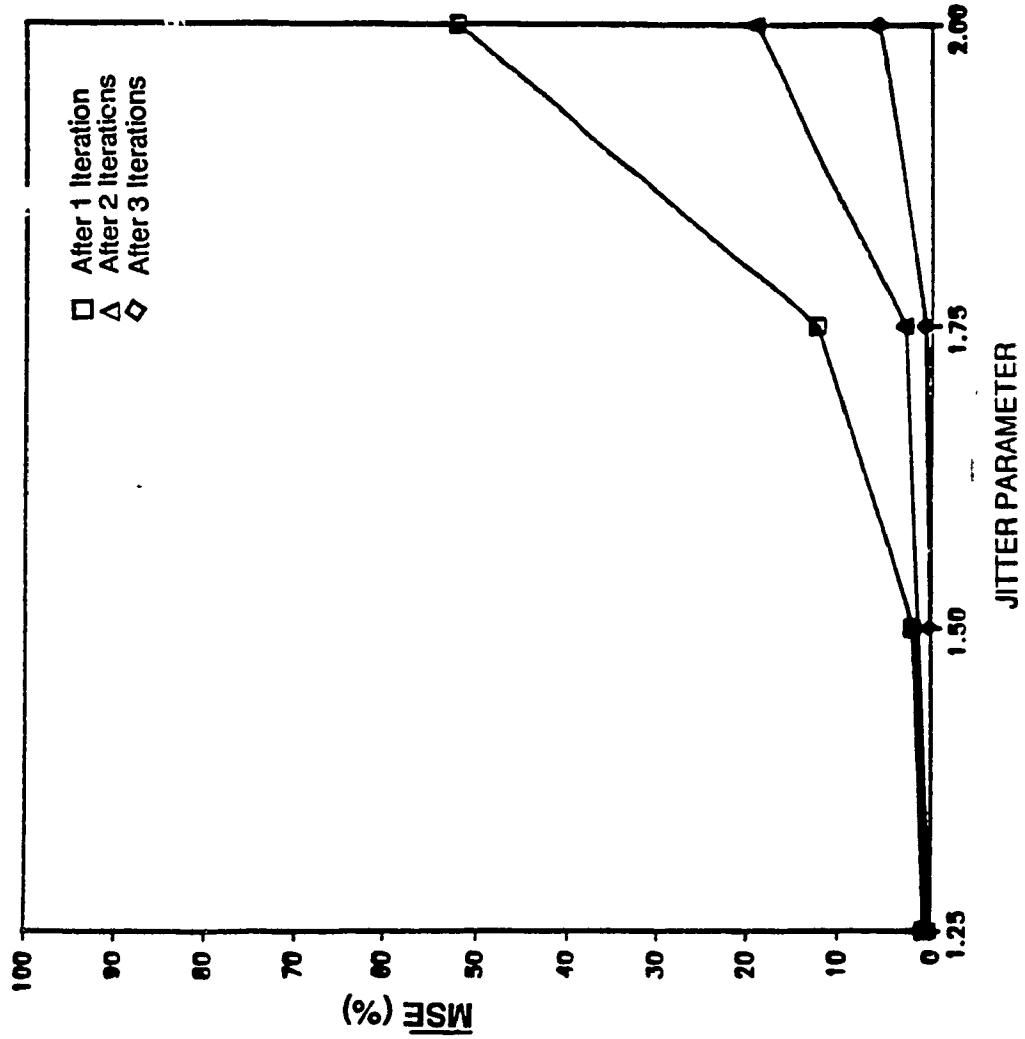


Fig. 5.13 (a): Mean of MSE for Uniformly Distributed Random Processes ($M = 5$)

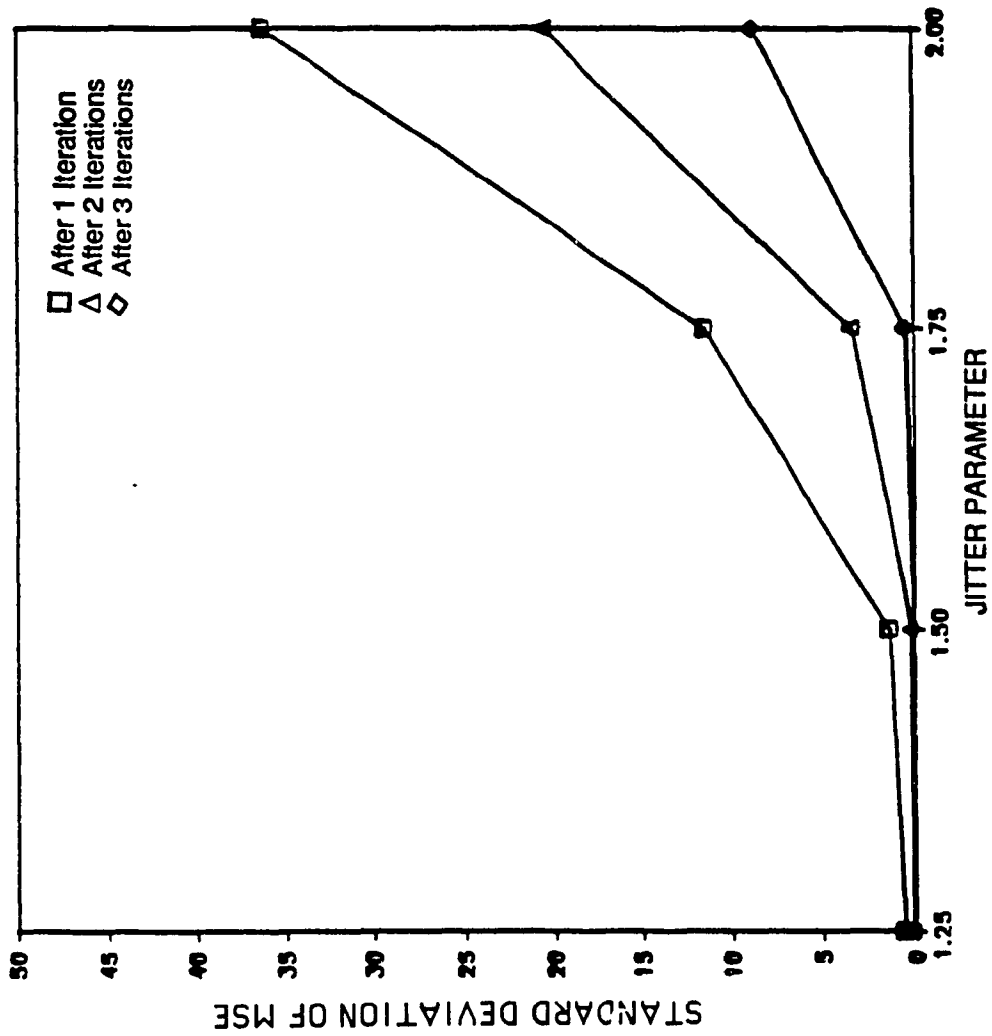


Fig. 5.13 (b): Standard deviation of MSE for uniformly distributed random processes ($M = 5$)

shown in the Fig. 5.13 (b). This shows the variation on the \overline{MSE} to be small. Thus it can be concluded that the MSE computed based on the first realization is about the same as \overline{MSE} obtained after 100 trials.

5.4.3 Sinusoidal Function in the Presence of Uniformly Distributed Random Process

This subsection carries a signal of nonstationary nature. The process considered is either a Gaussian or uniform distribution and they are reconstructed from their unequally spaced samples for different SNR_{IN} values. From section 5.3.2 it is found that the MSE variations for a uniform process behaves similar to that of a Gaussian distribution and thus the later is excluded from the present discussion of analyzing the effect of trials. Note that SNR_{IN} of Equation (5.6) is dependent on A_s and σ_n . Sample variance (σ_n) of the random noise may vary from trial to trial. In otherwords one should expect a slight variation in SNR_{IN} from one realization to another due to the variation in σ_n^2 . A_s is always kept constant as unity and not varied with realizations. The two statistical parameters are studied for SNR_{IN} of 20 db. The subinterval length (M) considered is 3 or 5 based on the range of J.

Consider a sequence of 42 samples extracted at $\{t_k\}$ instants with J ranging from 0 to 1.0. The other input conditions are $A_s = 1$, $N = 42$, $f_m = 1100\text{Hz.}$, $f_s = 2400\text{Hz.}$, $Iter = 2$ and $NT = 100$. As pointed out earlier, the initial phase is varied from trial to trial. The reconstruction is performed and the average values of the MSE are computed. The three curves namely without, 1 and 2 iterations are plotted in Fig. 5.14 (a). The second and third curves are displayed separately in order to

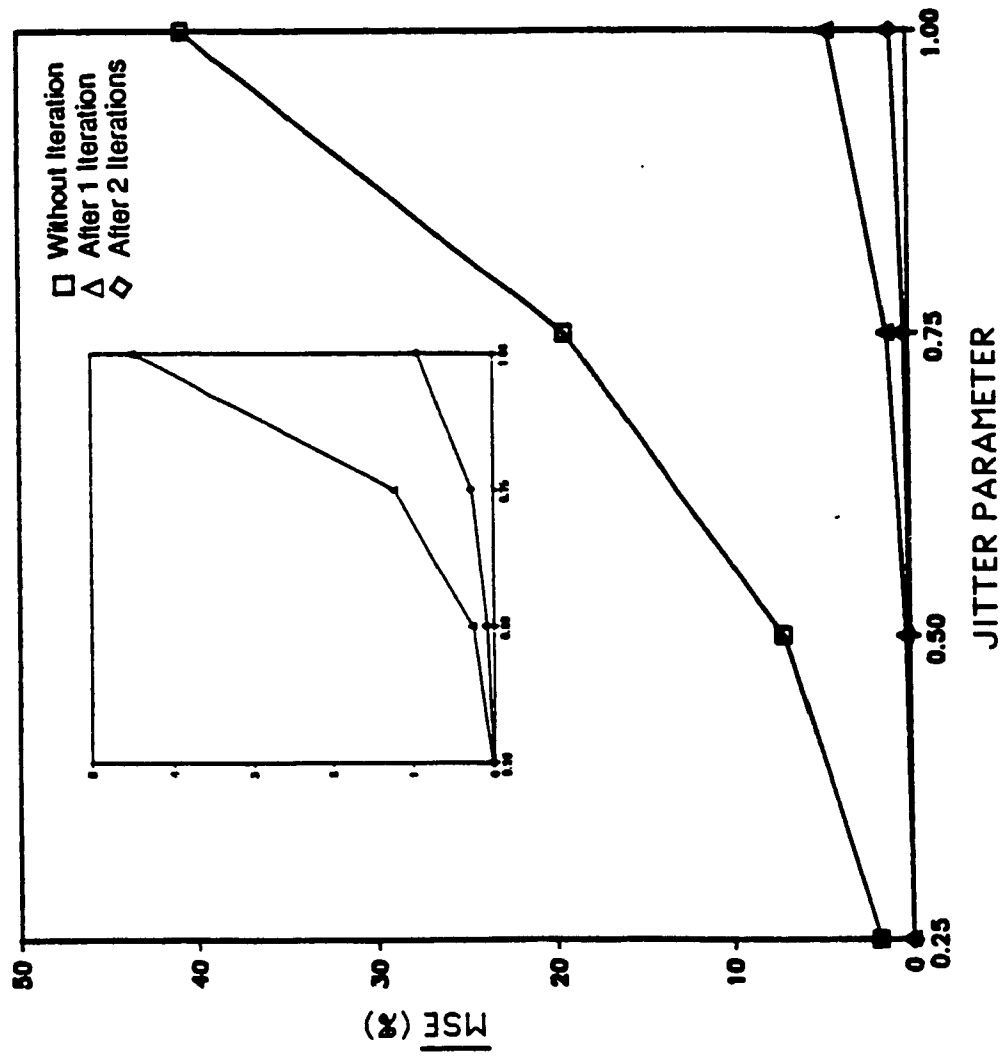


Fig. 5.14 (a): Mean of MSE for $SNR_N = 20\text{db}$. ($M = 3$)

Increase the clarity between the data points. The X and Y axes are respectively J and \overline{MSE} . \overline{MSE} of 1 and 2 iterations are close to 0.1% when J is 0.25 and 0.5. Considering $J = 0.5$, the \overline{MSE}_0 , \overline{MSE}_1 and \overline{MSE}_2 are computed as 7%, 0.3% and 0.08% respectively; however when $J = 1.0$ they are respectively 41%, 4.5% and 1%. Thus the mean of the error is increased when J is increased.

Fig. 5.14 (b) displays the corresponding analysis for the standard deviation. It has the same format as Fig. 5.13 (a). $\bar{\sigma}_0$, $\bar{\sigma}_1$ and $\bar{\sigma}_2$ are computed using equation (5.8) and they are 2, 0.2 and 0.04 for $J = 0.5$, whereas when J is increased to 1.0, they are respectively, 16, 3 and 0.8. Moreover, no abnormal changes are observed when the number of iterations are increased. Thus based on the mean and standard deviation it can be concluded that the simulated results hold good for the sum of a deterministic sinusoidal function and a random process.

Fig. 5.15 (a) and (b) illustrate the variation of mean and standard deviation for $1 < J \leq 2.0$, by choosing M as 5. Fig. 5.15 (a) displays three curves corresponding to \overline{MSE}_1 , \overline{MSE}_2 and \overline{MSE}_3 . The format is the same as Fig. 5.14 (a), however it has a different scale for the vertical axis. When $J = 2.0$, \overline{MSE} is found to be high. To reduce the \overline{MSE} without iteration one should increase the value of M from 5 to 7. Further, the second statistical function, standard deviation, is also computed and compared in Fig. 5.15 (b). Comparing the values of the second and third iterations, it is seen that the variation in the error is minimum. But when $J = 1.75$ and 2.0 it can be noted that the standard deviation is increased and this shows the deviation from \overline{MSE} is also high.

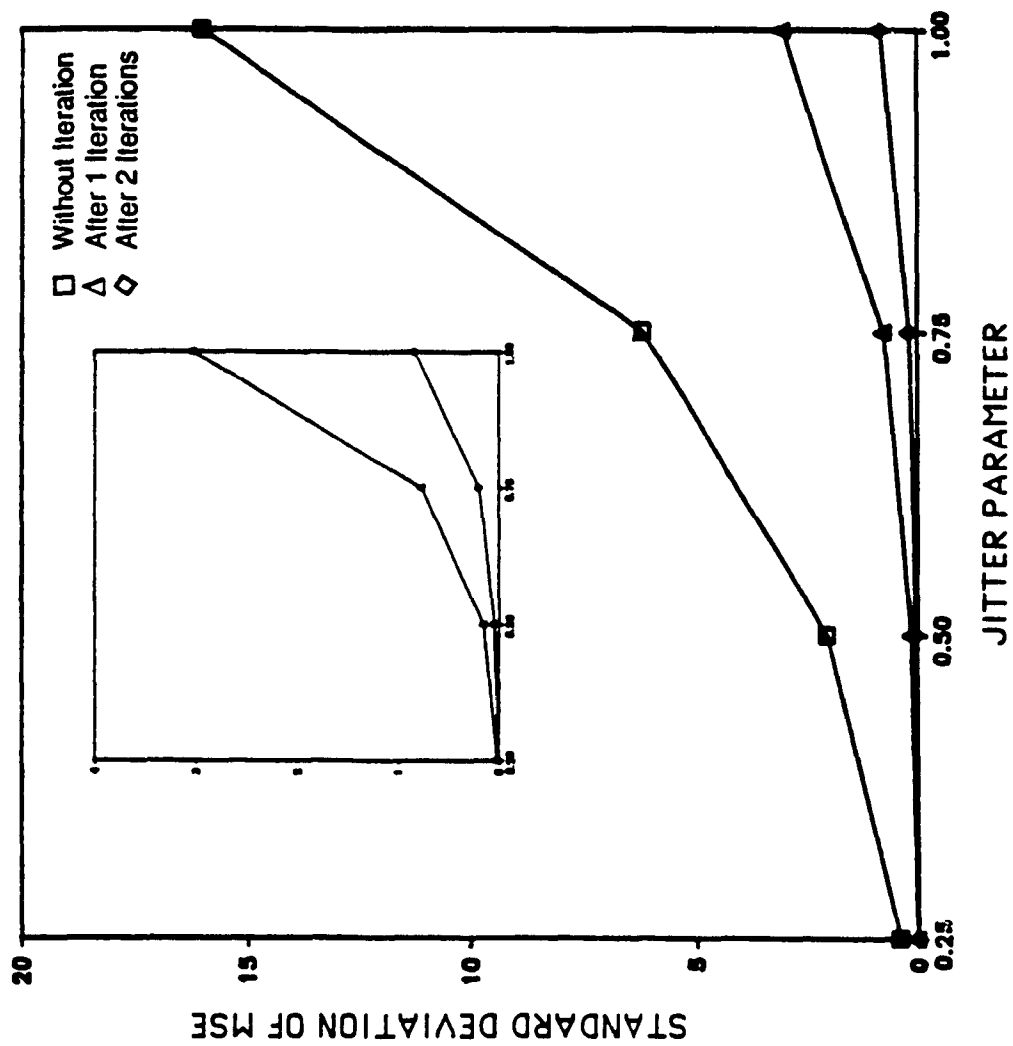


Fig. 5.14 (b): Standard deviation of MSE for $SNR_{1N} = 20\text{db}$. ($M = 3$)

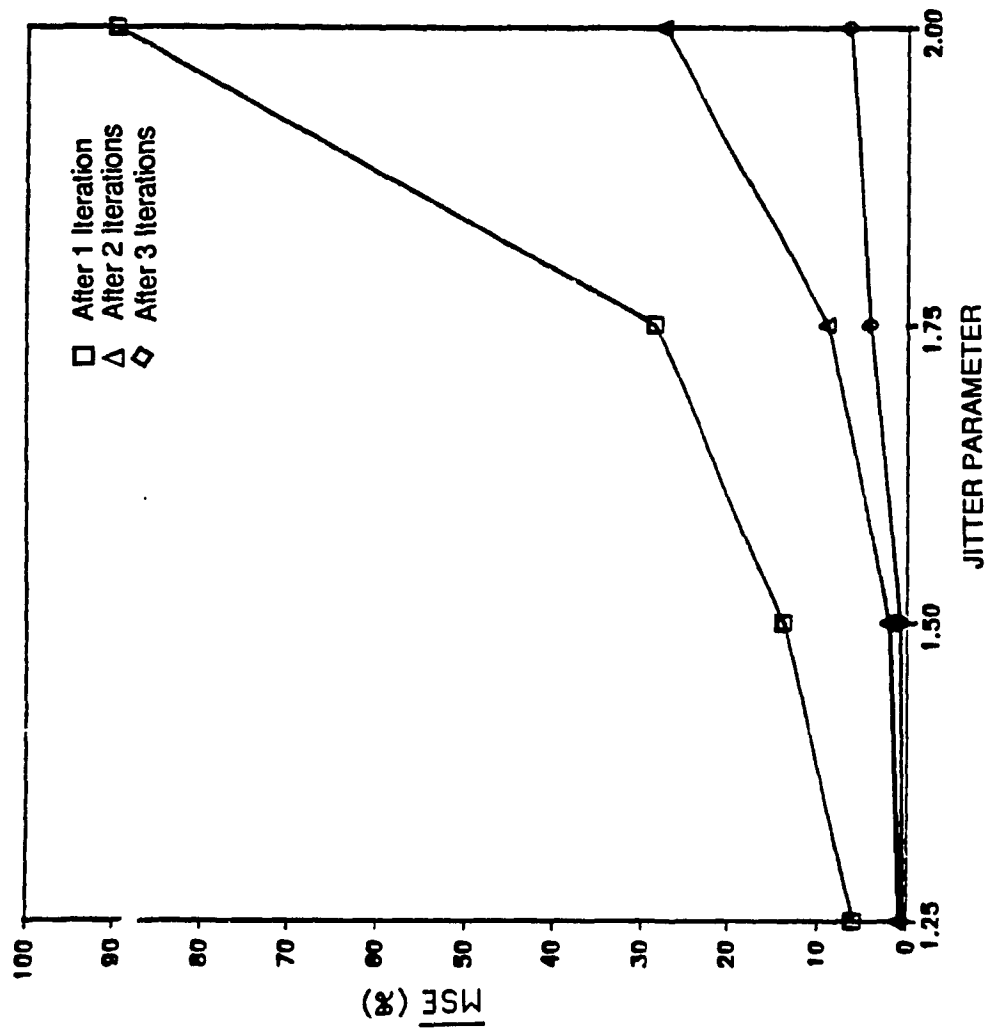


Fig 5.15 (a): Mean of MSE for $SNR_{IN} = 20\text{db}$. ($M = 5$)

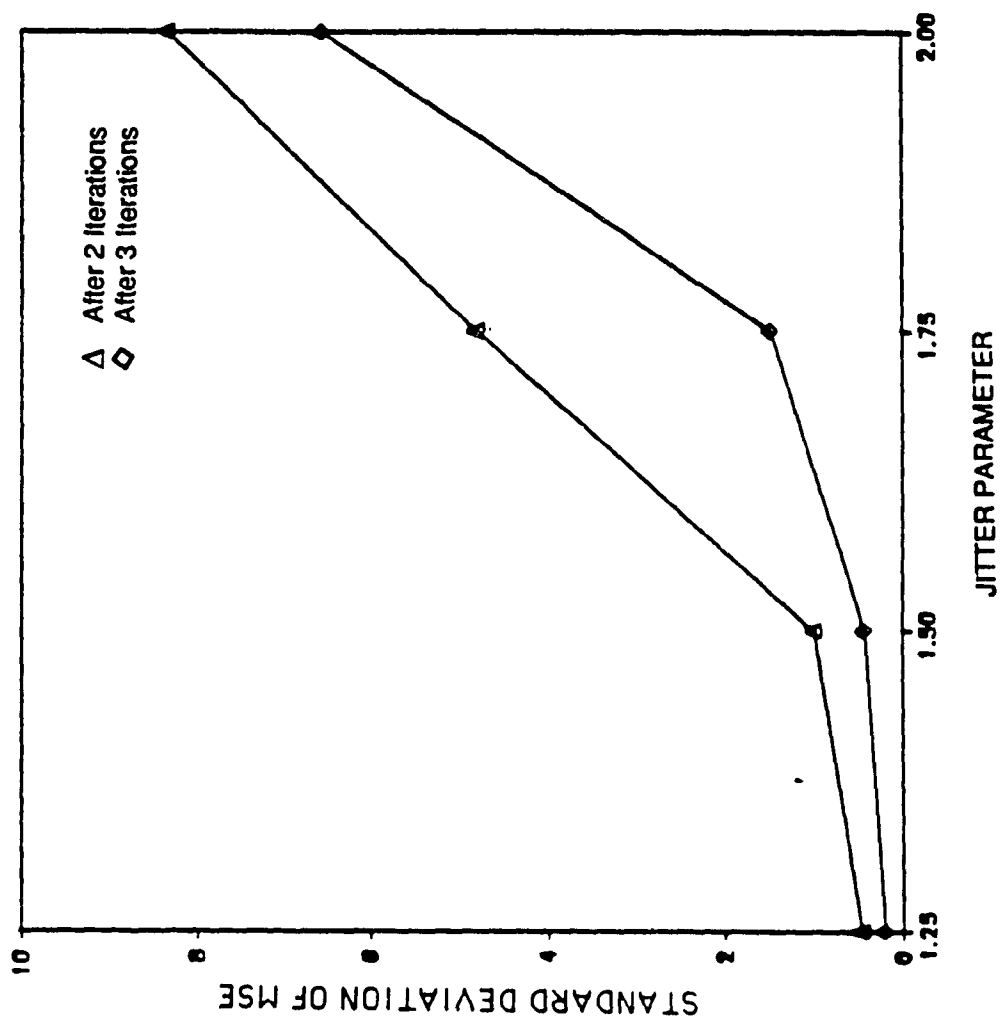


Fig. 5.15 (b): Standard deviation of MSE for $\text{SNR}_N = 20\text{db}$, ($M = 5$)

5.5 CONCLUSION

In this chapter various interesting simulations have been performed and the results presented. A random process has been generated and filtered to obtain a band-limited signal, which is further used for reconstruction. For reconstruction two types of random distributions were considered, namely, Gaussian and uniform distribution. In all cases the Mean Squared Error (MSE) was computed and its effects on the iterative procedure was also studied. Simulations for the case of a deterministic signal in the presence of a random noise was studied by considering different Signal to Noise Ratios (SNR_{IN}) during the reconstruction. Throughout the chapter the simulation results of the Present Study (PS) was compared with that of the "only one known on-line reconstruction procedure" from unequally spaced samples based on the sinc-composing functions (Marvasti and Analoul, 1989). At the end of the chapter, two statistical parameters (mean and standard deviation) for the MSE were calculated and compared. The effect of these parameters was also observed by varying the bounds of J which can be easily performed by suitably selecting M .

Based on the above discussion, the following can be concluded:

- (1) The iterative algorithm presented is extended for reconstructing a random distribution from unequally spaced data where the distribution can be either Gaussian or uniform.
- (2) The performance of the new algorithm was compared with Marvasti and Analoul's (1989) method for the reconstruction of a deterministic signal in the presence of noise. These results show that the present method performs better in all respects compared to that of Marvasti and Analoul (1989) one.

- (3) The effect of trials on the \overline{MSE} and $\bar{\sigma}$ for the ensemble of realizations is small, further reduction in their values are observed when the iterative procedure is implemented. This has been found to be true for the reconstruction of a sinusoidal signal with uniform distributed initial phase, uniformly distributed random process and for a deterministic signal in the presence of a random process.
- (4) From the calculated values of the standard deviations, only small variations between MSE and \overline{MSE} are observed.

CHAPTER 6

STABILITY

6.1 INTRODUCTION

In signal processing literature, many techniques such as lowpass filtering, polynomial holds, Yen's and Spline Interpolation have been presented to reconstruct a signal from its unequally spaced samples. These simulation techniques were analyzed and their performance were evaluated by Sankur and Gerhardt (1973). They compared the performance of these techniques by measuring the stability of the system. An index was defined using migration parameters of the deterministic signal. The extent to which the samples were allowed to migrate was also established by using uniform and Gaussian distributions.

$$SNR = \frac{\sum_{k=0}^N x^2(k\Delta t)}{\sum_{k=0}^N (x(k\Delta t) - \hat{x}(k\Delta t))^2} \quad (6.1)$$

where $x(k\Delta t)$ and $\hat{x}(k\Delta t)$ are respectively the original and the reconstructed samples respectively. In the above equation, the denominator expresses the error in the reconstruction procedure, in otherwords, the noise incorporated in the procedure. In the present study, the same principle is used to measure the index of performance not for its migration parameters but for variation in the input parameters. In the present study the sum of a deterministic sinusoidal signal and a random noise is considered for analysis instead of a deterministic signal. Therefore SNR is termed differently as Reconstruction Error (*RER*). Thus we define the term stability here as the system's insensitivity to *RER* for variations in the input parameters. The input parameters con-

sidered are the amplitude of the sine signal and the variance of the noise. The reasons for choosing these two parameters for sensitivity is explained in the following paragraph.

In section 5.3, the reconstruction of the sum of a deterministic (sinusoidal) function and a random process was considered for various SNR_{IN} . The various SNR_{IN} can be obtained by varying the two parameters: the amplitude of the sinusoidal function and the variance of the random noise, these are denoted respectively by A_s and σ_n^2 . Let us recall Equation (5.6):

$$SNR_{IN} = 10 \log_{10} \frac{A_s^2}{2\sigma_n^2} \quad (5.6)$$

From the above Equation it is clear that SNR_{IN} is directly and inversely proportional to A_s and σ_n^2 . Changes in these parameters affect the system performance. Recall the definition of RER used in Equation (4.6):

$$RER = 10 \log_{10} \frac{\sum_{k=0}^N x^2(k \Delta t)}{\sum_{k=0}^N (x(k \Delta t) - \hat{x}(k \Delta t))^2} \quad (4.6)$$

$x(k \Delta t)$ and $\hat{x}(k \Delta t)$ are the original and the recovered samples. The recovered samples are obtained as a result of two iterations and is denoted by $\hat{x}(k \Delta t)$. It implies that the iterative procedure is repeated twice ($Iter = 2$) for a sequence of N samples. It is decided to terminate the process after 2 iterations, since the simulated results as discussed in Chapters 4 and 5 have shown that the MSE levels are minimum even with 2 iterations. First, the effect of the amplitude variations in the simulated results are discussed and later the influence of the variance.

6.2 EFFECT OF AMPLITUDE ON THE STABILITY OF THE SYSTEM

The purpose of this section is to examine the sensitivity of the system performance by varying A_s in Equation (5.12). The variation in A_s under the assumption that $n(t)$ is a Gaussian process is considered as the first, and the variation in A_s using uniform noise is considered next.

Following are the input parameters considered for the stability criterion. A sequence of 42 samples are extracted at $\{t_k\}$ instants and these instants are randomly distributed with a uniform density function in the region of $-\Delta t/8$ to $\Delta t/8$. The average distance between the samples are $1/2400$ sec. (2400 Hz. is the sampling rate). For every subinterval length, three samples are selected for the partitioning scheme. In Equation (5.6), A_s is varied as 10, 20, ..., 100, with σ_n^2 remaining constant. A random Gaussian process having zero mean and unity variance (σ_n^2) is considered. For example, using $A_s = 10$, in Equation (5.6), SNR_{IN} is calculated approximately as 17 db. and when A_s is increased to 20, SNR_{IN} is increased to 23 db. The effect on RER due to a variation in SNR_{IN} is studied using the Equation (6.1). To evaluate the effect of J , it is increased from 0.25 to 1.5.

Fig. 6.1 summarizes the effect on RER due to variations in the J value. The four curves represent the RER variations for different jitter's namely, $J = 0.25, 0.5, 1.0$ and 1.5. It is clear from the figure that for an increase in SNR_{IN} , there is only a marginal variation in RER . The figure also demonstrates the insensitivity of A_s (SNR_{IN} from 17 db. to 37 db.) on the system performance. The other factor observed from the figure is that there is a reduction in RER for an increase in J and it can be explained as follows.

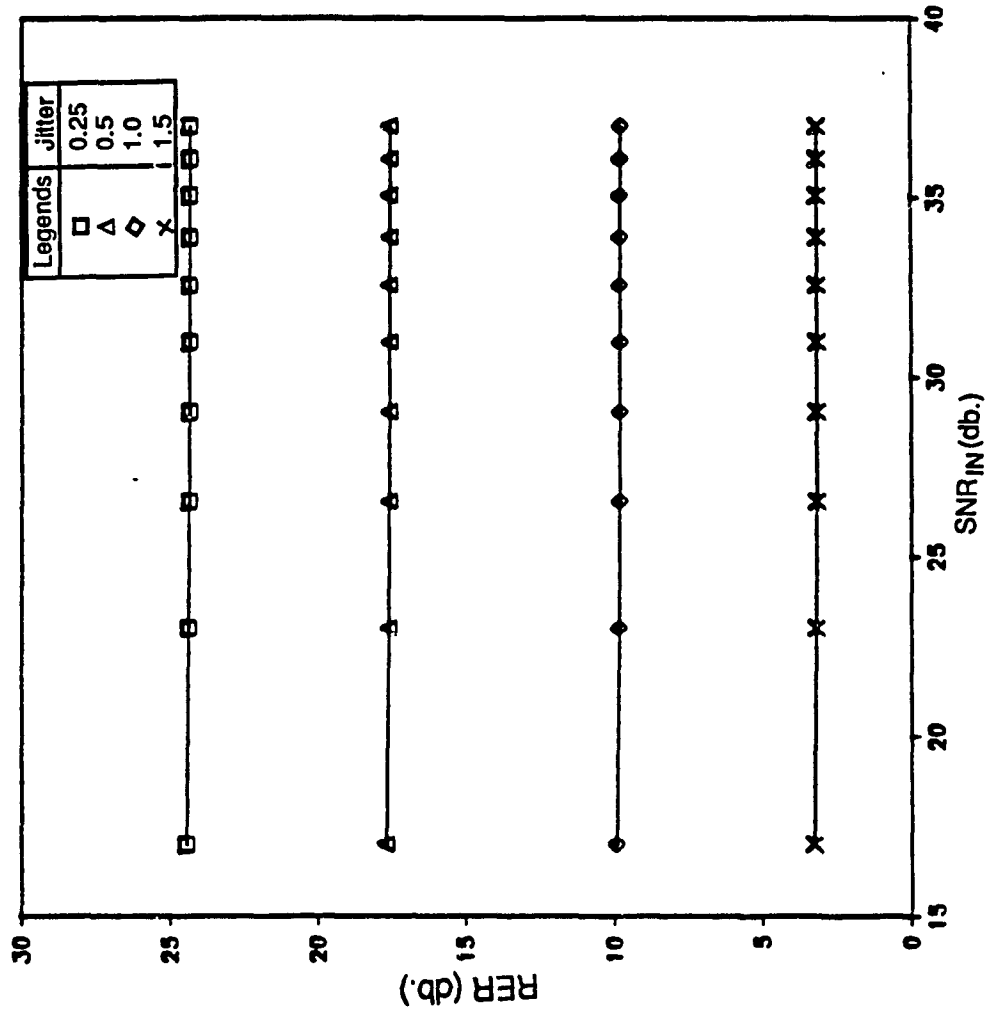


Fig.6.1: Influence of amplitude variation on the stability of a random Gaussian process

Referring to Fig. 3.2, Increase in J increases the deviations of time instants from their corresponding synchronous positions and this increase influences the iterative procedure. Hence the recovered uniformly spaced samples, $\hat{x}(k\Delta t)$, in the denominator of Equation (6.1) deviates away from the original samples, $x(k\Delta t)$. This increase in the denominator directly affects the RER and thus there is a reduction in the value of RER . For example when $J = 0.25$, for a value of 17 db. in SNR_{IN} , RER is approximately 24.4 db. When SNR_{IN} is increased to 37 db., RER is 24.3 db. Thus for an increase of 20 db. in SNR_{IN} , there is only a change of approximately .1 db. in RER . Consider $J = 1.0$ (larger time instants deviation), only 0.2 db. change is found when SNR_{IN} is increased from 17 db. to 37 db. Thus for the two curves ($J = 0.25$ and 1.0), when $SNR_{IN} = 17\text{ db.}$, RER are respectively 24.4 and 9.9 db. The reduction in RER is approximately 14.5 db., from $J = 0.25$ to $J = 1.0$. As pointed out earlier, this reduction in RER is due to the larger deviation of the time instants from their corresponding synchronous positions $\{k\Delta t\}$.

The above observations reveal that the present method is insensitive to variations in SNR_{IN} . In otherwords, the marginal variation in the reconstruction error for an increase in the input, SNR_{IN} , confirms that the system is stable. The discussion presented confirms the stability of the system performance for a sinusoidal signal in the presence of a Gaussian process. The analysis can be further extended to study the system performance in the presence of a sinusoidal signal with a random uniform process.

A random uniform process can be generated instead of a Gaussian process by initializing the random generator function to uniform distribution. The input

parameters remain the same as before and they are, $N = 42$, $f_m = 1100\text{Hz}$, $f_s = 2400\text{Hz}$, $M = 3$ and $Iter = 2$. J is also varied from 0.25 to 1.0. As before, A_s is varied from 10 to 100 in steps of 10 and σ_n^2 is chosen as 0.06. In Equation (5.6), for $A_s = 10$ and $\sigma_n^2 = 0.06$, the SNR_{IN} is found to be 41 db. The iterative procedure is implemented and the uniform samples are recovered after 2 iterations which are used to compute the RER . By following the same procedure, when A_s is equal to 20, the SNR_{IN} is computed as 47 db and its corresponding RER also measured.

Fig. 6.2 shows three curves corresponding to $J = 0.25$, 0.5 and 1.0. These curves follow the same trend as those in Fig. 6.1 and therefore the arguments of Fig. 6.1 are equally valid here. Considering typically two sample points on the X axis, namely 41 db. and 61 db., the RER is observed to be approximately constant. It is also clear from the figure that for an increase of 20 db. in SNR_{IN} , only a deviation of 0.1 db. is found. Thus the system is found to be stable even when a uniform process is considered.

6.3 INFLUENCE OF THE VARIANCE ON THE STABILITY OF THE SYSTEM

It is observed from above studies that the system is stable for variations in the input parameter, A_s . The above observation also holds for various values of J . However, the stability of the system has to be studied by varying the second input parameter namely, σ_n^2 . Hence, A_s is kept constant as unity and σ_n^2 varied.

As before, a sequence of 42 samples at $\{t_k\}$ instants are randomly distributed with uniform density function in the region of $-\Delta/8$ to $\Delta/8$, thus $J = 0.25$. M is

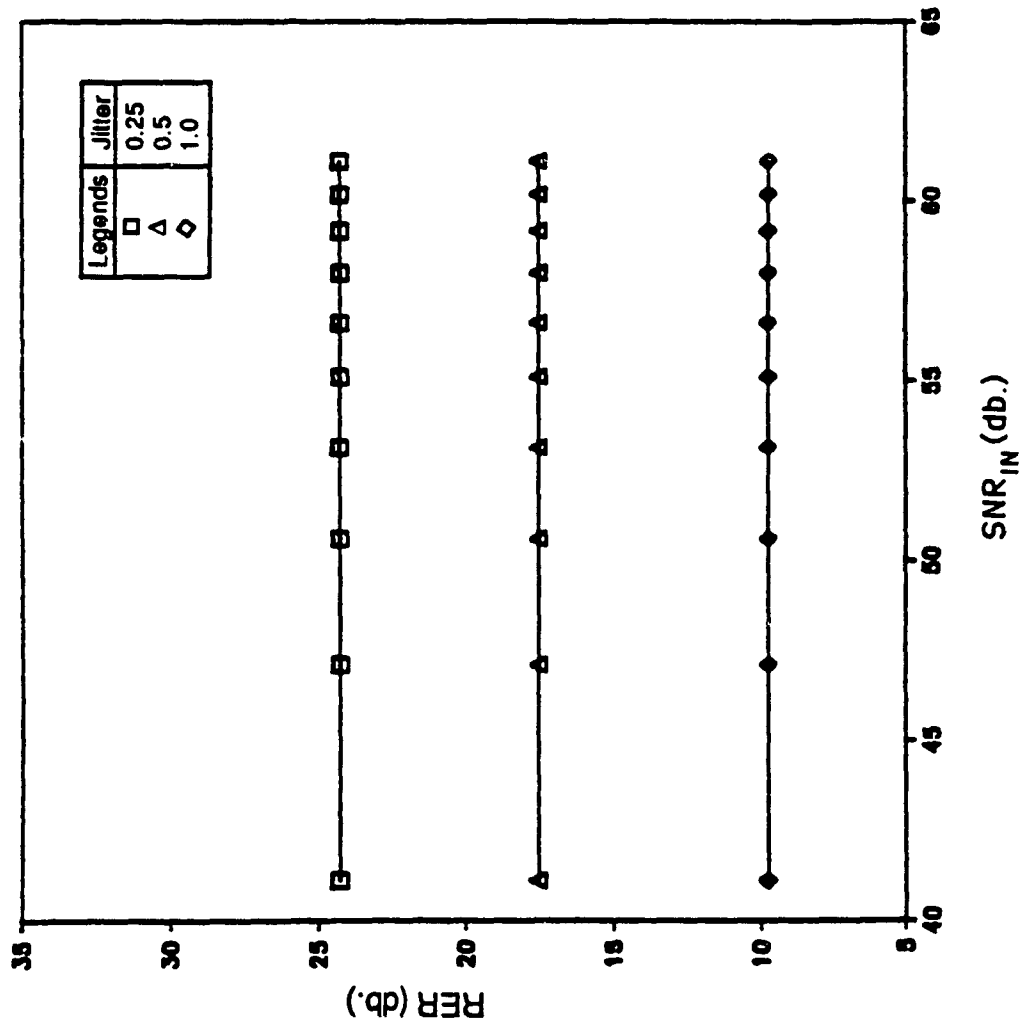


Fig.6.2: Influence of amplitude variation on the stability of a random uniform process

chosen 3, for the partitioning scheme. When $\sigma_n^2 = 1.0$, SNR_{IN} can be calculated as -3 db. by using Equation (5.6). The present iterative procedure is applied for this signal to noise ratio and uniform samples recovered after 2 iterations. $\hat{x}(k\Delta t)$ so obtained is further used to compute the RER .

Fig. 6.3 shows four curves corresponding to $J = 0.25, 0.5, 1.0$ and 1.5 . X and Y axes are respectively SNR_{IN} and RER . The range of the X axis is from -5 db. to ∞ db. According to Eq (4.6), when $\sigma_n^2 \rightarrow 0$, the value of $SNR_{IN} \rightarrow \infty$. From the figure it is also clear that the RER decreases when SNR_{IN} increases. This trend is well pronounced for the region of -3 db. to 10 db. and stabilized when SNR_{IN} is further increased. For example for the curve of $J = 0.25$, for $SNR_{IN} = -3db.$ and 9 db., RER are observed to be 25.8 db. and 23.2 db. respectively. There is a difference of approximately 2.6 db. in RER value for an increase of 12 db. in SNR_{IN} value. However when $SNR_{IN} = 35 db.$, RER is only 24.3 db. From $SNR_{IN} = 9db.$ to $SNR_{IN} = 35db.$, there is only a marginal variation in RER value. Thus changes are significant only in the region of -3 db. to 10 db. of SNR_{IN} and found to be insensitive there after. Comparing Fig. 6.1 and Fig. 6.3 for a typical sample point, say $SNR_{IN} = 35db.$, for $J = 0.25$, we see that the RER values are 24.3 db. and 24.4 db. respectively. Both have refer almost the same value for RER for the same SNR_{IN} value. This ensures the performance of the iterative procedure remains constant for the same SNR_{IN} value.

Let us now study the effect of the variation in σ_n^2 for the cases of the reconstruction of a random uniform process. The input conditions are the same as before. Fig. 6.4 shows the influence of variance on the stability of a random uniform process and it

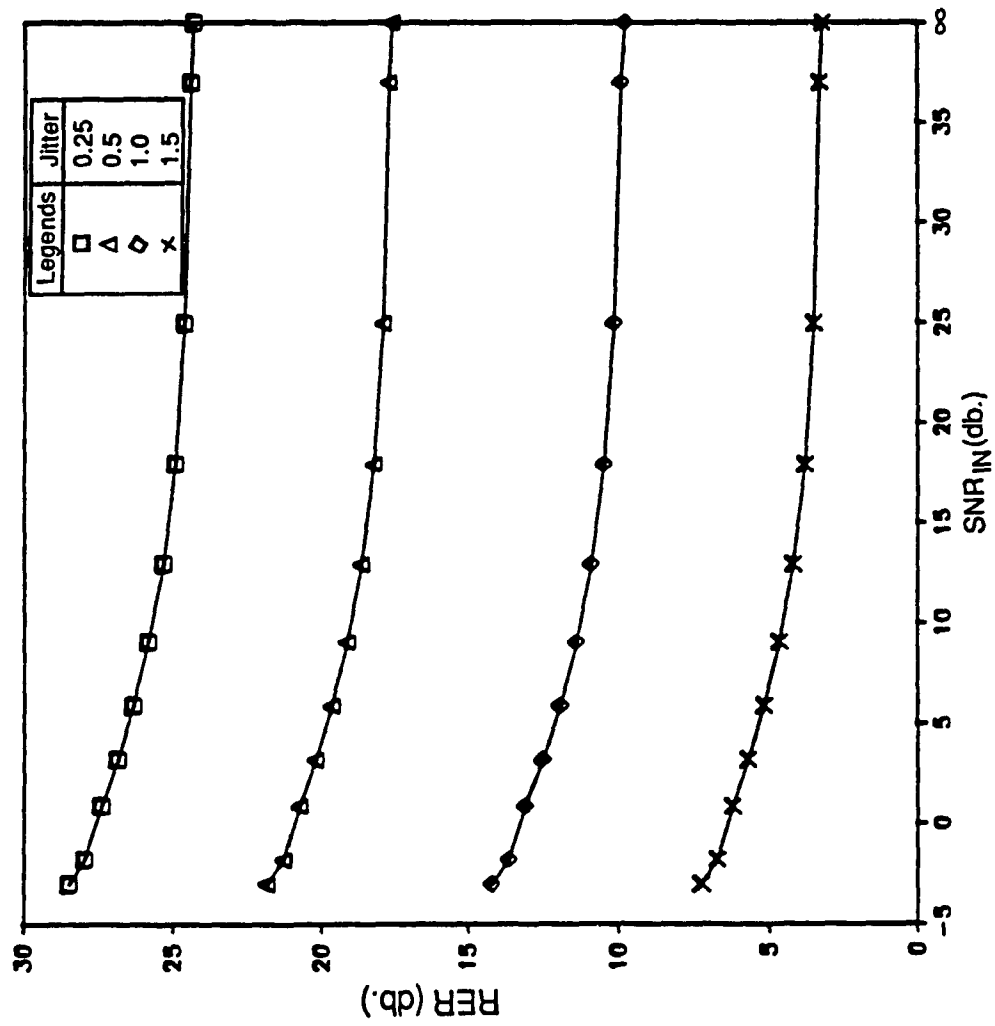


Fig.6.3: Influence of variance on the stability of a random Gaussian process

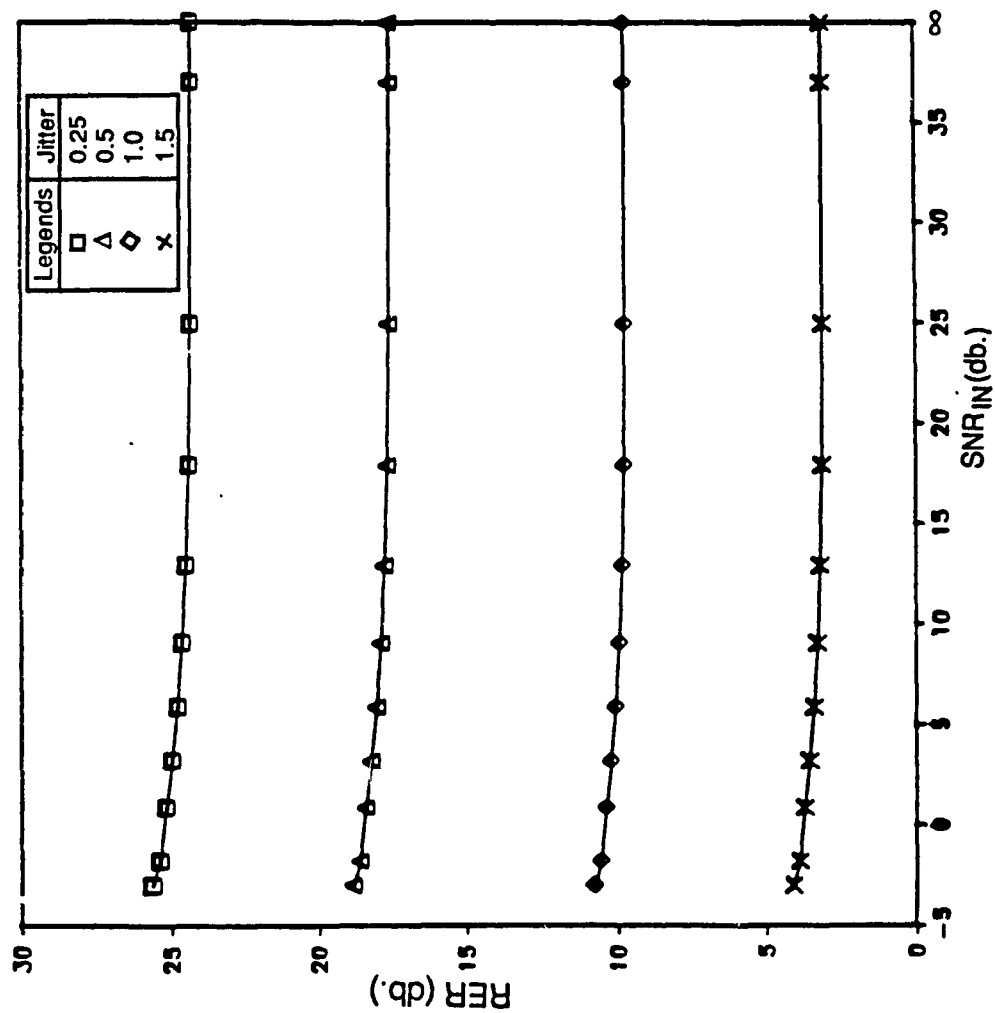


Fig.6.4: Influence of variance on the stability of a random uniform process

can be observed that the system is more insensitive to the variations in SNR_{IN} than the previous case. The analysis of these two cases confirm the stability of the system. Moreover it is clear that using a random uniform process, the system is more insensitive to variations in the input parameter, σ_n^2 , than in the presence of a Gaussian process. The analysis presented is restricted upto $J = 1.5$; however, it can also be further extended to $J = 2.0$ or 2.5 . For $J = 2.0$, one has to select M as 5, in order to perform the partitioning scheme.

6.4 CONCLUSION

Based on the above discussion, the following findings are formulated:

- (1) In the present study, RER is used as an index of performance to study the influence of the variation in the input parameters, namely, amplitude and variance.
- (2) Only marginal variation in the output of the system is noticed when there is an increase in the amplitude of the sinusoidal signal and this is found to be true both for the Gaussian and uniform processes.
- (3) The influence of the variance of a random process on the system stability is also studied. The results presented confirm that RER decreases when the input increases. This trend is observed only for a particular region of SNR_{IN} outside of which RER is constant.
- (4) These findings confirm that the present method is not only found to be efficient for reconstruction, but also the system is stable for variations in the input parameters.

CHAPTER 7

CONCLUSIONS

An iterative procedure for the reconstruction of a bandlimited signal from unequally spaced samples was presented. A Partitioning scheme was used for selecting the number of samples in a subinterval length. For the deterministic process, sine waves and sums of sine waves are reconstructed from the unequally spaced data points. The effect of the subinterval length and the jitter parameter on the reconstructed signal have also been studied. During the second part of the simulation a systematic approach for the reconstruction of a random process from unequally spaced samples was attempted. This has been performed by generating a random process and filtering it by using a Butterworth lowpass filter. Two types of random distributions, namely, Gaussian and Uniform were considered for the analysis. The iterative procedure has been further extended for the sum of a deterministic signal and a random noise by considering the Signal Noise Ratio (SNR) as the index. For each of the above cases, the value of the Mean Square Error (MSE) has been computed to evaluate the performance of the iterative procedure.

Based on the discussion of the results, the following findings can be formulated:

- 1) An increase either in the number of iterations or the subinterval length decreases the MSE level. This unique characteristic provides two options for the reconstruction procedure. One can either select the subinterval length or fix the number of iterations based on the MSE requirement.

- 2) A relationship has been formulated between the jitter parameter and the subinterval length such that it is always possible to obtain a less than 5% MSE level.
- 3) An increase either in the subinterval length or the number of iterations increases the CPU time of computation.
- 4) The calculated MSE for the reconstruction of a random process is much less than that of a deterministic signal, particularly for a sinusoidal signal with an operating frequency close to half the sampling frequency.
- 5) An increase in SNR increases the MSE level, which itself decreases when the iterative procedure is used.

Recently, Marvasti and Analoul (1989) developed an iterative adaptive method for reconstructing bandlimited signals. To evaluate the efficiency and show the superiority of the present study, considerable amount of effort has been made in simulating all the different cases discussed in the thesis. The MSE for both the methods were computed and compared. From these studies it is clear that the proposed method is not only better in MSE performance, but also can work for larger deviations of samples in comparison to Marvasti and Analoul (1989).

The above findings are applicable for a stochastic signal under the assumption of a stationary ergodic process. To validate this assumption, signals were also reconstructed for different realizations. The effect of trials on the average value of the MSE and standard deviation of the error were found to be minimum, further they decrease, when the iterative procedure is implemented. The stability of the system was also studied for variations in the input parameters, namely amplitude and variance, by using an index termed as Reconstruction Error (RER).

REFERENCES

- [1] Ahmad M., Plotkin E. I., Swamy M. N. S. and Wang J. D., (1989). "An Iterative Procedure for Uniform Resampling of 2-D Signal from Its Nonequally Spaced Samples", IEEE Int. Symposium on Circuits and Systems, 2, 1087-1090.
- [2] Balakrishnan A. V., (1962). "On the Problem of Jitter in Sampling", IRE Trans. on Inf. Theory, IT-8, 226-236.
- [3] Balakrishnan A. V., (1957). "A Note on the Sampling Principle for Continuous Signals", IRE Trans. on Inf. Theory, IT-3, 143-146.
- [4] Beutler F. E., (1966). "Error Free Recovery of Signals from Irregularly Spaced Samples", SIAM Rev., 8, 328-335.
- [5] Beutler F. E., (1961). "Sampling Theorems and Bases in Hilbert Space", Information and Control, 4, 97-117.
- [6] Black H. S., (1953). "Modulation Theory", D. Van Nostrand Co. Inc., New-York, NY.
- [7] Brown J. L., (1982). "Multichannel Sampling of Lowpass Signals", IEEE Trans. on Circuits and Syst., CAS-28, 101-106.
- [8] Brown W. M., (1960). "Sampling With Random Jitter", Jour. of SIAM, 11, 460-473.
- [9] Crochiere R. E. and Rabiner L.R., (1983). "Multirate Digital Signal Processing", Englewood Cliffs, Prentice-Hall, NJ.
- [10] Davis A. M., (1986). "Almost Periodic Extension of Band-limited Function and Its Applications to Nonuniform Sampling", IEEE Trans. on Circuits and Systems, CAS-33, 933-938.
- [11] Dunlop J. and Phillips V. J., (1974). "Signal Recovery From Repetitive Nonuniform Samples Patterns", Radio Electronic Engineer, 44, 491-503.
- [12] Ferrar W. L., (1927). "On the Consistency of Cardinal Function Interpolation", Proceeding Roy. Soc. Edinburgh, 47, 230-242.
- [13] Fogel L. J., (1955). "A Note on the Sampling Theory", IRE Trans. on Information Theory, IT-1, pp 12-13.
- [14] Forsythe G. E., Malcom M. A. and Moler C. B., (1977). "Computer Methods for Mathematical Computations", Prentice-Hall, NJ.

- [15] Gabor D., (1961). "Progress in Optics", E.Wolf., 1, Amsterdam, The Netherlands, North Holland.
- [16] Gardner N. T., (1972). "A Note on Multidimensional Sampling Theorem", IEEE Proc., 60, 247-248.
- [17] Jerri A. J., (1977). "The Shannon Sampling Theorem - Its Various Extensions and Applications: A Tutorial Review", Proc. of the IEEE, 65, 1585-1598.
- [18] Kramer H. P., (1960). "On the Best Approximation of Random Processes", IRE Trans. on Inf. Theory, IT-6, 52-53.
- [19] Mark J. N. and Todd T. D., (1981). "A Nonuniform Sampling Approach to Data Compression", IEEE Trans. Communication., COM-29, 24-32.
- [20] Marvasti F. and Analoui M., (1989). "Recovery of Signals from Nonuniform Samples Using Iterative Methods", Presented at ISCAS, 1021-1024.
- [21] Marvasti F., (1986). "Spectral Analysis of Random Sampling and Error Free Recovery by an Iterative Method", IECE Trans. of Inst. Electron. Comm. Eng., Japan (Section-E), E89, 2.
- [22] Mendelovitz E. and Sherman J. W., (1975). "Truncation Error for Signal Sampling", 9th Asilomar Rec. for Circuits Syst. Compu., 16-19.
- [23] Moler C., Little J., Bangert S. and Kleiman S., (1987). "Pro-matlab for Sun Workstations", The Mathworks Inc., Massachusetts.
- [24] Papoulis A., (1977.a.). "Generalized Sampling Expansions", IEEE Trans. on Circuits and Syst., CAS-24, 652-654.
- [25] Papoulis A., (1977.b.). "Signal Analysis", Mc Graw-Hill, New-York, NY.
- [26] Papoulis A., (1987. a.). "Truncated Sampling Expansion", IEEE Trans. on Auto. Control., 804-805.
- [27] Papoulis A., (1987. b.). "Limits on Band-limited Signals", Proceedings of the IEEE, 55, 1677-1681.
- [28] Papoulis A., (1986). "Error Analysis in Sampling Theory", Proc. of the IEEE, 54, 947-955.
- [29] Papoulis A., (1982. a.). "The Fourier Integral and Its Applications", Mc Graw-Hill, New-York, NY.

- [30] Papoulis A., (1962. b.). "Probability, Random Variables and Stochastic Processes", Mc Graw-Hill, NY.
- [31] Plotkin E. I. and Swamy M. N. S., (1989). "Non-linear Structural Model: Overview of Parameter Invariant Filtering and Non-uniform Sampling", Canadian Conference, Montreal, 1-4.
- [32] Plotkin E. I. and Swamy M. N. S., (1987). "Signal Reconstruction from Nonequally Spaced Samples with Jitter Error Reduction and Bandwidth Compression", IEE Proc., Int. Symposium on Signal Processing and Applications, ISSPA 87, Brisbane, 337-341.
- [33] Plotkin E. I., Roytman L. M. and Swamy M. N. S., (1984). "Reconstruction of Nonuniform Sampled Bandlimited Signals and Jitter Error Reduction", Signal Processing, 7, 151-160.
- [34] Plotkin E. I., Roytman L. M. and Swamy M. N. S., (1982). "Nonuniform Sampling for Bandlimited Modulated Signals", Signal Processing, 4, 295-303.
- [35] Rabiner L. R. and Gold B., (1975). "Theory and Applications of Digital Signal Processing", Eaglewood Cliffs, Prentice Hall, NJ.
- [36] Reza F. M., (1961). "An Introduction to Information Theory", Mc Graw-Hill, New-York, NY.
- [37] Sandberg I. W., (1963). "On the Properties of Systems that Distort Signals -1", Bell Syst. Tech. Journal, 42, 2033-2047.
- [38] Sankur B. and Gerhardt L., (1973). "Reconstruction of Signals from Nonuniform Samples", IEEE Int. Conf. on Comm. Rec., 15.13 - 15.18.
- [39] Shannon C. E., (1949). "Communication in the Presence of Noise", Proc. of IRE, 37, 10-21.
- [40] Smith M. J. T. and Barnwell T.P., (1986). "Exact Reconstruction Techniques for Tree-Structure Subband Coders", IEEE Trans. on Acc., Speech and Signal Processing, ASSP-36, 434-440.
- [41] Stanely D. W., (1982). "Electronic Communication Systems", Reston Publishing Company Inc., Prentice-Hall, Reston, Virginia.
- [42] Thomas J. B. and Liu B., (1964). "Error Problems in Sampling Representations", IEEE Int. Conv. Rec. (USA), 12, 269-277.
- [43] Valdhyanadhan P. P. and Liu V. C., (1988). "Classical Sampling Theorems in the Context of Multirate and Polyphase Digital Filter Band Structures", IEEE Trans. on Acoustics, Speech and Signal Processing, 36, 1480-1495.

- [44] Valdhyanadhan P. P., (1987.a). "Quadrature mirror Filter Banks, M-Band Extensions and Perfect Reconstruction Techniques", IEEE ASSP Mag., pp 15-18.
- [45] Valdhyanadhan P. P., (1987.b). "Theory and Design of M-channel Maximally Decimated Quadrature Mirror Filter with Arbitrary M, Having the Perfect Reconstruction Property, IEEE Trans. on Acc., Speech and Signal Processing, ASSP-35, 476-492.
- [46] Vetterli M., (1987). "A Theory of Multirate Filter Banks", IEEE Trans. on Acc., Speech and Signal Processing, ASSP-35, 356-371.
- [47] Whittaker J. M., (1929). "The Fourier Theory of the Cardinal Functions", Proc. of Math. Soc., Edinburgh, 1, 169-176.
- [48] Whittaker E. T., (1915). "On the Functions which are Represented by the Expansion of the Interpolating Theory", Proc. Roy. Soc. Edinburgh, 35, 181-194.
- [49] Wiley R. G., (1978). "Recovery of Bandlimited Signals for Unequally Spaced Samples", IEEE Trans. on Comm., 26, 135-137.
- [50] Wiley R. G., Schwarzlander H. and Weiner D. D., (1977). "Demodulation Procedure for Very Wideband FM", IEEE Trans. on Comm., 25, 318-327.
- [51] Yao K. and Thomas J. B., (1968). "On a Class of Nonuniform Sampling Representations", Presented at the Symposium on Signal Transmission and Processing, Columbia University, New-York, 69-75.
- [52] Yao K. and Thomas J. B., (1966). "On Truncation Error Bounds for Sampling Representations of Band-limited Signals", IEEE Trans. on Aerospace and Electronic Systems, AES-2, 640-647.
- [53] Yao K. and Thomas J. B., (1963). "On some Stability and Interpolatory Properties of Nonuniform sampling Expansion", IEEE Trans. on Circuit Theory, CT-14, 404-408.
- [54] Yen J. L., (1956). "On Nonuniform Sampling of Bandwidth Limited Signals", IRE Trans. on Circuit Theory, CT-3, 251-257.